Louisiana State University
LSU Digital Commons

LSU Doctoral Dissertations | Graduate School

2009

Derivatization of porphyrins for DNA and metal ion binding, especially by employing secondary sulfonamide links

Janet Manono
Louisiana State University and Agricultural and Mechanical College

Follow this and additional works at: https://digitalcommons.lsu.edu/gradschool_dissertations

 Part of the Chemistry Commons

Recommended Citation
Manono, Janet, "Derivatization of porphyrins for DNA and metal ion binding, especially by employing secondary sulfonamide links" (2009). *LSU Doctoral Dissertations*. 153.
https://digitalcommons.lsu.edu/gradschool_dissertations/153

This Dissertation is brought to you for free and open access by the Graduate School at LSU Digital Commons. It has been accepted for inclusion in LSU Doctoral Dissertations by an authorized graduate school editor of LSU Digital Commons. For more information, please contactgradetd@lsu.edu.

DERIVATIZATION OF PORPHYRINS FOR DNA AND METAL ION BINDING, ESPECIALLY BY EMPLOYING SECONDARY SULFONAMIDE LINKS

A Dissertation

Submitted to the Graduate Faculty of the
Louisiana State University and
Agricultural and Mechanical College
in partial fulfillment of the
requirements for the degree of
Doctor of Philosophy

in

The Department of Chemistry

by
Janet Manono
B.S., University of Nairobi, 2001
May 2009

DEDICATION

This dissertation is dedicated to my parents, **Job** and **Beatrice Manono** for their endless love, support and sacrifice throughout my life, and in memory of my late father **Mr. Job K. Manono**, who departed this earth a few months before completion of this Ph.D program.

ACKNOWLEDGEMENTS

I would like to express my gratitude to my advisor **Dr. Luigi G. Marzilli** for his support, guidance and patience during this career. I must thank **Dr. Patricia A. Marzilli** for endless reading of my dissertation. Special thanks to **Dr.Steve Watkins** and **Dr.Jayne Garno** for your encouragement and support when I needed it most, also thanks to **Dr. Anne Grove** and **Dr**. **Xu Zhimin** for serving in my committee.

I am very grateful to **Dr. Dale Treleaven** and **Dr. Thomas Weldeghiorghis**, for helping me when needed with the NMR spectrometers and **Dr. Frank Fronczeck** for the X-ray structures. Thanks to the past and present group members (**Dr. Anna Maria, Dr. Kristie Adams, Dr. Vidhi Maheshwari** and **Theshini Perara)** in addition to the Italian scholars, **Dr. Maria Carlone, Dr. Rosita Ronaldo and Dr. Patrizia Siega**. Thanks to my wonderful friends **Dr. Celinah, Dr. Cathrine** and **Dr. Annie** for the words of encouragement and always pushing me to be strong and positive in everything. Special thanks to Ms. Sherry Wilkes for helping me with all the official paper work during my graduate studies and the warm welcome to Louisiana State University.

I owe much thanks to my parents (**Job and Beatrice Manono**) for bringing me this far and working hard to see me achieve the highest education, Thank you for believing in me and working hard day and night to support my education. Special thanks to my family, **Emily, Priscah, Edwin, Evans, Josephine and Allan**.

Finally, I would like to thank my fiancée and my best friend **A. K. Mwatibo** for his love, constant support and encouraging words that have made me overcome all the stress in graduate school. Last but not least, thanks to **Dr. James Mwatibo**, **Joshua and Emily Mwatibo** and the rest of the **Mwatibo** family for your love and support.

TABLE OF CONTENTS

LIST OF TABLES

LIST OF FIGURES

ABSTRACT

Porphyrins are of exceptional importance in nature, science and technology: for instance, as ligands for metals in supramolecular synthesis, as photosensitizers in photodynamic therapy (PDT), and as building blocks for electronic devices. In addition to their application in cancer therapy, porphyrin species also exhibit antiviral activity. New *meso*-tetraarylporphyrins (TArP, Ar = -C_6H_4-) of the general formula, T($R^1R^2NSO_2Ar$)P, with R^1 = N-py-n-CH_2 (n = 2, 3 or 4) or SO_3^- and R^2 = H or CH_3 were synthesized. These groups were linked to the 4-position of the phenylene group of the porphyrin by a secondary (SO_2NHR) or tertiary (SO_2NR_2) sulfonamide group. The sulfonamide group was found to be a versatile way of expanding the porphyrin. The presence of a tertiary sulfonamide group instead of a dissociable proton improved the solubility of the new class of porphyrin compounds synthesized.

Adducts having four methylcobaloxime units ($CH_3Co(DH)_2$) bound to the pyridyl nitrogens of T(*N*-py-4-$CH_2(CH_3)NSO_2Ar$)P or TpyP(4) were synthesized for the first time and their solution properties studied by ^{1}H NMR spectroscopy. The ^{1}H NMR signal of the axial methyl of $CH_3Co(DH)_2L$ complexes shifts upfield with increasing L basicity, but the signal of the equatorial methyl is insensitive to L basicity. The axial methyl signal was used to examine the effect of coordination of the $CH_3Co(DH)_2$ moiety to the N-pyridyl group of the TpyP(4) and of the newly synthesized porphyrin, T(*N*-py-4-$CH_2(CH_3)NSO_2Ar$)P.

A new class of water-soluble porphyrins *meso*-tetraarylporphyrins and some metal derivatives were synthesized from the above class of compounds by simple alkylation and metallation with copper and zinc salt. Interactions of selected porphyrins and metalloporphyrins (Cu(II), Zn(II)) with calf thymus DNA were investigated by visible circular dichroism, absorption, and fluorescence spectroscopies. The main aim of studying this class of compounds

was to assess whether *N*-methylpyridinium (*N*-Mepy) groups must be directly attached to the porphyrin core in order for intercalative binding to DNA to occur.

Porphyrins have been known for some years to show antiviral activity against human immunodeficiency virus (HIV) infection in assays that measured inhibition of virus replication. One promising approach receiving increasing attention is the development of microbicides which, when applied topically, can prevent viral infection. These compounds could directly interact with HIV virions to decrease or prevent infectivity, thus providing a defense against sexual transmission of the virus. Sulfonated derivatives of tetraarylporphyrin have also been shown to exhibit activity HIV. A new class of porphyrins containing sulfonamide links was synthesized and characterized by ^{1}H NMR spectroscopy and mass spectrometry.

CHAPTER 1. INTRODUCTION

Porphyrins are a class of macrocyclic compounds, which contain four pyrrole rings linked by four methine bridges and their parent molecule is known as porphine (Figure 1.1). Substitution of some or all of the hydrogens on the pyrrole rings or at the methine bridge of the porphine results in *β*-substituted and *meso*-substituted (Figure 1.1) porphyrins.[1] Porphyrins and related compounds are the basic chromophores for a large number of biologically important natural products such as cytochromes, haemoproteins, chlorophylls and bacteriophylls.[2] Porphyrins are being studied widely because of their intriguing physical, chemical and biological properties.[1]

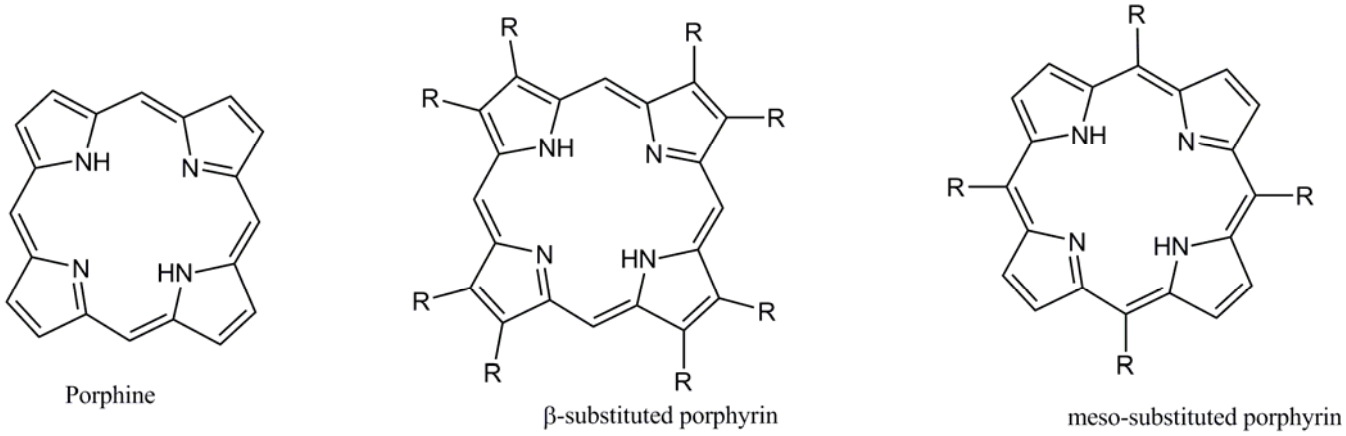

Figure 1.1. Structures of porphine, *β*-substitued and *meso*-subsituted porphyrins.

Porphyrins and their derivatives are highly colored and absorb strongly in the visible region near 400 nm (molar extinction coefficients are about 10^5 $mol^{-1}L$), characteristic of the macrocyclic conjugation and several weaker absorption bands (Q bands) between 450-700 nm.[3] The main intense absorption band is known as the *Soret* band, named after the biochemist who first observed it in hemoglobin.[4] The *Soret* band is a major characteristic of the optical spectrum of the porphyrin macrocycle as it disappears with the disruption of the macrocycle.[3] The intensity and wavelength of the absorption bands changes with variations in the peripheral

positions of the porphyrin macrocycle. Protonation of two of the inner nitrogen atoms or insertion of a metal into the porphyrin cavity changes the visible absorption spectrum.[3] The ^{1}H NMR spectrum of the aromatic porphyrin ring shows anisotropic effects.[5-7] The highly shielded NH protons in the porphyrins appear at very high field (-2 to -4 ppm), whereas the outer *meso* protons (shielded by the aromatic ring current) appear at very low field (8 to 10 ppm).[8,9]

The porphyrin macrocycle is very stable to concentrated acids (e.g. sulfuric acid), and can exhibit characteristics of both acids and bases.[2] The nitrogen atoms at the centre of the porphyrin core are responsible for this interesting characteristic.[2] In the free-base porphyrins, the central nitrogen atoms are free and the NHs (pK_b~ 9) can be protonated easily with acids such as trifluoroacetic acid.[1] Strong base such as alkoxides can remove the protons (p*K*a~16) from the inner nitrogen atoms of the porphyrin to form a dianion.[1] The inner protons can also be replaced by a metal. Various types of metals (e.g., Zn, Cu, Ni, Sn etc) can be inserted into the porphyrin cavity by using various metal salts.[10] Removal of the metal can be achieved by treatment of the metallated porphyrins with acids, and different types of acids are required for the removal of the different metals.

1.1 *Meso*-tetra(4-pyridyl)porphyrin (TpyP(4))

The development of new multiporphyrin assemblies is a subject of current research because of their potential applications in material science, reaction catalysis and energy transfer molecular devices for advanced technological tasks. [11-14] Porphyrins offer a variety of appealing features: rigid, planar geometries, high stability, intense electronic absorption bands in the visible region, a relatively long fluorescence decay time, facile tunability of their physicochemical properties by metallation or functionalization of the peripheral substituents.[15]

The metal-driven construction of multi-porphyrin assemblies exploits the formation of coordination bonds between peripheral basic site(s) on the porphyrins and metal centers. This has recently allowed the design and preparation of sophisticated supramolecular architectures.[12] Particularly attractive porphyrin arrays are those based on TpyP(4) (Figure 1.2). The electronic properties and solubility of TpyP(4) can be tuned by functionalization of the phenyl rings or the β-pyrrolic positions.[16] TpyP(4) or related compounds can provide geometrically well-defined connections to as many as four metal centers by the coordinating ability of the peripheral pyridyl groups.[17,18] 4-*meso* pyridyl groups can be coordinated to metal-containing fragments of various coordination numbers and geometries.[19] Adducts obtained by peripheral coordination of pyridylporphyrins to singly unsaturated metal centers have shown new, interesting photophysical properties.[20,21] Similarly, when polyunsaturated metal fragments are used to bridge two or more TpyP(4) units, supramolecular species of considerable structural and photophysical interest are obtained.[18]

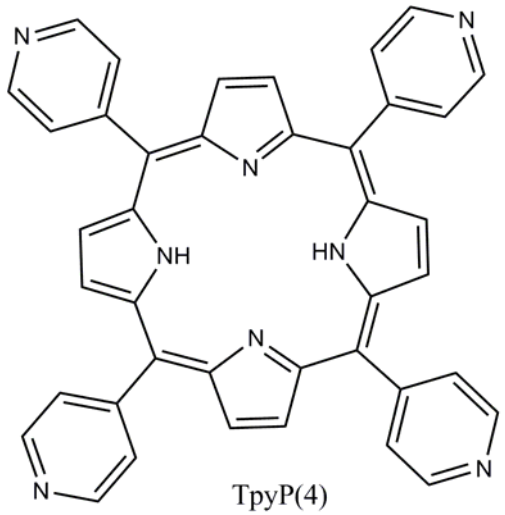

TpyP(4)

Figure 1.2. *Meso*-tetra(4-pyridyl)porphyrin.

1.2 Cationic Porphyrins

Most derivatives of cationic *meso*-tetraphenylporphyrins (TPPs) are based either on the pyridine or aniline structures, TpyP(4) and TMAP (Figure 1.3). The interaction of cationic porphyrins with DNA is of considerable interest due to their potential applications in medicine. The special properties of porphyrins such as high optical absorption, relatively high quantum yields of triplet state and fluorescence, or paramagnetism of some metal complexes provide the use of porphyrins in medicine, for instance, as active compounds in radiological therapy,[22,23] and magnetic resonance imaging of cancer detection[24] and as photosenstizers in photodynamic therapy (PDT) of cancer.[22,23,25]

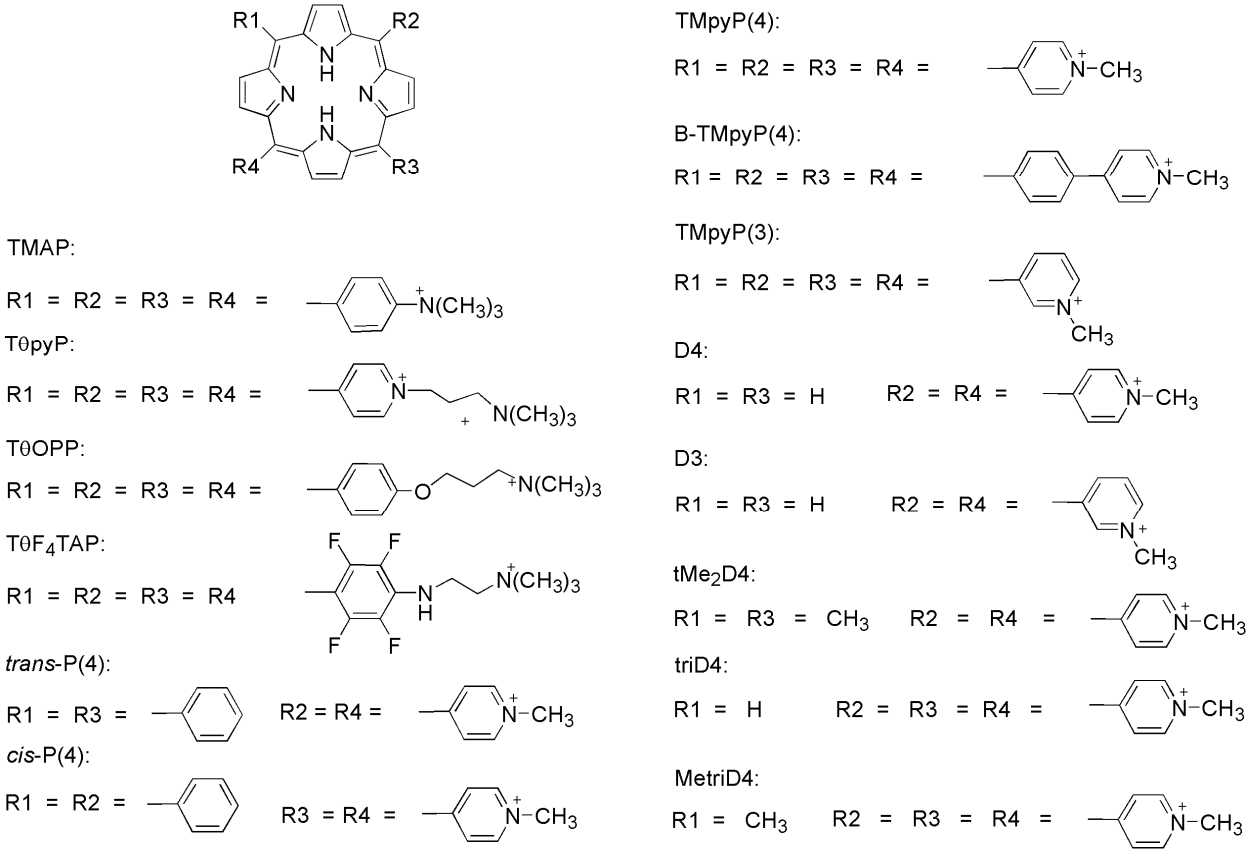

Figure 1.3. Structures of cationic porphyrins mentioned in this study.

Other work has demonstrated that cationic porphyrins can exhibit PDT against psoriasis atheromatous plaque, antiviral and antibacterial activity or act as artificial nucleases.[26-31] Porphyrins have been found to selectively accumulate in cancer cells more than in normal cells.[32-34] The ability of porphyrins to selectively accumulate in tumors, in addition to the characteristic red fluorescence has led to use of porphyrins in tumor diagnosis.[35] Interest in porphyrins and metalloporphyrins as photosensitizers and the need to understand their effect on DNA has led to extensive studies of porphyrin-DNA binding. From early studies of *meso*-tetra(4-*N*-methylpyridiniumyl)porphyrin(TMpyP(4)) and several of its derivatives, Fiel et al. proposed three major binding modes for the classification of porphyrin-DNA interactions: intercalation, outside binding with self-stacking of the porphyrin and simple outside binding (Figure 1.4).[36] The interaction of cationic porphyrins with synthetic or natural DNA has been widely studied using visible and fluorescence[37]spectroscopy, circular dichroism (CD)[36,38-40], Raman,[41-43] Nuclear Magnetic Resonance (NMR),[31,41,42] Electron Spin Resonance (ESR),[44] viscometry,[42,45] footprinting,[46] kinetic methods[47] and X-ray crystallography.[48]

One motivation for these spectroscopic investigations has been to establish reliable criteria for differentiating between intercalative and outside binding modes of porphyrins with various synthetic and natural DNAs. A thorough investigation conducted in Pasternak's laboratory showed that intercalating porphyrins are characterized by: (i) large red ($\Delta\lambda \geq 15$ nm) and hypochromic ($\%H \geq 35$) shifts of their Soret maxima, (ii) negative induced CD activity in the Soret region, and (iii) high selectivity for the GC-rich DNA regions.[40] In contrast outside binding porphyrins displayed: (i) much smaller red shifts ($\Delta\lambda \geq 8$ nm) and little hypochromicity ($\%H \leq 10$) and sometimes *hyper*chromicity) of their Soret maxima, (ii) positive induced CD bands in the Soret region, and (iii) a distinct selectivity for AT-rich DNA regions.[40]

The binding mode or modes of a specific porphyrin-DNA system are highly dependent on the location of the substituent groups of the porphyrin, the nature of the metal ion, and the type of DNA. In order to achieve intercalation, it has been proposed that the porphyrin must have a limited effective thickness. For example, the four planar *N*-methylpyridinium substituents of TMpyP(4) (Figure 1.3) allow intercalative binding,[36,45,49,50] whereas a similar porphyrin, TMAP, with non-planar *N*-trimethylammonium substituents, is an outside binder.[36,49] Metalloporphyrin derivatives of TMpyP(4) (MTMpyP(4)) having no axial ligands such as Au(III), Ni(II), Pt(II) and Cu(II) are also known to intercalate with calf thymus DNA (CT DNA) and poly(dG-dC)-poly(dG-dC) (abbreviated as $[poly(dG\text{-}dC)]_2$).[40,45,51-55] In contrast, MTMpyP(4) that maintain axial ligands (Zn(II), Co(III), Fe(III), and Mn(III) do not intercalate but bind preferentially to poly(dA-dT)-poly(dA-dT) (abbreviated as $[poly(dA\text{-}dT)]_2$) over poly $[poly(dG\text{-}dC)]_2$.[56-60] It's believed that intercalation does not occur because the axial ligands sterically prevent the insertion of the porphyrin ring between DNA base pairs. Interestingly, none of the metalloporphyin derivatives of TMpyP(4), regardless of ligation, intercalate into $[poly(dA\text{-}dT)]_2$. This finding has led to the conclusion that porphyrins selectively intercalate in regions of DNA with a high percentage of GC base pairs and undergo outside binding in regions high in AT base pairs.[31,59,61]

Fiel and co-workers presented a systematic study of position isomers of TMpyP(4), including *meso*-tetra(3-*N*-methylpyridiniumyl)porphyrin (TMpyP(3), TMpyP(2).[36,62] The absorbance, circular dichroism, and viscometric results indicated that TMpyP(3) could intercalate into CT DNA but that TMpyP(2) could not. [36] The metal-free porphyrin, *meso*-tetra(2-*N*-methylpyridiniumyl)porphyrin (TMpyP(2)), in which the rotation of the *N*-methyl pyridyl group is prevented because of steric hindrance does not intercalate, but rather binds

externally to DNA and shows high specificity for AT-rich regions of DNA.[36,40]A comprehensive study of the DNA binding characteristics of 33 porphyrins by Sari et al. has evaluated the effect of the number of charges and their position on the porphyrin.[37] All porphyrins were of the formula [*meso*-[*N*-methyl-4(or 3 or 2)-pyridiniuml]n(aryl)$_{4-n}$Porphyrin]. From competitive binding assays with ethidium bromide, apparent binding constants were calculated for each of the porphyrins with CT DNA. The binding affinity was found to increase linearly with the increase in number of positive charges on the porphyrin.[37] In addition, it was determined that the minimum requirement for intercalation was two freely rotating groups in a *cis* position. This result suggested that only half of the porphyrin needs to be in a planar conformation inorder to intercalate.[37]

Over the years multiple steric issues have come to light in the quest to understand the DNA-binding interactions of the TMpyP (4) and its related compounds. Recent studies have shown that intercalation versus outside binding may also be influenced by charge on the porphyrin core[63,64] and the ionic strength of the medium, which affects self association of the porphyrin.[65,66] For instance, when the n-butyl group is attached to the periphery of the pyridinium ring, the porphyrin intercalates between the DNA base pairs,[67] but when replaced by the tri-methyl group, the porphyrin exhibits an outside self-stacking binding mode,[45] therefore indicating the importance of the steric effect of the periphery of the pyridinium ring. Fiel et al. found that TMAP binds to CT DNA in a self-stacking manner, characterized by a conservative induced CD signal.[36] Pasternack and Gibbs et al. discovered extensive self-stacking of *cis*-bis(4-*N*-methylpyridyl)diphenylporphyrin (*cis*-P(4) (Figure 1.3) and *trans*-bis(4-*N*-methylpyridyl)diphenylporphyrin (*trans*-P(4) (Figure 1.3) along the DNA backbone.[51,66,68] Our laboratory has studied the interaction of three tentacle porphyrins; (meso-tetra[2,3,5,6-

tetrafluoro-4-(2-trimethylammoniumethylamine)phenyl]porphyrin (TθF$_4$TAP), *meso*-tetra[4-[3-trimethylammoniumpropyl)oxy]phenyl]porphyrin (TθOPP), meso-tetra[4-*N*-(3-(trimethylammonio)-propyl)pyridyl]porphyrin (TθpyP) (Figure 1.3) with natural and synthetic DNA. These tentacle porphyrins all have similar size and shape but differ in electronic properties. The electron-withdrawing fluoro substituents on the aromatic rings make the porphyrin ring of TθF$_4$TAP more electron deficient than that of TθOPP (electron-donating ability of the phenoxy aromatic substituents of TθOPP makes it more electron rich) and more like that of TθpyP which is electron deficient owing to the electron-withdrawing effect of the pyridinium groups.[64] Spectroscopic and viscometric studies indicated that TθpyP (Figure 1.3) is an intercalator, whereas TθOPP and TθF$_4$TAP are outside binders with self stacking along the backbone of CT DNA, [poly(dA-dT)]$_2$ and [poly(dG-dC)]$_2$ DNA.[38,69,70] The electron-richness of the core of TθOPP may act to stabilize the self-stacked, outside bound DNA adduct, disfavoring intercalation.[38] Sterically less demanding porphyrins 5-15-di(*N*-methylpyridinium-4-yl)porphyrin (D4) and 5-15-di(*N*-methylpyridinium-3-yl)porphyrin (D3) (Figure 1.4) have been synthesized by the McMillin group and the interaction of these porphyrins with DNA indicated that both porphyrins bind as intercalators, regardless of the base composition of the DNA host.[71]

Many porphyrins form dimers and higher order aggregates in aqueous solution. Generally, anionic porphyrins (carboxy- and sulfonato-porphyrins) have shown a stronger tendency to self-stack than cationic porphyrins. This behavior may be the result of a greater localized electron density in the core region, which would promote stronger van der Waals interactions in a face-face dimer.[72] Similarly, electron-donating substituents on cationic porphyrins, which produce relatively electron rich cores, also tend to promote the formation of dimers and higher order aggregates.[73] For example, TMAP is electron rich, as indicated by the relatively high pK_a values

of its pyrrolic nitrogens, and it aggregates in aqueous solution;[74] TθOPP also has an electronic rich core due to the electron-donating ability of the phenoxy aromatic substituents ($pK_a = 4.6$)[64] and exhibits aggregation properties similar to those of TMAP.[64] Aggregation of these porphyrins is promoted at high salt concentrations, where repulsions of like charges are reduced.

Cationic porphyrins aggregate quite readily in aqueous solution. Pasternack et al. first proposed[72] the idea that TMpyP(4) exists only as a monomer in aqueous solution. The original conclusion was based on a straight-line Beer's law plot over the concentration range 1-60 mM.[72] However, Kano et al., using mainly fluorescence techniques, argued that TMpyP(4) dimerizes very strongly even at concentrations below 0.1 μM.[75] They observed unresolved fluorescence bands which tended to separate upon dilution and with increasing temperature.[75] In ^{1}H NMR studies, a broad singlet corresponding to the pyrrole protons of TMpyP(4) was interpreted as evidence for face-to face dimer.[76] In contrast, other tetracationic porphyrins such as TMAP, TOpyP(4) (meso-tetra(4-*N*-octylpyridinium)porphyrin) aggregate spontaneously in aqueous solution in both the presence and absence of NaCl.[74] Moreover two dicationic porphyrin derivatives (*cis*-P(4) and *trans*-P(4)) are known to form self aggregates.[66,74] In particular, *trans*-P(4) readily forms large aggregate assemblies. McMillin and co-workers have synthesized less sterically demanding porphyrin having less bulk at the periphery (tMe_2D4) (Figure 1.3).[71] The tMe_2D4 system makes an interesting contrast with *trans*-P(4), tMe_2D4 is a less hydrophobic porphyrin and generally is less prone to aggregation than *trans*-P(4).[71] tMe_2D4 (Figure 1.3) was found to intercalate into DNA, in contrast to reports on *trans*-P(4), which binds externally, forming long-range stacked structures.[51,66,71]

The aggregation behavior of a porphyrin has a direct effect on its DNA-binding mode; porphyrins which aggregate strongly have a greater tendency to undergo outside binding with

self-stacking. Several porphyrins have been recognized as binding to DNA in this manner. TMAP binds to DNA in an outside binding with self-stacking mode and forms aggregates on DNA under higher ionic strength that differs from those that are formed under low ionic strength.[77] Fe(II) form of TMAP outside bind to DNA under low ionic strength but at higher ionic strength the binding mode is outside binding with self-stacking.[77] Other porphyrins which bind to DNA by this mode include *cis*-and *trans*-P(4), two dicationic porphyrins that exhibit intense conservative CD signals with CT DNA.[51,66] Cu(II)TMpyP(4) is an outside binder with self-stacking with $[poly(dA\text{-}dT)]_2$ at high porphyrin/DNA ratios, even though it can also intercalate at GC sites.[78] TθOPP has positive charges on the side chains off the TPP.[38,69] TθOPP bind to CT DNA with stacking of the porphyrin along the exterior of the DNA.[38,69]

1.3 Porphyrins Containing Sulfonamide Links

In this dissertation, the synthesis and applications of porphyrins containing sulfonamide groups (Figure 1.5) will be discussed. Part one of this dissertation presents the synthesis of new porphyrin derivatives of *meso*-tetraarylporphyrins (TArP) of the general formula $T(R^1R^2NSO_2Ar)P$ with R^1 = *N*-py-CH_2, in which n = 2 or 4 and R^2 = H or CH_3. These porphyrins are neutral, bearing pyridy groups linked to the 4-position of the phenylene group of the porphyrin by secondary ($-SO_2NHR$) or tertiary ($-SO_2NR_2$) sulfonamide groups. The reaction of T(*N*-py-4-$CH_2(CH)_3NSO_2Ar$)P and its model porphyrin, *meso*-tetra(4-pyridyl)porphyrin (TpyP(4)), with methylcobaloxime ($CH_3Co(DH)_2H_2O$ will be discussed. The newly synthesized porphyrin (T(*N*-py-4-$CH_2(CH)_3NSO_2Ar$)P) contain a 4-pyridyl group attached to the aryl group of the porphyrin at the *meso* position through a sulfonamide link, and a methine group links the sulfonamide group and the pyridyl group; as a result, the pyridyl group is insulated from the porphyrin core. The effect of coordination of the methylcobaloxime ($CH_3Co(DH)_2$) to the *N*-

pyridyl moeity of TpyP(4) and of the newly synthesized porphyrin (T(*N*-py-4-$CH_2(CH_3)NSO_2Ar$)P) has been examined by ^1H NMR, visible, and fluorescence spectroscopic techniques.

In part two of this dissertation, the synthesis, solution properties and the DNA-binding characteristics of the alkylated derivatives of the porphyrin with the general formula $[MT(R^2R^1NSO_2Ar)P]X_{4/8}$ are presented (where M = 2H, Cu(II) or Zn(II); $R^1 = CH_3$ or H and R^2 = *N*-Mepy-n-CH_2- (*N*-Mepy = *N*-methylpyridinium group and n = 2, 3 or 4) or $R^1 = R^2 = Et_3NCH_2CH_2$; and Ar = 4-$C_6H_4$-). The DNA binding modes of both the free base and the selected metalloporphyrins derivatives have been evaluated by absorbance, circular dichroism, and fluorescence spectroscopy for the metal-free derivatives. The main goal of the second part of this dissertation was to assess if *N*-Mepy groups must be directly attached to the porphyrin core in order for intercalative binding of porphyrins to DNA to take place.

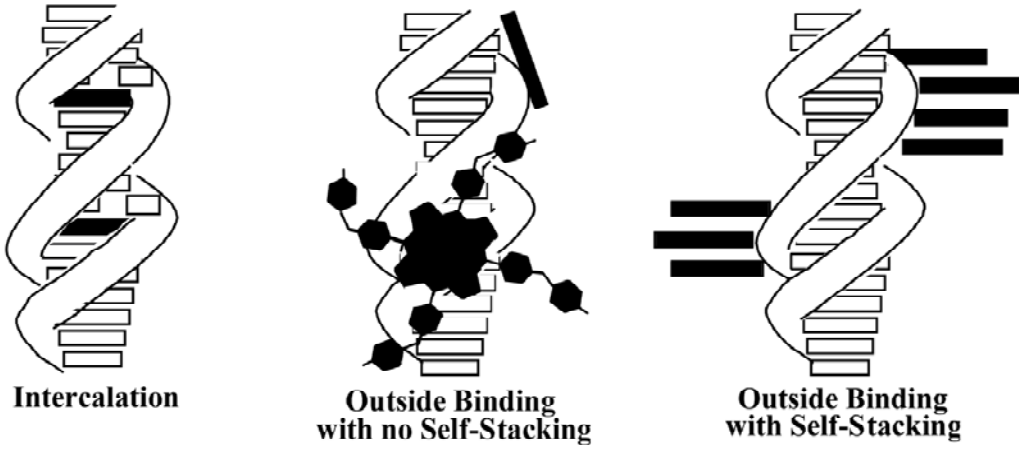

Figure 1.4. Three modes of porphyrin-DNA binding. Edge-on view of the porphyrin is represented as the dark rectangle, while the face on view is the pyrrole-shaped figure in the center.

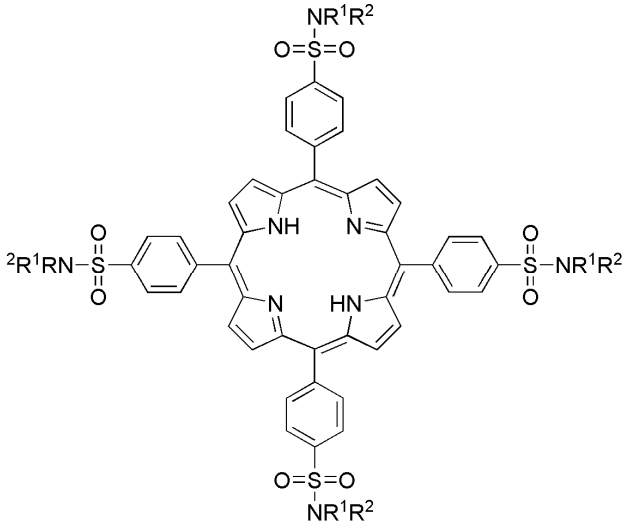

Figure 1.5. General structure of the newly synthesized porphyrins.

1.5 References

1. Falk, J. E. In *General chemistry: In Porphyrins and metalloporphyrins*; Elsevier: Amsterdam, 1964; Vol. 2, pp 3-29.

2. Smith, K. M., Ed. *Porphyrins and Metalloporphyrins*; Elsevier: Amsterdam, 1975.

3. Weiss, C. *J. Mol. Spectrosc.* **1972**, *44*, 37-80.

4. Soret, J. L. *C. R. Acad. Sci.,* **1883**, *97*, 1267.

5. Kevin M. Smith, D. A. G. R. J. A. *Org. Magn. Reson.* **1984**, *22*, 779-783.

6. Senge, M. O.; Smith, K. M. *Photochem. Photobiol.* **1991**, *54*, 841-846.

7. Smith, K. M.; Unsworth, J. F. *Tetrahedron* **1975**, *31*, 367-375.

8. Abraham, R. J.; Medforth, C. J.; Smith, K. M.; Goff, D. A.; Simpson, D. J. *J. Am. Chem. Soc.* **1987**, *109*, 4786-4791.

9. Abraham, R. J.; Rowan, A. E.; Mansfield, K. E.; Smith, K. M. *J. Chem. Soc., Perkin Trans. 2* **1991**, 515-521.

10. Buchler, J. W. In *Porphyrins and Metalloporphyrins*; Smith, K. M., Ed.; Elsevier: Amsterdam, 1975; Vol. Chapter 5, p 157.

11. Blau, W.; Byrne, H.; Dennis, W. M.; Kelly, J. M. *Opt. Commun.* **1985**, *56*, 25-29.

12. Iengo, E.; Scandola, F.; Alessio, E. In *Non-Covalent Multi-Porphyrin Assemblies Synthesis and Properties*, 2006, pp 105-143.

13. Scandola, F.; Chiorboli, C.; Prodi, A.; Iengo, E.; Alessio, E. *Coord. Chem. Rev.* **2006**, *250*, 1471-1496.

14. Su, W.; Cooper, T. M.; Brant, M. C. *Chem. Mater.* **1998**, *10*, 1212-1213.

15. BarbosaNeto, N. M.; DeBoni, L.; Mendonca, C. R.; Misoguti, L.; Queiroz, S. L.; Dinelli, L. R.; Batista, A. A.; Zilio, S. C. *J. Phys. Chem. B* **2005**, *109*, 17340-17345.

16. Iengo, E.; Zangrando, E.; Alessio, E. *Acc. Chem. Res.* **2006**, *39*, 841-851.

17. Prodi, A.; Indelli, M. T.; Kleverlaan, C. J.; Alessio, E.; Scandola, F. *Coord. Chem. Rev.* **2002**, *229*, 51-58.

18. Prodi, A.; Kleverlaan, C. J.; Indelli, M. T.; Scnadola, F.; Alessio, E.; Iengo, E. *Inorg. Chem.* **2001**, *40*, 3498-3504.

19. Gianferrara, T.; Serli, B.; Zangrando, E.; Iengo, E.; Alessio, E. *New J. Chem.* **2005**, *29*, 895-903.

20. Alessio, E.; Macchi, M.; Heath, S. L.; Marzilli, L. G. *Inorg. Chem.* **1997**, *36*, 5614-5623.

21. Araki, K.; Toma, H. E. *J. Photochem. Photobiol., A* **1994**, *83*, 245-250.

22. Hambright, P.; Fawwaz, R.; McRae, J.; Bearden, A. J.; Valk, P. *Bioinorg. Chem.* **1975**, *5*, 87-92.

23. Zanelli, D. G.; Kaclin, C. A. *Br. J. Radiol* **1981**, *54*, 403-407.

24. Chen, C.; Cohen, J. S.; Myers, C. E.; Sohn, M. *FEBS Lett.* **1984**, *168*, 70-74.

25. Bonnett, R. *Chem. Soc. Rev.* **1995**, *24*, 19-33.

26. Ben-Hur, E.; Horowitz, B. *Photochem. Photobiol.* **1995**, *62*, 383-388.

27. Aasanaka, M.; Kurimura, T.; Toya, H.; Ogaki, K.; Kato, Y. *AIDS* **1989**, *3*, 403-404.

28. Dixon, D. W.; Gill, A. F.; Giribabu, L.; Vzorov, A. N.; Alam, A. B.; Compans, R. W. *J. Inorg. Biochem.* **2005**, *99*, 813-821.

29. Dixon, D. W.; Schinazi, R.; Marzilli, L. G. *Ann. N.Y. Acad. Sci.* **1990**, *616*, 511-513.

30. Lia, H.; Fedorovaa, O. S.; Grachevc, A. N.; Trumbleb, W. R.; Bohachb, G. A.; Czuchajowskia, L. *Biochim. Biophys. Acta, Gen. Struct. Expr.* **1997**, *1354*, 252-260.

31. Marzilli, L. G. *New J. Chem.* **1990**, *14*, 409-420.

32. Tronconi, M.; Colombo, A.; De Cesare, M.; Marchesini, R.; Woodburn, K. W.; Reiss, J. A.; Phillips, D. R.; Zunino, F. *Cancer Letters* **1995**, *88*, 41-48.

33. Winkelma.J; Slater, G.; Grossman, J. *Cancer Research* **1967**, *27*, 2060.

34. Woodburn, K. W.; Bellinger, G. C. A.; Phillips, D. R.; Reiss, J. A. *Aust. J. Chem.* **1992**, *45*, 1745-1751.

35. Lipson, R. L.; Baldes, E. J.; Gray, M. *Cancer* **1967**, *20*, 2255-2257.

36. Carvlin, M. J.; Fiel, R. J. *Nucleic Acids Res.* **1983**, *11*, 6121-6139.

37. Sari, M. A.; Battioni, J. P.; Dupre, D.; Munsuy, D.; Le Pecq, J. B. *Biochemistry* **1990**, *29*, 4205-4215.

38. Mukundan, N. E.; Petho, G.; Dixon, D. W.; Marzilli, L. G. *Inorg. Chem.* **1995**, *34*, 3677-3687.

39. Pasternack, R. F. *Chirality* **2003**, *15*, 329-332.

40. Pasternack, R. F.; Gibbs, E. J.; Villafranca, J. J. *Biochemistry* **1983**, *22*, 2406-2414.

41. Bütje, K.; Schneider, J. H.; Nakamoto, K.; Kim, J. P.; Wang, Y.; Ikuta, S. *J. Inorg. Biochem.* **1989**, *37*, 119-134.

42. Gray, T. A.; Marzilli, L. G.; Yue, K. T. *J. Inorg. Biochem.* **1991**, *41*, 205-219.

43. Schneider, J. H.; Odo, J.; Nakamoto, K. *Nucleic Acids Res.* **1988**, *16*, 10323-10338.

44. Dougherty, G.; Pasternack, R. F. *Biophys. Chem.* **1992**, *44*, 11-19.

45. Banville, D. L.; Marzilli, L. G.; Strickland, J. A.; Wilson, W. D. *Biopolymers* **1986**, *25*, 1837-1858.

46. Ford, K.; Fox, R. K.; Neidle, S.; Waring, J. M. *Nucleic Acids Res.* **1987**, *15*, 2221-2234.

47. Pasternack, R. F.; Gibbs, E. J.; Villafranca, J. J. *Biochemistry* **1983**, *22*, 5409-5417.

48. Lipscomb, L. A.; Zhou, F. X.; Presnell, S. R.; Woo, R. J.; Peek, M. E.; Plaskon, R. R.; Williams, L. D. *Biochemistry* **1996**, *35*, 2818-2823.

49. Carvlin, M. J.; Dattagupta, N.; Fiel, R. J. *Biochem. Biophys. Res. Commun.* **1982**, *108*, 66-73.

50. Fiel, R. J.; Howard, J. C.; Mark, E. H.; Dattagupta, N. *Nucleic Acids Res.* **1979**, *6*, 3093-3118.

51. Gibbs, E. J.; Tinoco, I.; Maestre, M. F.; Ellinas, P. A.; Pasternack, R. F. *Biochem. Biophys. Res. Commun.* **1988**, *157*, 350-358.

52. Pasternack, R. F.; Brigandi, R. A.; Abrams, M. J.; Williams, A. P.; Gibbs, E. J. *Inorg. Chem.* **1990**, *29*, 4483-4486.

53. Strickland, J. A.; Banville, D. L.; Wilson, W. D.; Marzilli, L. G. *Inorg. Chem.* **1987**, *26*, 3398-3406.

54. Strickland, J. A.; Marzilli, L. G.; Wilson, W. D. *Biopolymers* **1990**, *29*, 1307-1323.

55. Strickland, J. A.; Marzilli, L. G.; Wilson, W. D.; Zon, G. *Inorg. Chem.* **1989**, *28*, 4191-4198.

56. Pasternack, R. F.; Gibbs, E. J.; Gaudemer, A.; Antebi, A.; Bassner, S.; Depoy, L.; Turner, D. H.; Williams, A.; Laplace, F.; Lansard, M. H.; Merienne, C.; Perreefauvet, M. *J. Am. Chem. Soc.* **1985**, *107*, 8179-8186.

57. Ward, B.; Skorobogaty, A.; Dabrowiak, J. C. *Biochemistry* **1986**, *25*, 7827-7833.

58. Geacintov, N. E.; Ibanez, V.; Rougee, M.; Bensasson, R. V. *Biochemistry* **1987**, *26*, 3087-3092.

59. Lin, M. F.; Lee, M. H.; Yue, K. T.; Marzilli, L. G. *Inorg. Chem.* **1993**, *32*, 3217-3226.

60. Strickland, J. A.; Marzilli, L. G.; Gay, K. M.; Wilson, W. D. *Biochemistry* **1988**, *27*, 8870-8878.

61. Fiel, R. J. *J. Biomol. Struct. Dyn.* **1989**, *6*, 1259-1275.

62. Carvlin, M. J.; Mark, E.; Fiel, R.; Howard, J. C. *Nucleic Acids Res.* **1983**, *11*, 6141-6154.

63. Kuroda, R.; Takahashi, E.; Austin, C. A.; Fisher, L. M. *FEBS Lett.* **1990**, *262*, 293-298.

64. Marzilli, L. G.; Petho, G.; Lin, M. F.; Kim, M. S.; Dixon, D. W. *J. Am. Chem. Soc.* **1992**, *114*, 7575-7577.

65. Dixon, D. W.; Steullet, V. *J. Inorg. Biochem.* **1998**, *69*, 25-32.

66. Pasternack, R. F.; Bustamante, C.; Collings, P. J.; Giannetto, A.; Gibbs, E. J. *J. Am. Chem. Soc.* **1993**, *115*, 5393-5399.

67. Sehlstedt, U.; Kim, S. K.; Carter, P.; Goodisman, J.; Vollano, J. F.; Norden, B.; Dabrowiak, J. C. *Biochemistry* **1994**, *33*, 417-426.

68. Pasternack, R. F.; Giannetto, A.; Pagano, P.; Gibbs, E. J. J. *J. Am. Chem. Soc.* **1991**, *113*, 7799-7800.

69. Mukundan, N. E.; Petho, G.; Dixon, D. W.; Kim, M. S.; Marzilli, L. G. *Inorg. Chem.* **1994**, *33*, 4676-4687.

70. McClure, J. E.; Baudouin, L.; Mansuy, D.; Marzilli, L. G. *Biopolymers* **1997**, *42*, 203-217.

71. Shelton, A. H.; Rodger, A.; McMillin, D. R. *Biochemistry* **2007**, *46*, 9143-9154.

72. Pasternack, R. F.; Centuro, G. C.; Boyd, P.; Hinds, L. D.; Huber, P. R.; Francesconi, L.; Fasella, P.; Engasser, G.; Gibbs, E. *J. Am. Chem. Soc.* **1972**, *94*, 4511-4517.

73. Bütje, K.; Nakamoto, K. *Inorg. Chim. Acta* **1990**, *167*, 97-108.

74. Kano, K.; Takei, M.; Hashimoto, S. *J. Phys. Chem.* **1990**, *94*, 2181-2187.

75. Kano, K.; Miyake, T.; Uomoto, K.; Sato, T.; Ogawa, T.; Hashimoto, S. *Chem. Lett.* **1983**, 1867-1870.

76. Kano, K.; Nakajima, T.; Takei, M.; Hashimoto, S. *Bull. Chem. Soc. Jpn.* **1987**, *60*, 1281-1287.

77. Ghaderi, M.; Bathaie, Z. S.; A., S.; Sharghi, H.; Tangestaninejad, S. *Int. J. Biol. Macromol.* **2007**, *41*, 173-179.

78. Hudson, B. P.; Sou, J.; Berger, D. J.; McMillin, D. R. *J. Am. Chem. Soc.* **1992**, *114*, 8997-9002.

CHAPTER 2. NEW PORPHYRINS BEARING PYRIDYL PERIPHERAL GROUPS LINKED BY SECONDARY OR TERTIARY SULFONAMIDE GROUPS: SYNTHESIS AND STRUCTURAL CHARACTERIZATION

2.1 Introduction

The special characteristics of porphyrins have led to numerous studies and applications both by nature and by mankind.[1-3] Pyridylporphyrins (PyPs) in which the pyridine ring is directly attached to the porphyrin core have been used in supramolecular systems, usually with metal centers providing the linking group.[4-6] A number of complexes with different coordination numbers involving ruthenium, rhenium and platinum have been coordinated symmetrically to N atoms of the peripheral pyridyl groups of *meso*-tetrapyridylporphyrins (TpyPs).[5,7-10] Most studies have involved the *meso*-tetra(4-pyridyl)porphyrin (TpyP(4)) isomer, Chart 2.1. It has been shown that coordination of the different metal fragments to N atoms of the peripheral pyridyl groups not only solubilizes the porphyrin but also introduces useful functionalities into the system.[6] For example, Alessio and co-workers recently reported adducts between a TpyP(4) pyridyl group and either one or four Re(I) bipyridine tricarbonyl units, and they have compared their photophysical properties to those of the parent TpyP(4).[11]

A second type of application for PyPs, such as TpyP(4), is to convert them into water-soluble *N*-alkylpyridinium derivatives. These compounds have been shown to possess interesting biomedical properties such as antiviral activity, anticancer activity, etc. and to interact with DNA by a variety of binding modes.[12-16] In many cases, metals bound to the center of the porphyrin influence the DNA binding mode.[17-21] Organometallic complexes such as areneruthenium(II) compounds (e.g., $[Ru(\eta^6\text{-}C_6H_5CH_3)(\mu\text{-}Cl)Cl]_2$) have been coordinated to the pyridyl groups of TpyP(4) in order to combine the photodynamic action of the porphyrin with the cytotoxicity effect of the areneruthenium complexes.[22] These PyPs are generally relatively rigid, a property

that may be helpful in constructing supramolecular systems,[23,24] but it would be interesting to examine less rigid systems, particularly after the pyridines are converted to N-alkyl pyridinium groups. As a first step in this direction, we wanted to overcome some of the problems in constructing suitable porphyrins, chiefly the low-yield syntheses that hamper porphyrin chemistry and the poor solubility of such PyPs as TpyP(4). PyPs reported here were prepared from the simple *meso*-tetraphenylporphyrin (TPP). TPP can be modified by connecting to it different peripheral substituents, changing the central metal, or expanding the size of the macrocycle. In this initial report, we describe a very useful strategy to meet our goals of finding a versatile synthetic approach to preparing soluble PyPs. Good solubility allows facile addition of the metal to either the inner core of the porphyrin or to a peripheral pyridyl group. Furthermore, we report a method of making poorly soluble porphyrins (e.g., TpyP(4)) more soluble by using a dissociable metal-protecting group such as an organocobaloxime moiety, $RCo(DH)_2$ (DH = the monoanion of dimethylglyoxime).

Organocobaloximes ($RCo(DH)_2L$), in which L is an N-donor ligand such as pyridine, have been used extensively to understand the fundamental chemistry related to the organocobalt B_{12} coenzymes.[25-31] In this work we exploit the lability and the well-understood NMR properties to explore the new porphyrins we have prepared. In particular, we describe the synthesis of new pyridyl porphyrins containing sulfonamide groups of the general formula, $MT(R^1R^2NSO_2Ar)P$. Using ^1H NMR, visible absorption and fluorescence spectroscopic techniques, we have examined the effect of coordination of the methylcobaloxime ($CH_3Co(DH)_2$) moiety to the *N*-pyridyl group of TpyP(4) and of the newly synthesized porphyrin, T(*N*-py-4-$CH_2(CH_3)NSO_2Ar)P$.

2.2 Experimental Section

2.2.1 Materials and Methods. 4-Cyanopyridine (4-CNpy), pyridine (py), 3,5-lutidine (3,5-lut), 4-dimethylaminopyridine (4-Me_2Npy), n-pyridylcarboxaldehyde (n = 2 or 4), n-pyridylmethylamine (n = 2 or 4),Methyl sulfonyl chloride (CH_3SO_2Cl), methylamine (CH_3NH_2), *meso*-tetra(4-pyridyl)porphyrin (TpyP(4)), and all solvents were obtained from Sigma-Aldrich. 5,10,15,20-tetra(4-chlorosulfonylphenyl)porphyrin ($TClSO_2PP$ (**1**)**,** Scheme 2.1) was synthesized by a known method, and the ^{1}H NMR chemical shifts in $CDCl_3$ matched the reported values. [32] $CH_3Co(DH)_2H_2O$ was prepared as previously reported.[30]

All ^{1}H NMR spectra were recorded on a 400 MHz Bruker NMR spectrometer. Peak positions are relative to TMS or solvent residual peak, with TMS as reference. Visible absorption spectra were recorded with a Cary 3 spectrophotometer. Excitation and fluorescence spectra of 5.0 μM porphyrin solutions (CH_2Cl_2) were recorded on a Fluorolog-3 spectrofluorimeter (Horiba Jobin Yvon) at room temperature.

2.2.2 X-ray Data Collection and Structure Determination. All single crystals suitable for X-ray crystallography were obtained by slow diffusion of methanol into dichloromethane solution. Single crystals were placed in a cooled nitrogen gas stream at 90 K on a Nonius Kappa CCD diffractometer fitted with an Oxford Cryostream cooler with graphite-monochromated Mo Kα (λ = 0.71073 Å) radiation. Data reduction included absorption corrections by the multi-scan method, with HKL SCALEPACK.[33] All X-ray structures were determined by direct methods and difference Fourier techniques and refined by full-matrix least squares, using SHELXL97.[34] All hydrogen atoms were visible in difference maps, but were placed in idealized positions. A torsional parameter was refined for each methyl group.

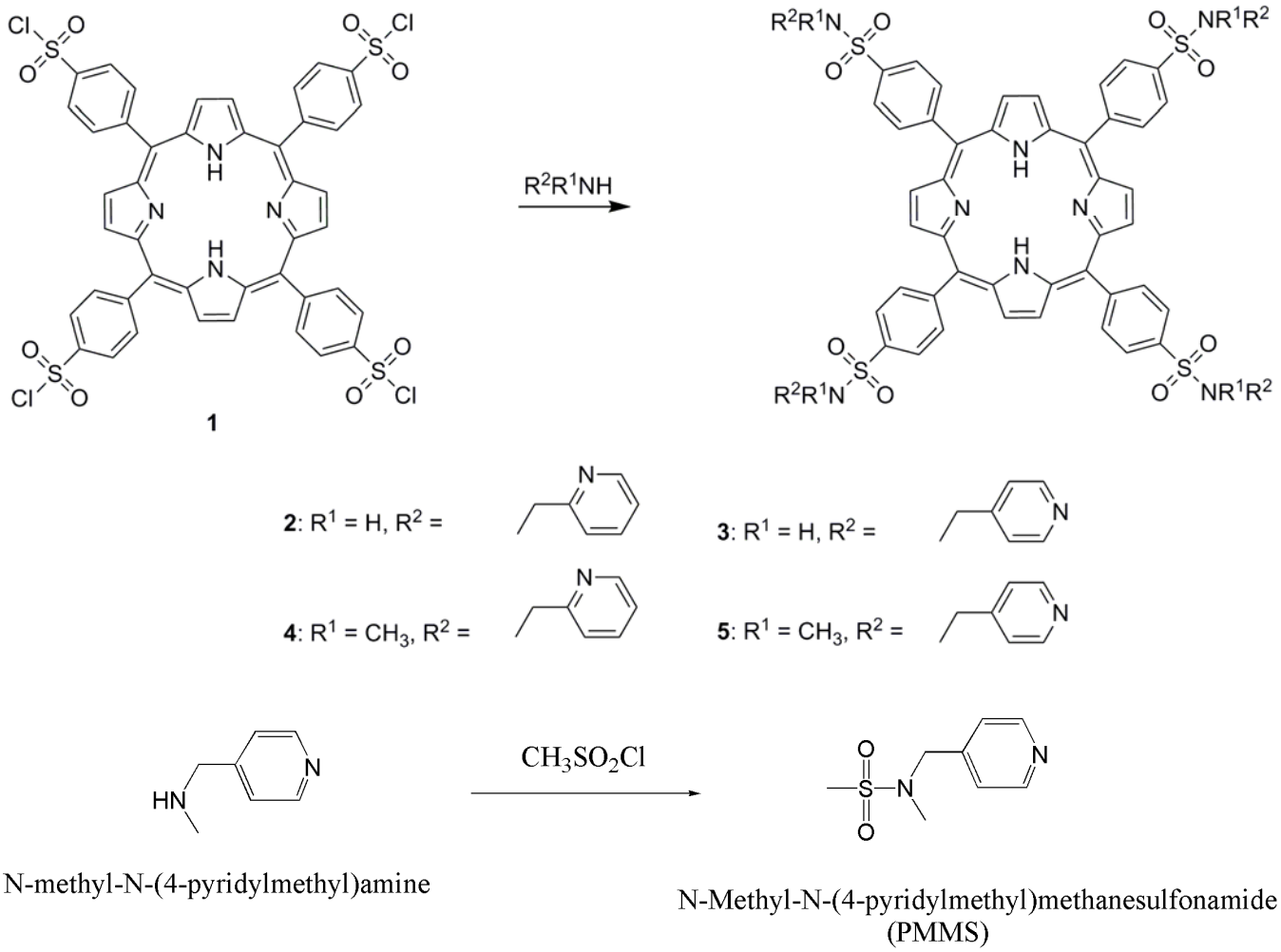

Scheme 2.1. Synthesis of porphyrin ligands and **PMMS**.

2.2.3 Synthesis of T(*N*-py-2-CH_2(H)NSO_2Ar)P (2) and T(*N*-py-4-CH_2(H)NSO_2Ar)P (3). A suspension of **1** (0.1 g, 0.1 mmol) in acetonitrile (15 mL) was treated with a solution of the respective amine in acetonitrile (0.5 mmol in 5 mL) at RT overnight. The suspension was filtered, and the purplish solid collected on the filter was washed with water several times (3 × 15 mL), followed by diethyl ether, and then air-dried.

T(*N*-py-2-CH_2(H)NSO_2Ar)P (2). Treatment of **1** (0.1 g, 0.1 mmol) with 2-pyridylmethylamine (50 μL, 0.5 mmol) as described above afforded porphyrin **2** as a purple powder (0.128 g, 83% yield). ^{1}H NMR (ppm) in DMSO-d_6: 8.80 (8H, s, β-pyrrole), 8.54 (4H, br,

NH-sulfonamide), 8.36 (8H, d, ArH), 8.18 (8H, d, ArH), 7.86 (4H, t, pyH), 7.52 (4H, d, pyH), 7.35 (4H, t, pyH), 8.17-8.13 (4H, t, pyH), 4.45 (8H, d, CH_2), -2.99 (2H, br, NH).

T(*N*-py-4-CH_2(H)NSO_2Ar)P (3) Treatment of **1** (0.1 g, 0.1 mmol) with 4-pyridylmethylamine (50 μL, 0.5 mmol) as described above afforded porphyrin **3** as a purple powder (0.11 g, 76% yield). ^{1}H NMR (ppm) in DMSO-d_6: 8.76 (12H, s, β-pyrrole and NH-sulfonamide), 8.60 (8H, d, pyH), 8.36 (8H, d, ArH), 8.19 (8H, d, ArH), 7.43 (8H, d, pyH), 4.42 (8H, d, CH_2), -3.01 (2H, br, NH).

2.2.4 Synthesis of T(N-py-n-CH_2(CH_3)NSO_2Ar)P Porphyrins (n = 2 or 4). Porphyrins **4** and **5** (below) were synthesized from secondary amines, prepared by a slight modification of a published procedure.[35] A solution of 1.0 g (9.34 mmol) of n-pyridylcarboxaldehyde (n = 2 or 4) in water (5 mL) was saturated with methylamine gas until the solution was cloudy. The resulting solution was stirred at RT for 2 h. Solvent removal under vacuum left a pale yellow oil of the Schiff base (~1.0 g); Schiff base formation was confirmed by a characteristic ^{1}H NMR imine signal (*N*-(4-pyridylmethylene)methylamine at 8.16 ppm, *N*-(2-pyridylmethylene)methylamine at 8.35 ppm). The yellow oil (9.34 mmol) was dissolved in 10 mL of methanol, 0.472 g of $NaBH_4$ was added, and the reaction mixture then left stirring at RT for 30 min. The solvent was evaporated under vacuum; the residue was dissolved in water (10 mL) and extracted into CH_2Cl_2 (3 × 10 mL). The organic phase was dried over anhydrous Na_2SO_4 and the solvent evaporated under vacuum to yield pale yellow oils that were characterized by ^{1}H NMR spectroscopy. These oils were used to synthesize porphyrins **4** and **5** as follows: a solution of **1** (0.2 g, 0.198 mmol) in CH_2Cl_2 (20 mL) was treated with 0.11 g (0.89 mmol) of *N*-methyl-*N*-(n-pyridylmethyl)amine (n = 2 or 4) in CH_2Cl_2 (5 mL). The reaction mixture was stirred at RT overnight, and the precipitate that formed was removed by filtration. The filtrate was washed with water (3 × 15 mL), dried

over anhydrous Na_2SO_4, and the solvent removed under vacuum. The residue was recrystallized from CH_2Cl_2/methanol.

T(*N*-py-2-$CH_2(CH_3)NSO_2$Ar)P (4). The general method described above, starting with 2-pyridylcarboxaldehyde (9.34 mmol, 1 g) and CH_3NH_2, yielded *N*-methyl-*N*-(2-pyridylmethyl)amine as a pale yellow oil (0.89 g, 76% yield). ^{1}H NMR (ppm) in $CDCl_3$: 8.53 (1H, d, ArH), 7.66 (1H, t, ArH), 7.28 (1H, d, ArH), 7.16 (1H, s, ArH), 3.83 (2H, s, CH_2), 2.50 (3H, s, CH_3).1.86 (1H, br, NH). GC-MS(m/z): M^+ = 123.2. Calcd for M^+ = 123.17. Treatment of **1** (0.2 g, 0.198 mmol) with *N*-methyl-*N*-(2-pyridylmethyl)amine (0.11g, 0.89 mmol) as described above afforded porphyrin **4** as a purple powder (0.16 g, 59% yield). ^{1}H NMR (ppm) in DMSO-d_6: 8.90 (8H, s, β-pyrrole), 8.59 (4H, d, pyH), 8.47 (8H, d, ArH), 8.25 (8H, d, ArH), 7.90 (4H, m, pyH), 7.56 (4H, d, pyH), 7.39 (4H, m, pyH), 4.60 (8H, s, CH_2), 2.99 (12H, CH_3), -2.94 (2H, br, NH). ESI-MS(m/z): $[M + H]^+$ = 1351.4077, $[M + 2H]^{+2}$ = 676.2076, $[M + 3H]^{+3}$ = 451.1437. Calcd for $[M + H]^+$ = 1351.3775, $[M + 2H]^{+2}$ = 676.1926, $[M + 3H]^{+3}$ = 451.1310.

T(*N*-py-4-$CH_2(CH_3)NSO_2$Ar)P (5). The general method described above, starting with 4-pyridylcarboxaldehyde (9.34 mmol, 1 g) and CH_3NH_2, yielded *N*-methyl-*N*-(4-pyridylmethyl)amine as a pale yellow oil (0.94 g, 83% yield). The ^{1}H NMR spectrum in $CDCl_3$ matches that reported in the literature.[36] ^{1}H NMR (ppm) in $CDCl_3$: 8.53 (2H, d, ArH), 7.24 (2H, d, ArH), 3.77 (2H, s, CH_2), 2.46 (3H, s, CH_3), 1.98 (1H, br, NH). GC-MS(m/z): M^+ = 123.0. Calcd for M^+ = 123.17. Treatment of **1** (0.2 g, 0.198 mmol) with *N*-methyl-*N*-(4-pyridylmethyl)amine (0.11g, 0.89 mmol) as described above afforded porphyrin **5** as a purple powder (0.15 g, 55% yield). ^{1}H NMR (ppm) in DMSO-d_6: 8.92 (8H, s, β-pyrrole), 8.65 (8H, d, pyH), 8.51 (8H, d, ArH), 8.30 (8H, d, ArH), 7.46 (8H, d, pyH), 4.54 (8H, s, CH_2), 2.93 (12H, s, CH_3), -2.92 (2H, br, NH). ESI-MS(m/z): $[M + H]^+$ = 1351.4107, $[M + 2H]^{+2}$ = 676.2096, [M +

$3H]^{+3}$ = 451.1451. Calcd for $[M + H]^{+}$ = 1351.3775, $[M + 2H]^{+2}$ = 676.1926, $[M + 3H]^{+3}$ = 451.1310.

Table 2.1. Characteristic Absorption and Emission Maxima of Methylcobaloxime–Porphyrin Adducts and of the Porphyrin Models in CH_2Cl_2

compound	absorption (λ_{max}/nm)		emission	
	Soret band	Q bands	λ_{em} (nm)[a]	
T(*N*-py-4-$CH_2(CH_3)NSO_2$Ar)P (**5**)	420	514, 548, 589, 644	650	714
Cu(II)**5**	416	540		
Zn(II)**5**	424	550, 596	603	649
$[CH_3Co(DH)_2]_4$Por**5** (**6**)	420	514, 548 589, 644	650	714
$[CH_3Co(DH)_2]_4$Cu(II)**5** (**7**)	416	540		
$[CH_3Co(DH)_2]_4$Zn(II)**5** (**8**)	424	550, 596	599	648
TpyP(4)	416	510, 544, 587, 642	649	712
Cu(II)TpyP(4)	418	538		
Zn(II)TpyP(4)	424	550, 596	602	652
$[CH_3Co(DH)_2]_4$TpyP(4) (**9**)	422	515, 550, 590, 646	652	714
$[CH_3Co(DH)_2]_4$Cu(II)TpyP(4) (**10**)	418	540		
$[CH_3Co(DH)_2]_4$Zn(II)TpyP(4) (**11**)	424	551, 594	603	646

[a] λ_{exc} = 420 nm.

Cu(II)T(*N*-py-4-$CH_2(CH_3)NSO_2$Ar)P (Cu(II)5). A solution of **5** (50 mg, 0.037 mmol) in CH_2Cl_2 (10 mL) was treated with copper(II) acetate (6.4 mg, 0.037 mmol) in methanol (5 mL). The solution was left stirring at RT for about 1 h. Completion of the reaction was indicated by

the collapse of the four Q bands of the free base to one Q band (Table 2.1). The reaction mixture was reduced in volume to about 1 mL, and acetone was added to precipitate Cu(II)**5** as a red powder. (48 mg, 92% yield). ^{1}H NMR (ppm) in $CDCl_3$: 8.74 (8H, br, pyH), 8.05 (8H, br ArH), 7.49 (8H, d, pyH), 4.46 (8H, br, CH_2), 2.92 (12H, br, CH_3).

Zn(II)T(*N*-py-4-$CH_2(CH_3)NSO_2$Ar)P (Zn(II)5). A solution of **5** (50 mg, 0.037 mmol) in CH_2Cl_2 (10 mL) was treated with zinc(II) acetate (40 mg, 0.19 mmol) in methanol (2 mL). The solution was left stirring at RT for 2 h, after which an aliquot of the reaction mixture was analyzed by using visible spectroscopy. The metal insertion was complete, as indicated by the collapse of the four Q bands to two Q bands (Table 2.1). After the CH_2Cl_2 was removed by rotary evaporation, the purple precipitate that formed was collected on a filter and washed with methanol to remove the excess of zinc acetate and air dried to afford Zn(II)**5** (30 mg, 58% yield). ^{1}H NMR (ppm) in DMSO-d_6: 8.85 (8H, s, β-pyrrole), 8.64 (8H, d, pyH), 8.46 (8H, d, ArH), 8.28 (8H, d, ArH), 7.46 (8H, d, pyH), 4.55 (8H, d, CH_2), 2.93 (12H, s, CH_3).

2.2.5 Synthesis of ([$CH_3Co(DH)_2$])4T(*N*-py-4-$CH_2(CH_3)NSO_2$Ar)P (6). $CH_3Co(DH)_2H_2O$ (95 mg, 0.30 mmol) was added to a solution of **5** (0.1 g, 0.074 mmol) in CH_2Cl_2 (20 mL) and stirred until a clear solution resulted (~5 min). The solution was filtered and treated with 5 mL of ethyl acetate. After partial evaporation of the solution, a brownish precipitate was collected on a filter, washed with diethyl ether, and vacuum dried to afford **6** (Chart 2.1) as a brown precipitate (0.17 g, 92% yield). ^{1}H NMR (ppm) in $CDCl_3$: 18.34 (8H, s, OH), 8.85 (8H, s, β-pyrrole), 8.67 (8H, d, pyH), 8.44 (8H, d, ArH), 8.26 (8H, d, ArH), 7.44 (8H, d, pyH), 4.54 (8H, d, CH_2), 3.00 (12H, CH_3), 2.15 (48H, s, CH_3), 0.82 (12H, d, Co-CH_3), -2.79 (2H, br, NH).

Chart 2.1

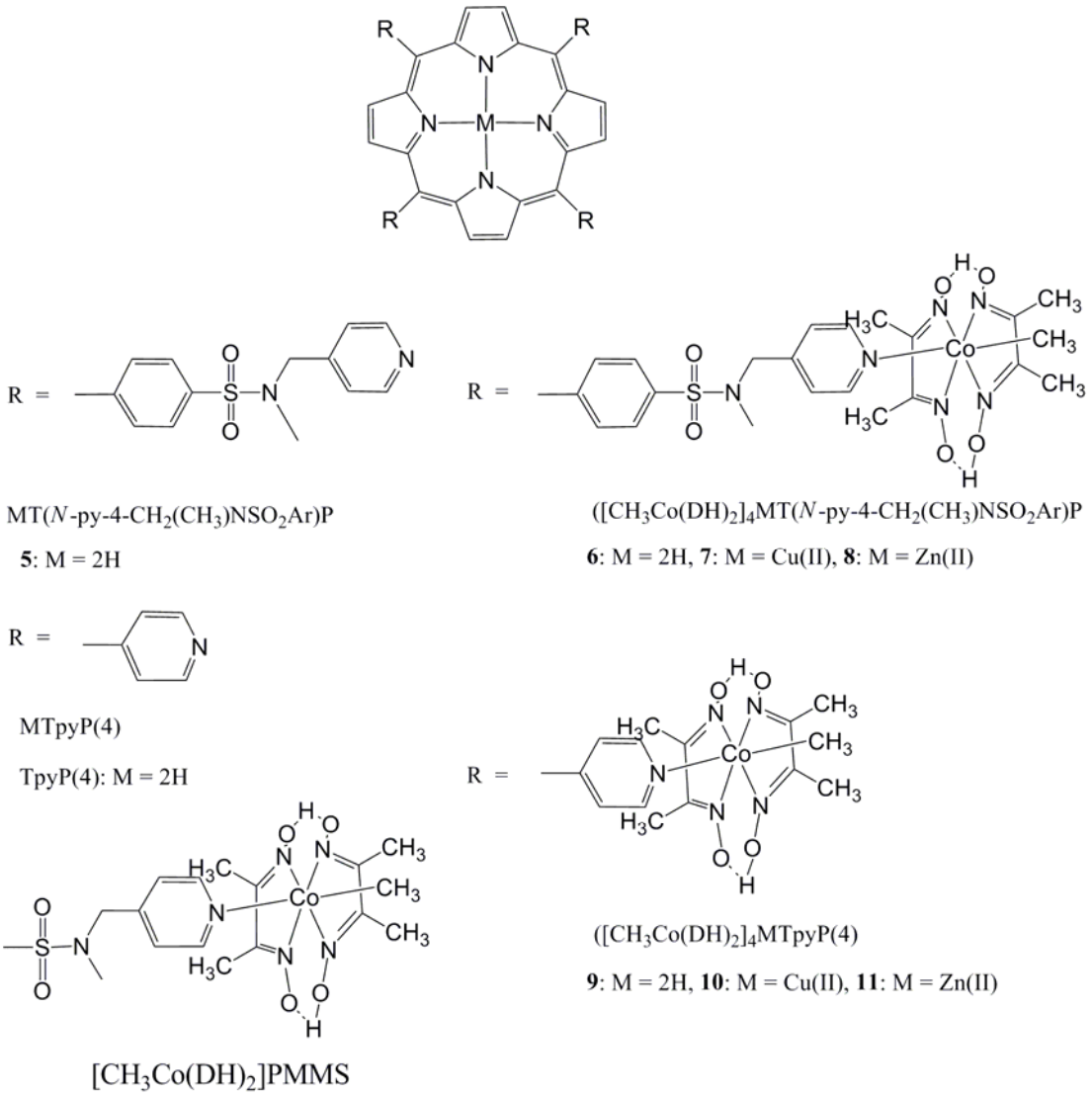

[$CH_3Co(DH)_2$]$_4$Cu(II)T(*N*-py-4-$CH_2(CH_3)NSO_2Ar$)P (7). The general method described above with $CH_3Co(DH)_2H_2O$ (45 mg, 0.14 mmol) and Cu(II)**5** (50 mg, 0.035 mmol) afforded **7** (Chart 2.1) as a red precipitate (65 mg, 69% yield). ^{1}H NMR (ppm) in $CDCl_3$: 18.30, (8H, s, OH), 8.62 (8H, br, pyH), 8.02 (8H, br ArH), 7.38 (8H, d, pyH), 4.44 (8H, d, CH_2), 2.90 (12H, CH_3), 2.14 (48H, s, CH_3), 0.81 (12H, d, Co-CH_3).

[$CH_3Co(DH)_2$]$_4$Zn(II)T(*N*-py-4-$CH_2(CH_3)NSO_2Ar$)P (8). The general method described above with $CH_3Co(DH)_2H_2O$ (45 mg, 0.14 mmol) and Zn(II)**5** (50 mg, 0.035 mmol) afforded **8**

(Chart 2.1) as a purple precipitate (50 mg, 53% yield). ^{1}H NMR (ppm) in $CDCl_3$: 18.18 (8H, s, OH), 8.94 (8H, s, β-pyrrole), 8.63 (8H, d, ArH), 8.44 (8H, d, ArH), 8.24 (8H, d, ArH), 7.41 (8H, d, pyH), 4.54 (8H, d, CH_2), 3.01 (12H, CH_3), 2.12 (48H, s, CH_3), 0.77 (12H, d, Co-CH_3).

[$CH_3Co(DH)_2$]$_4$TpyP(4) (9). $CH_3Co(DH)_2H_2O$ (0.21 g, 0.64 mmol) was added to a suspension of TpyP**(4)** (0.1 g, 0.16 mmol) in CH_2Cl_2 (10 mL). After stirring (~5 min), the suspension became a solution, which was then filtered and 5 mL of ethyl acetate was added. After partial evaporation of the solution, a reddish precipitate was collected on a filter, washed with diethyl ether, and vacuum dried to afford **9** (Chart 2.1, 0.28 g, 94% yield). ^{1}H NMR (ppm) in $CDCl_3$: 18.53 (8H, s, OH), 9.03 (8H, d, pyH), 8.75 (8H, s, β-pyrrole), 8.15 (8H, d, pyH), 2.33 (48H, s, CH_3), 1.03 (12H, s, Co-CH_3), -3.04 (2H, br, NH).

[$CH_3Co(DH)_2$]$_4$Cu(II)TpyP(4) (10). A solution of **9** (50 mg, 0.027 mmol) in CH_2Cl_2 (10 mL) was treated with a methanol solution (5 mL) of Cu(II) acetate (8.2 mg, 0.041 mmol). The solution was stirred at RT for 2 h, then filtered and left standing at RT overnight. The precipitate that formed was collected on a filter and vacuum dried, affording **10** (Chart 2.1) as a red precipitate (43 mg, 85%). ^{1}H NMR (ppm) in $CDCl_3$: 18.23 (8H, s, OH), 8.79 (8H, br, pyH), 2.26 (48H, s, CH_3), 0.96 (12H, s, Co-CH_3).

[$CH_3Co(DH)_2$]$_4$Zn(II)TpyP(4) (11). Treatment of a solution of **9** (50 mg, 0.027 mmol) with a methanol solution (5 mL) of Zn(II) acetate (8.9 mg, 0.041 mmol) as described for **10** above afforded **11** (Chart 2.1) as a purple precipitate (39 mg, 77% yield). ^{1}H NMR (ppm) in $CDCl_3$: 18.42(8H, s, OH), 8.97 (8H, d, pyH), 8.82 (8H, s, β-pyrrole), 8.13 (8H, d, pyH), 2.29 (48H, s, CH_3), 0.97 (12H, s, Co-CH_3).

***N*-Methyl-*N*-(4-pyridylmethyl)methanesulfonamide (PMMS).** A solution of 0.57 g (5 mmol) of CH_3SO_2Cl in CH_2Cl_2 (50 mL) was added dropwise over the course of ~0.5 h to a

solution of 1.12 g of *N*-methyl-*N*-(4-pyridylmethyl)amine (10 mmol) in of CH_2Cl_2 (50 mL). The reaction mixture was stirred at RT overnight. The reaction mixture was filtered and washed with water (3 × 50 mL). The CH_2Cl_2 was dried over anhydrous Na_2SO_4 and the solvent evaporated under vacuum to yield a pale yellow oil (0.76 g, 68% yield). ^{1}H NMR (ppm) in $CDCl_3$: 8.60 (1H, d, ArH), 7.29 (1H, d, ArH), 4.32 (2H, s, CH_2), 2.89 (3H, s, CH_3), 2.80 (3H, s, CH_3).

Synthesis of [$CH_3Co(DH)_2$]PMMS. $CH_3Co(DH)_2H_2O$ (100 mg, 0.31 mmol) was added to a solution of PMMS (62 mg, 0.31 mmol) in CH_2Cl_2 (20 mL) and stirred until a clear solution resulted (~5 min). The solution was filtered and treated with 5 mL of ethyl acetate. After partial evaporation of the solution, an orange precipitate was collected on a filter, washed with diethyl ether, and vacuum dried to afford [$CH_3Co(DH)_2$]PMMS as an orange precipitate (0.14 g, 90% yield). ^{1}H NMR (ppm) in $CDCl_3$: 18.29, (8H, s, OH), 8.59 (8H, d, pyH), 7.31 (8H, d, pyH), 4.32 (8H, d, CH_2), 2.91 (3H, CH_3), 2.84 (3H, s, CH_3), 2.13 (12H, s, CH_3), 0.83 (12H, d, Co-CH_3).

2.3 Results and Discussion

2.3.1 Crystal Structures of T(*N*-py-4-$CH_2(CH_3)NSO_2Ar$)P (5) and Cu(II)T(*N*-py-4-$CH_2(CH_3)NSO_2Ar$)P (Cu(II)5). X-ray quality crystals of porphyrin **5** and its copper complex were obtained by slow diffusion of methanol into a dichloromethane solution of the respective compound. Crystal data and structural refinement details are summarized in Table 2.2. ORTEP drawings of **5** and Cu(II)**5** are shown in Figure 2.1; **5** and Cu(II)**5** lie on an inversion center. The 24-atom core of **5** is planar. The two distances (2.018 and 2.091 Å) from the centroid (C_t) of the pyrrole nitrogens to $N_{pyrrole}$ and $NH_{pyrrole}$, respectively, in **5** are comparable to the respective values of 2.026 and 2.099 Å for TPP.[37] The phenyl rings of **5** are almost perpendicular to the plane of the porphyrin, with dihedral angles of 84.9(2)° and 73.3(2)°. Two of the pyridyl rings of **5** are almost in the plane of the porphyrin, with a dihedral angle of 4.6(3)° and the other two

pyridyl rings are slightly out of the plane of the porphyrin with a dihedral angle of 36.1(3)°.The coordination about the copper atom of Cu(II)**5** is square planar (Figure 2.1). The two Cu-N distances are 2.001(5) and 2.002(6) Å, which are comparable to that for Cu(II)TPP (1.995(2) Å).[38] The phenyl rings of Cu(II)**5** are almost perpendicular to the plane of the porphyrin with dihedral angles of 83.5(3)° and 84.0(3)°. Two of the pyridyl rings of Cu(II)**5** are almost in the plane of the porphyrin with a dihedral angle of 3.7(4)°, while the dihedral angle for the other two pyridyl rings is 31.2(5)°.

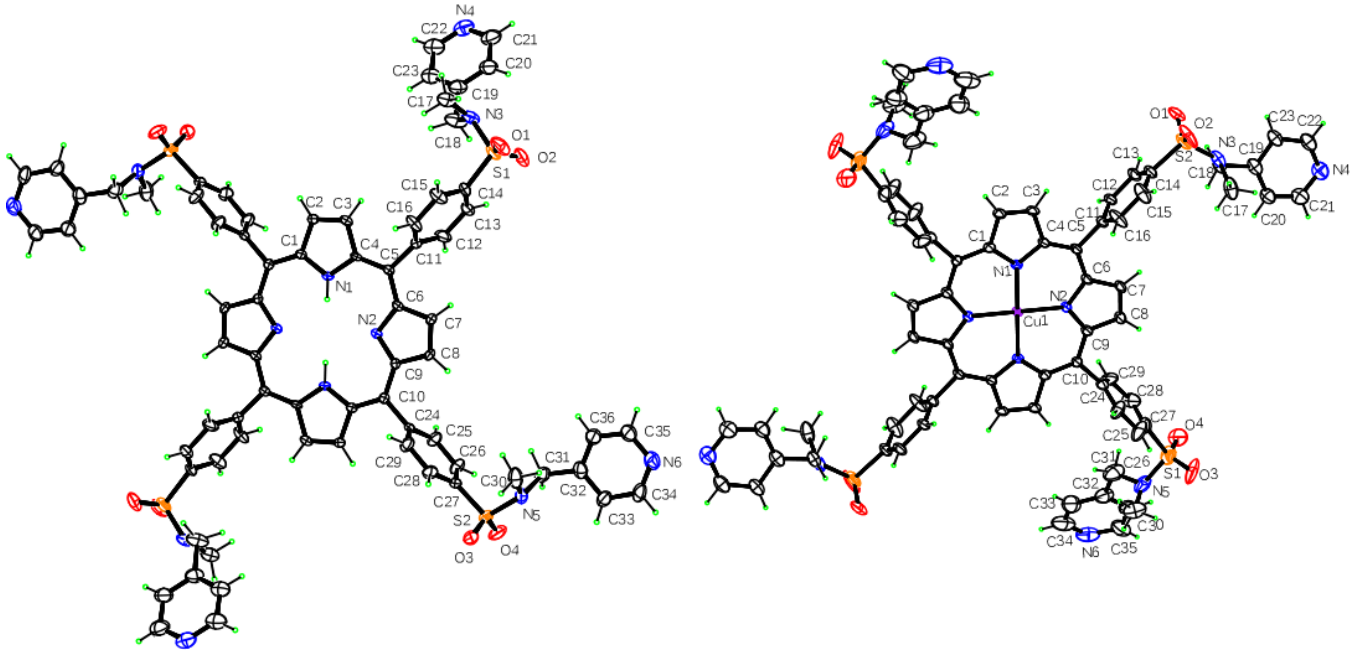

Figure 2.1. ORTEP drawings of T(*N*-py-4-$CH_2(CH_3)NSO_2Ar$)P (**5**) and Cu(II)**5** with 50% ellipsoids.

The overlay of the porphyrin core of Cu(II)TPP and Cu(II)**5** gave an RMS value of 0.0136 Å. This good fit implies that having substituents at the periphery of the porphyrin does not affect the planarity of the core. Preliminary X-ray results also confirmed the synthesis of **4** (Figure A1).

Table 2.2. Crystal Data and Structure Refinement for T(*N*-py-4-$CH_2(CH_3)NSO_2Ar$)P (**5**), Cu(II)**5**, and $[CH_3Co(DH)_2]_4$TpyP(4) (**9**)

	5	Cu(II)**5**	**9**
formula	$C_{72}H_{62}N_{12}O_8S_4$•$4CH_3OH$	$C_{72}H_{60}CuN_{12}O_8S_4$•$4CH_3OH$	$C_{76}H_{94}Co_4N_{24}O_{16}$•$12CHCl_3$
fw	1479.74	1541.27	3267.89
color	red	orange	orange
cryst syst	monoclinic	monoclinic	triclinic
space group	$P2_1/c$	$P2_1/c$	$P\bar{1}$
		unit cell dimensions	
a (Å)	13.879(5)	13.530(4)	13.356(2)
b (Å)	12.776(4)	12.967(4)	13.893(2)
c (Å)	21.131(8)	21.020(7)	19.974(4)
α (deg)	90	90	72.830(9)
β (deg)	99.184(15),	97.227(14)	73.905(7)
γ (deg)	90	90	75.270(9)
V (Å^3)	3699(2)	3659(2)	3341.7(10)
Z	2	2	1
T (K)	90	90	90
ρ_{calc} (mg m^{-3})	1.329	1.399	1.624
abs coeff (mm^{-1})	0.20	0.48	1.27
2 $_{max}$ (deg)	46.0	46.0	46.0
R indices[a]	0.090	0.096	0.051
wR2 = [I > 2σ(I)][b]	0.247	0.280	0.136
data/params	5081 / 471	5066 / 477	9107 / 795

[a] $R = (\sum||F_o| - |F_c||)/\sum|F_o|$. [b] $wR2 = [\sum[w(F_o^2 - F_c^2)^2]/\sum[w(F_o^2)^2]]^{1/2}$.

2.3.2 Crystal Structure of $[CH_3Co(DH)_2]_4$TpyP(4) (9). Crystals of porphyrin **9** were obtained by layering hexane in a chloroform solution of **9**. The crystals permitted the first X-ray

structural determination of the TpyP(4) molecule with four $CH_3Co(DH)_2$ units, each bound to a pyridyl nitrogen (Table 2.2, Figure 2.2). In the crystal, the porphyrin has an inversion center. The planes of the pyridyl groups make dihedral angles of 78.1(2)° and 64.1(2)° with the plane of the porphyrin. The equatorial plane of the pseudo-octahedral methylcobaloxime units is nearly perpendicular to the plane of the porphyrin, with dihedral angles of 89.6(1)° and 81.4(1)°. The $Co–N_{eq}$ bond distances range from 1.882(4)–1.892(5) Å (Table A1), which is close to the range reported for $CH_3Co(DH)_2py$ (1.877(2)–1.905(5) Å).[39] The Co–N(axial) distances of **9** are 2.055(4) and 2.079(4) Å (Table A1), in good agreement with the value reported for $CH_3Co(DH)_2py$ (2.068(3) Å).[39] The $Co–CH_3$ bond lengths of **9** (1.999(5) and 2.002(5) Å) are very close to the value reported for $CH_3Co(DH)_2py$ (1.998(5) Å).[39]

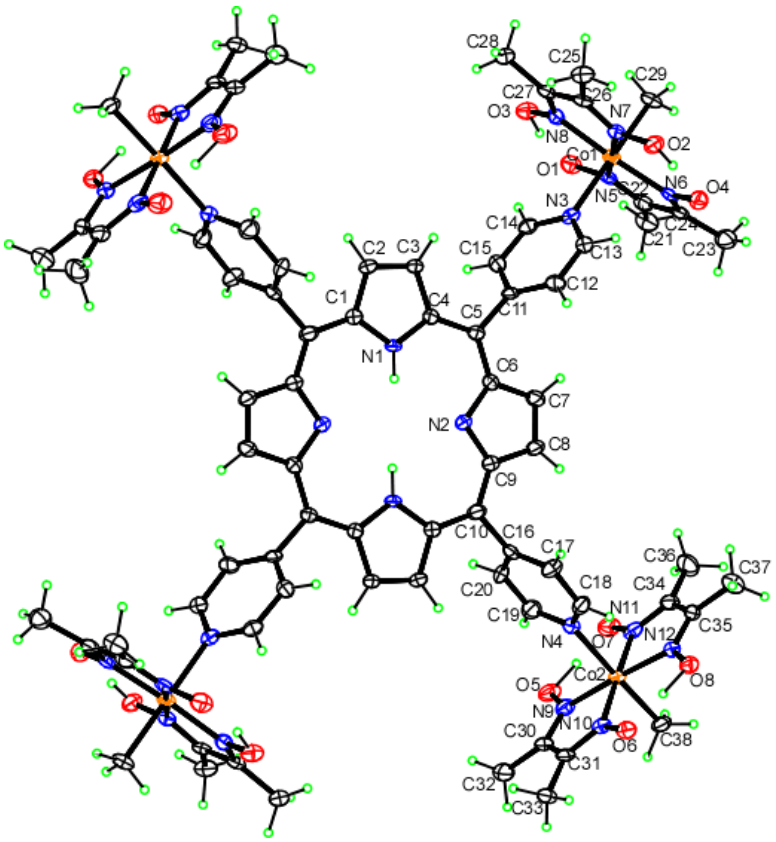

Figure 2.2. ORTEP drawing of $[CH_3Co(DH)_2]_4TpyP(4)$ **(9)** with 50% ellipsoids.

2.3.3 Synthesis of the Porphyrins, Porphyrin-Cobaloxime Adducts, and Their Metal Complexes. Treatment of **1** ($TClSO_2PP$, Scheme 2.1) with primary amines such as 2- or 4-pyridylmethylamine generated porphyrins containing secondary sulfonamide groups (**2** and **3**). Metallation of such porphyrins resulted in an insoluble material, possibly because the metal coordinates to the sulfonamide group through both the sulfonyl oxygen and the deprotonated sulfonamide nitrogen.[40-42] The potential for secondary sulfonamides to coordinate to metals led us to investigate the synthesis of porphyrins containing only tertiary sulfonamide groups. The presence of an N-Me group in place of the dissociable NH group allowed us to prepare porphyrins (**4** and **5**) that are very soluble in organic solvents; these were characterized by mass spectrometry and ^{1}H NMR spectroscopy. Cu(II) and Zn(II) complexes of porphyrin **5** were also prepared.

Methylcobaloxime complexes ($CH_3Co(DH)_2L$) are generally synthesized from $CH_3Co(DH)_2H_2O$ by substitution of water in the presence of an excess of L in methanol solution[30] or in a CH_2Cl_2 suspension.[29] Addition in a 4:1 ratio of $CH_3Co(DH)_2H_2O$ to L (L = T(*N*-py-4-$CH_2(CH_3)NSO_2Ar$)P and TpyP(4)) in dichloromethane produced $[CH_3Co(DH)_2]_4L$ adducts. The related metalloporphyrin adducts can be prepared by reaction of the metalloporphyrin with $CH_3Co(DH)_2H_2O$ or by insertion of the metal ion into the isolated $[CH_3Co(DH)_2]_4L$ adducts. Both methods were efficient and afforded the corresponding zinc and copper complexes in good yield. Because TpyP(4) is not very soluble in chloroform or dichloromethane and the adduct is soluble, metal insertion into the $[CH_3Co(DH)_2]_4$TpyP(4) adduct (**9**) is the preferred method. Insertion of Zn(II) into ($[CH_3Co(DH)_2]_4$T(*N*-py-4-$CH_2(CH_3)NSO_2Ar$)P) (**6**) and **9** led to two Q bands instead of four and a 2 nm red shift of the

Soret band, while insertion of Cu(II) led to one Q band and a 4 nm blue shift of the Soret band; these changes are similar to those found upon metallation of other porphyrins by these metals.[43]

2.3.4 Solution Studies. Porphyrins **2** to **5** were characterized by ^{1}H NMR spectroscopy in $CDCl_3$ and DMSO-d_6 (Tables 2.2 and A2). As a result of shielding by the porphyrin ring current, the β-pyrrole proton signals are downfield (~ 8.8 ppm) and the NH signals appear upfield (~-2.9 to -3.0 ppm).

The ^{1}H NMR spectra of T(*N*-py-4-$CH_2(CH_3)NSO_2Ar$)P (**5**) and $[CH_3Co(DH)_2]_4$T(*N*-py-4-$CH_2(CH_3)NSO_2Ar$)P (**6**) are compared in Figure 2.3. The ^{1}H NMR shifts of the β-pyrrole, H2,6, and H3,5 signals of **6** in $CDCl_3$ are slightly upfield (by (0.02-0.03 ppm) to those of **5** (Table 2.3).

Table 2.3. Selected ^{1}H NMR Shifts (ppm) of Porphyrin and $[CH_3Co(DH)_2]_4$–Porphyrin Signals[a]

compound	O–H···O	Hβ[b]	H3,5 (py)	H2,6 (py)	dmgH	CH_3–Co	-NH
T(*N*-py-4-$CH_2(CH_3)NSO_2Ar$)P (**5**)		8.87	7.42	8.70			-2.79
$[CH_3Co(DH)_2]_4$Por**5** (**6**)	18.34	8.85	7.44	8.67	2.15	0.82	-2.79
$[CH_3Co(DH)_2]_4$Cu(II)**5** (**7**)	18.30		7.38	8.62	2.14	0.80	
$[CH_3Co(DH)_2]_4$Zn(II)**5** (**8**)	18.18	8.94	7.41	8.63	2.12	0.77	
TpyP(4)		8.87	8.16	9.06			-2.92
$[CH_3Co(DH)_2]_4$TpyP(4) (**9**)	18.53	8.75	8.15	9.03	2.33	1.03	-3.04
$[CH_3Co(DH)_2]_4$Cu(II)TpyP(4) (**10**)	18.23			8.79	2.26	0.96	
$[CH_3Co(DH)_2]_4$Zn(II)TpyP(4) (**11**)	18.42	8.82	8.13	8.97	2.29	0.98	
py			7.29	8.61			
$CH_3Co(DH)_2$py	18.32		7.33	8.61	2.13	0.83	

[a] 5 mM in $CDCl_3$. [b] β-pyrrole.

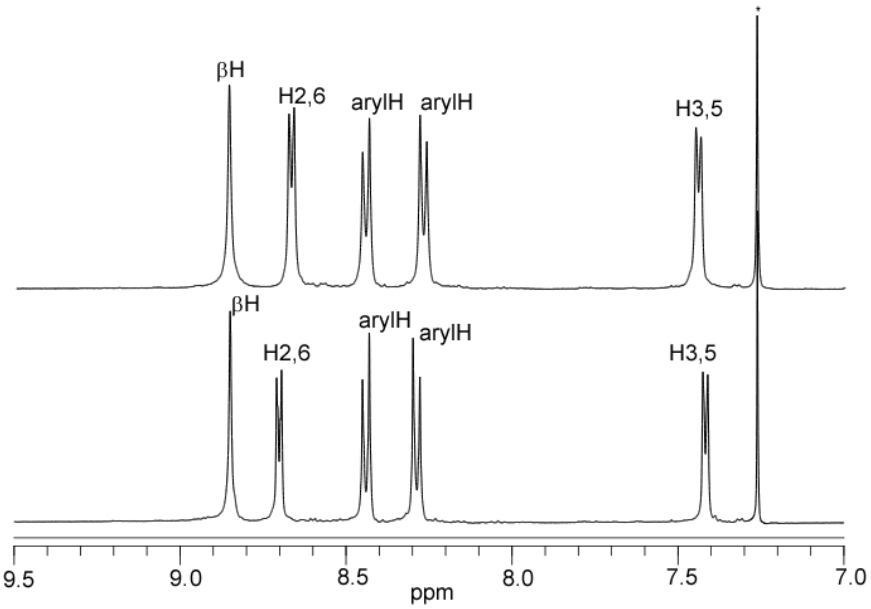

Figure 2.3. Comparison of the ^{1}H NMR spectra of T(*N*-py-4-$CH_2(CH_3)NSO_2Ar$)P (**5)** (bottom) and $[CH_3Co(DH)_2]_4$T(*N*-py-4-$CH_2(CH_3)NSO_2Ar$)P (**6**) (top) in $CDCl_3$.

Normally coordination of a metal would cause downfield shifts of such signals. The upfield shift of H2,6 arises from the anisotropic shielding by Co,[27,28] which more than counteracts the deshielding typically resulting from the inductive effect of a metal. The sharp singlet for the equatorial DH methyls and the broad signal of the oxime O–H–O bridge of the $CH_3Co(DH)_2$ moieties for **6** have shifts of 2.15 ppm and 18.34 ppm, respectively. These shifts are similar to the 2.13 ppm and 18.32 ppm values observed for $CH_3Co(DH)_2$py,[27] as expected. For the axial methyls, a singlet was observed at 0.82 ppm for **6**. Insertion of Cu(II) and Zn(II) into porphyrin **6** resulted in a general upfield shift for the axial methyl signal (Table 2.4). The H3,5 and H2,6 ^{1}H NMR signals of TpyP(4) and $[CH_3Co(DH)_2]_4$TpyP(4) (**9**) **(**shown in $CDCl_3$ in Figure 2.4) are respectively ~0.7 and 0.35 downfield from those of **5** and **6**. Such downfield shifts for TpyP(4) and **9**, as well as the greater downfield shift of H3,5 vs. H2,6, could be explained either by an inductive or by an anisotropic effect of the porphyrin core.

Table 2.4. ^{1}H NMR Chemical Shifts (ppm) for $CH_3Co(DH)_2L$ Complexes in $CDCl_3$

L	pK_a	CH_3–Co	DH methyls
4-CNpy[a]	1.9	0.90	2.13
py[a]	5.9	0.83	2.13
3,5-lut[a]	6.2	0.77	2.13
4-Me_2Npy[a]	9.7	0.72	2.13

[a] Values from reference 27.

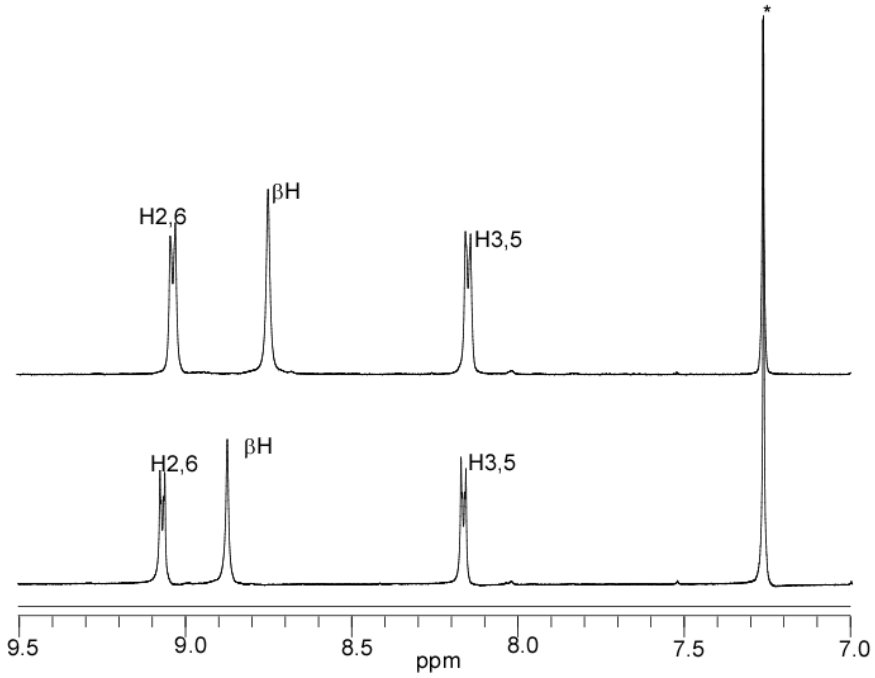

Figure 2.4. Comparison of the ^{1}H NMR spectra of TpyP(4) (bottom) and $[CH_3Co(DH)_2]_4$TpyP(4) **(9)** (Top) in $CDCl_3$.

When compared to the shifts of the parent TpyP(4), several signals of **9** (Table 2.3) are moderately or slightly upfield (the β-pyrrole proton signal by 0.12 ppm, the pyridyl H2,6 signal by 0.03 ppm, and the H3,5 signal by 0.01 ppm). The upfield shifts of the pyridyl signals arise from the anisotropy of Co.[27,28] In a previous study,[5] coordination of four *cis*,*cis*,*cis*-$RuCl_2$(dimethylsulfoxide)$_2$CO units to the pyridyl groups of TpyP(4) was found to cause downfield shifts of the β-pyrrole (0.07 ppm), H2,6 (0.45 ppm) and H3,5 (0.06 ppm) signals.[5]

This result is in contrast to the upfield-shifted porphyrin signals we have observed with $[CH_3Co(DH)_2]_4$TpyP(4) (**9**). The NH signal of **9** (-3.04 ppm) is shifted upfield by 0.12 ppm, as compared to that of TpyP(4) (-2.92 ppm) (Table 2.3).

Sharp singlets observed at 2.33 ppm and at 1.03 ppm for the equatorial and axial methyl protons of $[CH_3Co(DH)_2]_4$TpyP(4) (**9**) are shifted downfield by 0.20 ppm when compared to the corresponding signals for $CH_3Co(DH)_2$py.[27] The axial methyl signal of $CH_3Co(DH)_2L$ shifts upfield with increasing L basicity;[28] thus, the downfield shift of the axial methyl observed with L = TpyP(4) indicates either that TpyP(4) peripheral pyridyls are much less basic than pyridine or that the signal is shifted by porphyrin anisotropy. Unlike the axial methyl signal, the equatorial methyl signal of $CH_3Co(DH)_2L$ compounds is insensitive to L basicity and tends not to vary much from compound to compound unless L is anisotropic.[25] The usual value is ~2.15 ppm; the much further downfield signal for $[CH_3Co(DH)_2]_4$TpyP(4) (**9**) indicates that anisotropy, not basicity, is responsible. Insertion of a metal into **9** to form the Cu(II) (**10**) and Zn(II) (**11**) derivatives resulted in a general upfield shift of the signals of the $CH_3Co(DH)_2$ and pyridyl moieties (Table 2.3). Previous studies have shown that insertion of Zn(II) into TpyP(4) increases the basicity of the pyridyl nitrogen.[44-46] This increased basicity is confirmed by the more upfield shift of the axial methyl signal of **11** compared to **9**. Nevertheless, the downfield shift position of the axial methyl signal of **9**, **10**, and **11** indicates either low pyridyl basicity or a porphyrin anisotropic effect extending out to this long distance. More basic L form more stable $CH_3Co(DH)_2L$ compounds, and thus we assessed relative binding ability.

A $CDCl_3$ solution initially 10 mM in 3,5-lut and 5 mM in $[CH_3Co(DH)_2]_4$TpyP(4) (**9**) gave a ^{1}H NMR spectrum (Figure 2.5) with signals for $CH_3Co(DH)_2$(3,5-lut), indicating some

displacement of the $CH_3Co(DH)_2$ moiety from **9**. In addition to the NH signal for **9** at -3.04 ppm, NH signals for new species were observed at -3.01, -2.97, -2.94 and -2.92 ppm (Figure 2.5).

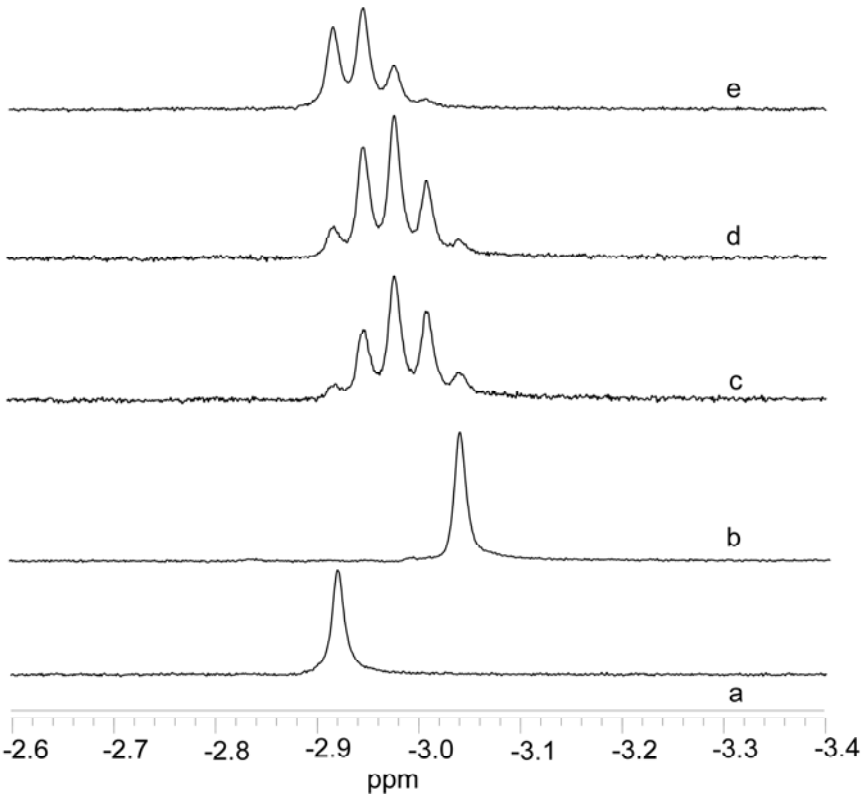

Figure 2.5. Inner NH signals of the ^{1}H NMR spectra of TpyP(4) (a); $[CH_3Co(DH)_2]_4$TpyP(4) (b); $[CH_3Co(DH)_2]_4$TpyP(4) : 3,5-lut = 1:2 (c); $[CH_3Co(DH)_2]_4$TpyP(4) : 3,5-lut = 1:4 (d); $[CH_3Co(DH)_2]_4$TpyP(4) : 3,5-lut = 1:8 (e) in $CDCl_3$.

In a similar study performed with 40 mM 3,5-lut, the relative size of the NH signals changed. This change and the relative shift trend (the NH signal shifted downfield as the number of $CH_3Co(DH)_2$ moieties displaced increased) allowed assignment of the NH signal to the different adducts. The distribution of the TpyP(4) adducts differing in the number of $CH_3Co(DH)_2$ moieties is summarized in Table 2.5. The shifts for the NH and other signals are given in Table A3.

Table 2.5. Distribution[a] (%) of Various $[CH_3Co(DH)_2]$ Adducts after Addition of Pyridines to a $CDCl_3$ Solution of $[CH_3Co(DH)_2]_4$TpyP(4) (**9**)

9 : pyridine ratio	number of coordinated $[CH_3Co(DH)_2]$ units				
	0	1	2	3	4
9 : 4-CNPy (1:2)	0	6	21	42	31
9 : 4-CNPy (1:8)	6	22	37	27	8
9 : 3,5-lut (1:2)	4	16	35	32	13
9 : 3,5-lut (1:8)	49	36	12	3	0

[a] Distribution determined from NH signals.

Addition of a 40 mM solution of 3,5-lut led to considerable displacement of the porphyrin ligand, with 49% of the porphyrin completely lacking a $CH_3Co(DH)_2$ moiety (Table 2.5). Two DH methyl peaks were observed. One peak of the signal is for $CH_3Co(DH)_2$(3,5-lut) (2.13 ppm), a value similar to that observed previously.[27,28] The second peak (2.33 ppm) is broad and arises from overlapping signals of $[CH_3Co(DH)_2]_n$TpyP(4) adducts (n = 1, 2, 3 and 4). In solutions of **9** containing 3,5-lut, two signals were observed for the axial methyls. The signal at 0.77 ppm matches that of $CH_3Co(DH)_2$(3,5-lut), while the other signal (1.03 ppm) is broad and matches that of the $[CH_3Co(DH)_2]_n$TpyP(4) adducts (where n = 1, 2, 3 and 4). By integration of the axial methyl signals, the percentage of $CH_3Co(DH)_2$ moiety bound in TpyP(4) adducts and the percentage in $CH_3Co(DH)_2$(3,5-lut) could be determined (Table 2.6). In the experiment with 10 mM 3,5-lut (**9**:3,5-lut = 1:2), 51% of the $CH_3Co(DH)_2$ was bound to 3,5-lut, while 49% was still bound to the porphyrin (Table 2.6); however, in the presence of 40 mM 3,5-lut (**9**:3,5-lut = 1:8), these values were 79% and 21%, respectively (Table 2.6).

A procedure similar to that described above was used to assign the different adducts of 4-CNpy and **9**. When 4-CNpy (40 mM) was added to a solution of **9** (5 mM) several TpyP(4) adducts

were observed. Only 6% of the porphyrin lacked a $CH_3Co(DH)_2$ moiety (Table 2.5). In the **9**:4-CNpy = 1:2 experiment, only 28% of the 4-CNpy was bound to $CH_3Co(DH)_2$ (Table 2.6).

The pyridyl group is not directly linked to the porphyrin in $[CH_3Co(DH)_2]$Por**5** (**6**); consequently, the NH signal of **6** is not shifted relative to that of **5**. Also, the aromatic signals overlap. Hence, the distribution of the various $[CH_3Co(DH)_2]_n$Por**5** adducts after addition of pyridine ligands could not be assessed. By using the axial methyl signal the percent distribution of the $CH_3Co(DH)_2$ moiety between the porphyrin adduct and the $CH_3Co(DH)_2$(pyridine ligand) complex could be determined, and the results are summarized in Table 2.6. The distribution of the pyridine ligands between $CH_3Co(DH)_2$(pyridine ligand) and the $[CH_3Co(DH)_2]_n$Por adducts is very similar for Por = **5** or TpyP(4). Thus, these two porphyrins have similar basicity.

The ^{1}H NMR chemical shifts for the axial methyl group of $CH_3Co(DH)_2$(pyridine ligand)[27] are summarized in Table 2.4. As mentioned, the axial methyl signal shifts upfield with greater 4-substituted pyridine ligand basicity. The shifts when L = **5**, TpyP(4), 4-CNpy, 3,5-lut and 4-Me_2Npy are given in Figure 2.6 and Table 2.4. When L = **5**, the axial methyl shift at 0.82 ppm matches that of $CH_3Co(DH)_2$py. These results suggest that the basicity of the pyridyl groups of **5** is close to that of pyridine. The similarity of the adduct distribution in Table 2.6 thus confirms that TpyP(4) has comparable basicity to **5**. Without doubt the porphyrin ring anisotropy and not low porphyrin basicity is responsible for the downfield position of the signals in $[CH_3Co(DH)_2]_n$TpyP(4) (**9**).

2.3.5 Visible Absorption Spectra. Soret and Q bands for **5** and TpyP(4) and their respective methylcobaloxime adducts (**6** and **9**) were measured in CH_2Cl_2 (Table 2.1). The Q and Soret bands correspond respectively to the first and second excited singlet states of the porphyrins.[47-49] The change in the number of Q bands to two or one observed upon insertion of metals (zinc and

copper) into the porphyrin results from the increased molecular symmetry (C_{4v} and D_{4h}, respectively), and is typical of patterns observed for metalloporphyrins with the respective metals.[47] The lower symmetry of the Zn porphyrin is attributable to one axial ligand, and X-ray results (although of crystals with less than desirable diffraction intensity) confirmed that an axial water is coordinated in $[CH_3Co(DH)_2]_4$Zn(II)TpyP(4) (Figure A2).

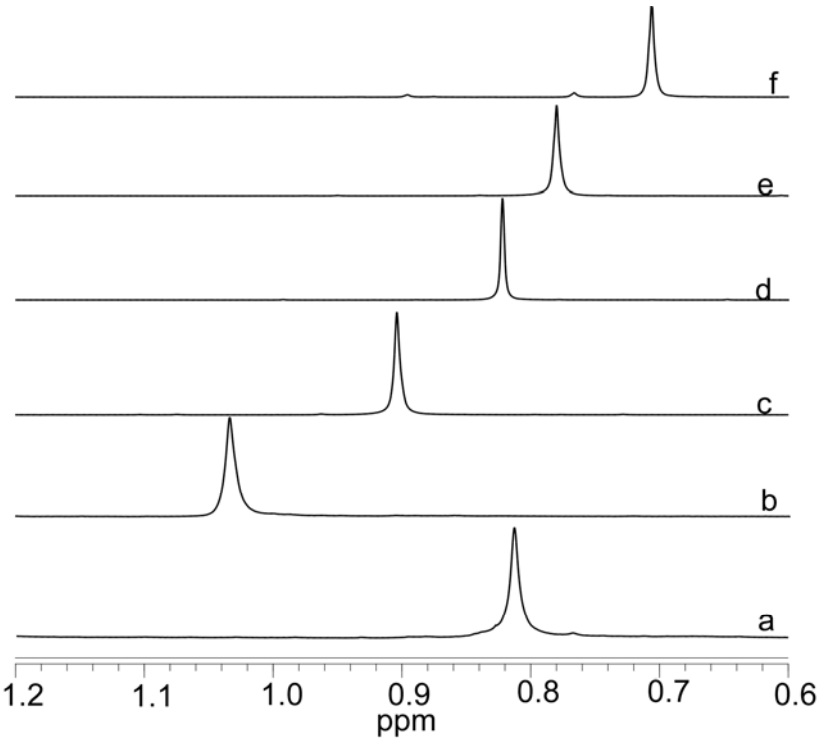

Figure 2.6. ^{1}H NMR spectra (Co-CH_3) region of $CH_3Co(DH)_2$L with **L** = T(*N*-py-4-$CH_2(CH_3)NSO_2Ar$)P (a); TpyP(4) (b); 4-CNpy (c); py (d); 3,5-lut (e) and 4-Me_2Npy (f) in $CDCl_3$.

Compared to the bands of the parent porphyrin (TpyP(4)**)**, the Soret and Q bands of **9** show 6 nm and ~4 nm red shifts, respectively (Table 2.1). The spectrum of **6** retains the characteristic Soret and Q bands of the parent porphyrin **5**, with no shifts (Table 2.1). The red shift of the Soret band observed with the $[CH_3Co(DH)_2]_4$TpyP(4) adduct (**9**) and its Cu and Zn complexes (Table 2.1) suggests that there is a reduction of the electron density as a result of cobalt coordination to the pyridyl groups. In contrast, the lack of a shift for the $[CH_3Co(DH)_2]_4$T(*N*-py-4-

$CH_2(CH_3)NSO_2Ar)P$ adduct (**6**) is expected because the pyridyl groups are not directly linked to the porphyrin core. The blue shift (4 nm) of the Soret band and of one Q band (540 nm) observed for copper complexes **7** and **10** (Table 2.1) are consistent with observations reported for other copper porphyrins.[50,51] In copper porphyrins the delocalized π bonding decreases the average electron density, which increases the energy needed for electronic transitions, and thus a blue shift of the Soret band is observed.[52] Complexes **8** and of **11** show a red shift (< 10 nm) of the Soret band and two Q bands (550, 596 nm), as observed previously with other zinc porphyrins.[51] For zinc porphyrins the delocalized π bonding increases the average electron density of the porphyrin, thus lowering the energy for electronic transition and leading to a red shift of the Soret band.[52]

2.3.6 Emission Spectra. The emission of T(*N*-py-4-$CH_2(CH_3)NSO_2Ar)P$ (**5)** and of TpyP(4) in dichloromethane is compared to that of the $CH_3Co(DH)_2$adducts (Table 2.1). The fluorescence intensity of **5** is comparable to that of TpyP(4) upon selective excitation at the Soret band (420 nm) (Figure 2.7). The adducts ($[CH_3Co(DH)_2]_4$T(*N*-py-4-$CH_2(CH_3)NSO_2Ar)P$ (**6**) and $[CH_3Co(DH)_2]_4$TpyP(4) (**9**)) show typical porphyrin-based intense fluorescence spectra (Figure 2.7) characterized by two bands at ~650 and ~714 nm (λ_{exc} = 420 or 515 nm).[43] A small red shift (~3 nm) of the emission bands of **9** was observed with respect to the parent porphyrin (TpyP(4)). Insertion of zinc (**8** and **11)** changed the general shape of the emission spectra and led to a blue shift (50 nm, λ_{exc} = 420 nm) of the emission bands (~600 and 650 nm) (Table 2.1) compared to those of the metal-free porphyrins (**6** and **9**). The intensity of spectra obtained on optically matched (λ_{exc} = 420 nm) solutions showed that the emission of **6** is slightly lower (25-35%) for both bands (650 and 714 nm) than that of **5**. The fluorescence intensity of **9 (**λ_{exc} = 420 nm) is generally much lower (90%, for both bands 652, 714 nm) than that of TpyP(4) (Figure 2.7).

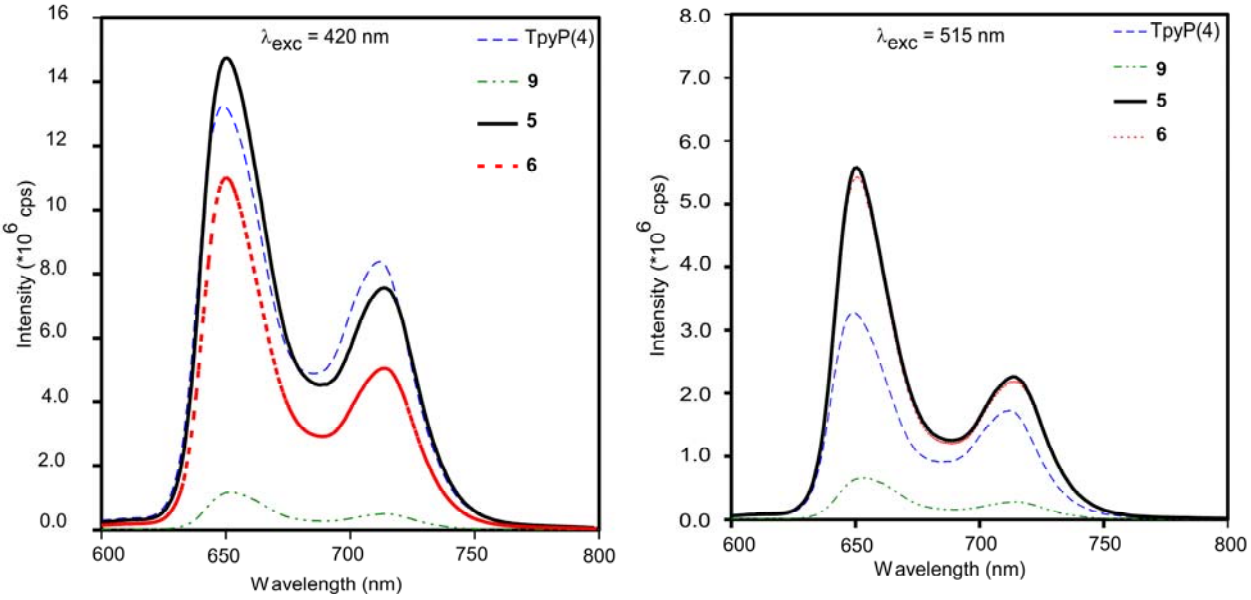

Figure 2.7. Emission spectra of TpyP(4), T(*N*-py-4-$CH_2(CH_3)NSO_2Ar$)P (**5**), $[CH_3Co(DH)_2]_4$T(*N*-py-4-$CH_2(CH_3)NSO_2Ar$)P (**6**) and $[CH_3Co(DH)_2]_4$TpyP(4) (**9**) in CH_2Cl_2.

The much greater effect of adduct formation on **9** than on **6** is attributable to the direct and indirect attachment of the pyridyl group to TpyP(4) and T(*N*-py-4-$CH_2(CH_3)NSO_2Ar$)P, respectively, resulting from a much shorter distance of the methylcobaloxime moieties to the porphyrin in **9** than in **6**. The quenching of the emission of **9** is attributed to the cobalt heavy atom effect. Heavy atoms enhance spin-orbit coupling of a formally spin-forbidden deactivation process of the singlet state of the porphyrin.[11]

The titrations of 4-CNpy, 3,5-lut and 4-Me_2Npy into 5 μM solutions of adducts **6** and **9** in dichloromethane were monitored by fluorescence spectroscopy; results for 4-CNpy and 4-Me_2Npy are shown for **6** and **9** in Figures A3, A4, 2.8. When a solution of **9** was titrated with these pyridine ligands, fluorescence intensity restoration was observed. Upon addition of 4-Me_2Npy (80 μM) (Figure 2.8), the restored fluorescence intensity at 650 nm was 12 times that of

the original solution of **9**; the values obtained with 3,5-lut and 4-CNpy (80 μM) (Figure A4) were 11 and 5 times the original fluorescence, respectively.

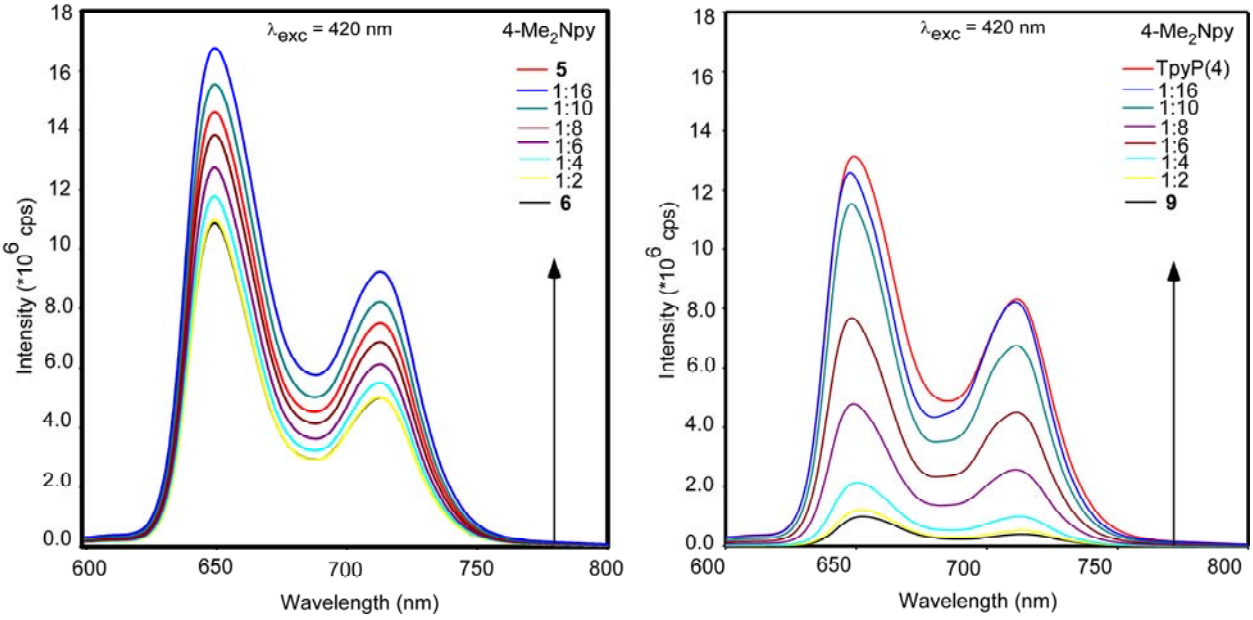

Figure 2.8. Emission spectra of $[CH_3Co(DH)_2]_4T(N\text{-py-4-}CH_2(CH_3)NSO_2Ar)P$ (**6**) (left) and $[CH_3Co(DH)_2]_4$TpyP(4) (**9**) (right) (5.0 μM) in CH_2Cl_2 with increasing amounts (**6/9** : pyridine ratio) of 4-Me_2Npy.

The titration of TpyP(4) with 4-Me_2Npy resulted in an intensity ~1.2 times that of the original value of TpyP(4)**.** These results support the conclusion that restoration of fluorescence intensity upon addition of the different pyridine ligands is caused by the displacement of the $CH_3Co(DH)_2$ moieties, releasing the TpyP(4).

The fluorescence intensity of **6** increased by 1.5 times upon the addition of 4-CNpy (Figure A3), 3,5-lut, or 4-Me_2Npy (Figure 2.8) (80 μM). The titration of **5** with 4-Me_2Npy led to a ~1.2 times increase of the original fluorescence intensity. This higher intensity is similar to that observed upon titrating **6** with the different pyridine derivatives; as a result, we conclude that the increase in fluorescence intensity of solutions of **6** arises from a combined effect of the pyridine

ligands, which displace the $CH_3Co(DH)_2$ moieties and which then interact weakly with the displaced porphyrin.

2.4 Conclusions

The synthetic scheme developed in this work is useful and versatile for preparing metalloporphyrins having sulfonamides. However, it is necessary to employ a tertiary sulfonamide because otherwise intractable species are formed. New pyridyl-containing porphyrins with a sulfonamide linker have been synthesized and characterized by ^{1}H NMR spectroscopy and mass spectrometry. Adducts with four methylcobaloxime units bound to pyridylporphyrins (TpyP(4) and T(*N*-py-4-$CH_2(CH_3)NSO_2Ar$)P) have been synthesized and their photophysical properties investigated and compared to those of the parent porphyrin. Upon excitation of the porphyrin core, the typical porphyrin fluorescence is partially quenched for the ($[CH_3Co(DH)_2]_4$T(*N*-py-4-$CH_2(CH_3)NSO_2Ar$)P adduct, whereas the fluorescence of the $[CH_3Co(DH)_2]_4$TpyP(4) adduct is strongly quenched. These observations suggest that the porphyrin core of T(*N*-py-4-$CH_2(CH_3)NSO_2Ar$)P is insulated from the pyridyl group, and consequently coordination of the methylcobaloxime moiety to the pyridyl group does not modulate greatly the photophysical properties of the porphyrin. A comparison of the ^{1}H NMR signal of the axial methyl of the T(*N*-py-4-$CH_2(CH_3)NSO_2Ar$)P and the TpyP(4) methylcobaloxime adducts with those of the other methylcobaloxime compounds with different pyridine ligands allows us to estimate the pK_a of the pyridyl groups of T(*N*-py-4-$CH_2(CH_3)NSO_2Ar$)P) and of TpyP(4) to be close to that of pyridine.

In summary, the additional linker insulates the porphyrin core from any effects of coordination of metals to the peripheral groups. Likewise, the linker extends the distance of the peripherally coordinated metals from the porphyrin core and this core does not affect the properties of the

peripheral metal. In contrast the core and the peripheral metals have mutual effects upon each other when adducts are prepared with the prototypical porphyrin, TpyP(4) .

2.5 References

1. Kadish, K. M.; Smith, K. M.; Guilard, R., Eds. *The Porphyrin Handbook*; Academic Press: New York, 2000; Vol. 1-10.

2. Kumar, R. K.; Goldberg, I. *Chem. Commun. (Cambridge, U. K.)* **1998**, 1435-1436.

3. Liu, J.; Huang, J.-W.; Fu, B.; Zhao, P.; Yu, H.-C.; Ji, L.-N. *Spectrochim. Acta, Part A* **2007**, *67*, 391-394.

4. Alessio, E.; Iengo, E.; Marzilli, L. G. *Supramol. Chem.* **2002**, *14*, 103-120.

5. Alessio, E.; Macchi, M.; Heath, S. L.; Marzilli, L. G. *Inorg. Chem.* **1997**, *36*, 5614-5623.

6. Gianferrara, T.; Serli, B.; Zangrando, E.; Iengo, E.; Alessio, E. *New J. Chem.* **2005**, *29*, 895-903.

7. Anson, F. C.; Shi, C. N.; Steiger, B. *Acc. Chem. Res.* **1997**, *30*, 437-444.

8. Castriciano, M.; Romeo, A.; Romeo, R.; Scolaro, L. M. *Eur. J. Inorg. Chem.* **2002**, 531-534.

9. Araki, K.; Silva, C. A.; Toma, H. E.; Catalani, L. H.; Medeiros, M. H. G.; Di Mascio, P. *J. Inorg. Biochem.* **2000**, *78*, 269-273.

10. Kon, H.; Tsuge, K.; Imamura, T.; Sasaki, Y.; Ishizaka, S.; Kitamura, N. *Inorg. Chem.* **2006**, *45*, 6875-6883.

11. Ghirotti, M.; Chiorboli, C.; Indelli, M. T.; Scandola, F.; Casanova, M.; Iengo, E.; Alessio, E. *Inorg. Chim. Acta* **2007**, *360*, 1121-1130.

12. Carvlin, M. J.; Fiel, R. J. *Nucleic Acids Res.* **1983**, *11*, 6121-6139.

13. Fiel, R. J. *J. Biomol. Struct. Dyn.* **1989**, *6*, 1259-1275.

14. Fiel, R. J.; Howard, J. C.; Mark, E. H.; Dattagupta, N. *Nucleic Acids Res.* **1979**, *6*, 3093-3118.

15. Fiel, R. J.; Munson, B. R. *Nucleic Acids Res.* **1980**, *8*, 2835-2842.

16. Marzilli, L. G. *New J. Chem.* **1990**, *14*, 409-420.

17. Banville, D. L.; Marzilli, L. G.; Strickland, J. A.; Wilson, W. D. *Biopolymers* **1986**, *25*, 1837-1858.

18. Pasternack, R. F.; Gibbs, E. J.; Villafranca, J. J. *Biochemistry* **1983**, *22*, 5409-5417.

19. Strickland, J. A.; Banville, D. L.; Wilson, W. D.; Marzilli, L. G. *Inorg. Chem.* **1987**, *26*, 3398-3406.

20. Ward, B.; Skorobogaty, A.; Dabrowiak, J. C. *Biochemistry* **1986**, *25*, 7827-7833.

21. Gibbs, E. J.; Tinoco, I.; Maestre, M. F.; Ellinas, P. A.; Pasternack, R. F. *Biochem. Biophys. Res. Commun.* **1988**, *157*, 350-358.

22. Schmitt, F.; Govindaswamy, P.; ss-Fink, G.; Ang, W.; Dyson, P. J.; Juillerat-Jeanneret, L.; Therrien, B. *J. Med. Chem.* **2008**, *51*, 1811-1816.

23. Atwood, L. J.; Davies, D. E. J.; Mac Nicol, D. D.; Vogtle, F.; Reinhoudt, N. D., Eds. *Comprehensive Supramolecular Chemistry*; Pergamon Press: Oxford, 1996.

24. Balzani, V.; Scandola, F. *Supramolecular Photochemistry,* Horwood, Chichester, UK, 1991.

25. Bresciani-Pahor, N.; Forcolin, M.; Marzilli, L. G.; Randaccio, L.; Summers, M. F.; Toscano, P. J. *Coord. Chem. Rev.* **1985**, *63*, 1-125.

26. Marzilli, L. G.; Summers, M. F.; Bresciani-Pahor, N.; Zangrando, E.; Charland, J. P.; Randaccio, L. *J. Am. Chem. Soc.* **1985**, *107*, 6880-6888.

27. Parker, W. O.; Zangrando, E.; Bresciani-Pahor, N.; Randaccio, L.; Marzilli, L. G. *Inorg. Chem.* **1986**, *25*, 3489-3497.

28. Siega, P.; Randaccio, L.; Marzilli, P. A.; Marzilli, L. G. *Inorg. Chem.* **2006**, *45*, 3359-3368.

29. Summers, M. F.; Toscano, P. J.; Bresciani-Pahor, N.; Nardin, G.; Randaccio, L.; Marzilli, L. G. *J. Am. Chem. Soc.* **1983**, *105*, 6259-6263.

30. Toscano, P. J.; Chiang, C. C.; Kistenmacher, T. J.; Marzilli, L. G. *Inorg. Chem.* **1981**, *20*, 1513-1519.

31. Toscano, P. J.; Marzilli, L. G. *Prog. Inorg. Chem.* **1984**, *31*, 105-204.

32. Gonsalves, A. M. R.; Johnstone, R. A. W.; Pereira, M. M.; de SantAna, A. M. P.; Serra, A. C.; Sobral, A. J. F. N.; Stocks, P. A. *Heterocycles* **1996**, *43*, 829-838.

33. Otwinowski, Z.; Minor, W. *Macromolecular Crystallography, part A*; New York Academic Press: New York, 1997; Vol. 276.

34. Sheldrick, G. M. *SHELX-97, Program for Crystal Structure Solution and Refinement*; University of Göttingen: Göttingen, Germany, 1997.

35. Tanaka, K.; Shiraishi, R. *Green Chem.* **2000**, *2*, 272-273.

36. Varney, M. D.; Palmer, C. L.; Deal, J. G.; Webber, S.; Welsh, K. M.; Bartlett, C. A.; Morse, C. A.; Smith, W. W.; Janson, C. A. *J. Med. Chem.* **1995**, *38*, 1892-1903.

37. Fleischer, E. B.; Webb, L. E.; Miller, C. K. *J. Am. Chem. Soc.* **1964**, *86*, 2342-2347.

38. He, H. S. *Acta Crystallogr., Sect. E: Struct. Rep. Online* **2007**, *63*, M976-M977.

39. Bigotto, A.; Zangrando, E.; Randaccio, L. *J. Chem. Soc., Dalton Trans.* **1976**, 96-104.

40. Saladini, M.; Iacopino, D.; Menabue, L. *J. Inorg. Biochem.* **2000**, *78*, 355-361.

41. Christoforou, A. M.; Fronczek, F. R.; Marzilli, P. A.; Marzilli, L. G. *Inorg. Chem.* **2007**, *46*, 6942-6949.

42. Christoforou, A. M.; Marzilli, P. A.; Fronczek, F. R.; Marzilli, L. G. *Inorg. Chem.* **2007**, *46*, 11173-11182.

43. Akins, D. L.; Zhu, H. R.; Guo, C. *J. Phys. Chem.* **1996**, *100*, 5420-5425.

44. Drain, C. M.; Batteas, J. D.; Flynn, G. W.; Milic, T.; Chi, N.; Yablon, D. G.; Sommers, H. *Proc. Natl. Acad. Sci. U. S. A.* **2002**, *99*, 6498-6502.

45. Drain, C. M.; Nifiatis, F.; Vasenko, A.; Batteas, J., D *Angew. Chem., Int. Ed. Engl.* **1998**, *37*, 2344-2347.

46. Drain, C. M.; Nifiatis, F.; Vasenko, A.; Batteas, J., D *Angew. Chem.* **1998**, *110*, 2478-2481.

47. Spellane, P. J.; Gouterman, M.; Antipas, A.; Kim, S.; Liu, Y. C. *Inorg. Chem.* **1980**, *19*, 386-391.

48. Dolphin, D., Ed. *The Porphyrin*; Academic Press: New York, 1978; Vol. 3.

49. Even, U.; Magen, J.; Jortner, J. *J. Chem. Phys.*, *77*, 4374-4383.

50. Butje, K.; Nakamoto, K. *Inorg. Chim. Acta* **1990**, *167*, 97-108.

51. Sun, X.; Chen, G.; Zhang, J. *Dyes Pigm.* **2008**, *76*, 499-501.

52. Zheng, W.; Shan, N.; Yu, L.; Wang, X. *Dyes Pigm.* **2008**, *77*, 153-157.

CHAPTER 3. NEW PORPHYRINS BEARING POSITIVELY CHARGED PERIPHERAL GROUPS LINKED BY A SULFONAMIDE GROUP TO *MESO*-TETRAPHENYLPORPHYRIN: INTERACTIONS WITH CALF THYMUS DNA

3.1 Introduction

The ability of cationic porphyrins to associate with DNA and RNA has prompted studies of medical and biological applications of porphyrins.[1-3] Pioneering work by Fiel and co-workers demonstrating that TMpyP (*meso*-tetra(*N*-Mepy)porphyrin tetracation, *N*-Mepy = *N*-methylpyridinium group, Figure 3.1) has a strong affinity for DNA[3] stimulated many subsequent studies.[4-8] TMpyP(4) (having the 4-Mepy group with the pyridinium moiety linked through the 4- position) and its derivatives exhibit activity against human immunodeficiency virus, the virus responsible for AIDS.[9] TMpyP(4) has also been used in various therapeutic applications, e.g., as photo-sensitizers in photodynamic therapy,[2,3,10-13] inhibitors of telomerase DNA cleavage,[14-16] and anticancer agents.[17,18]

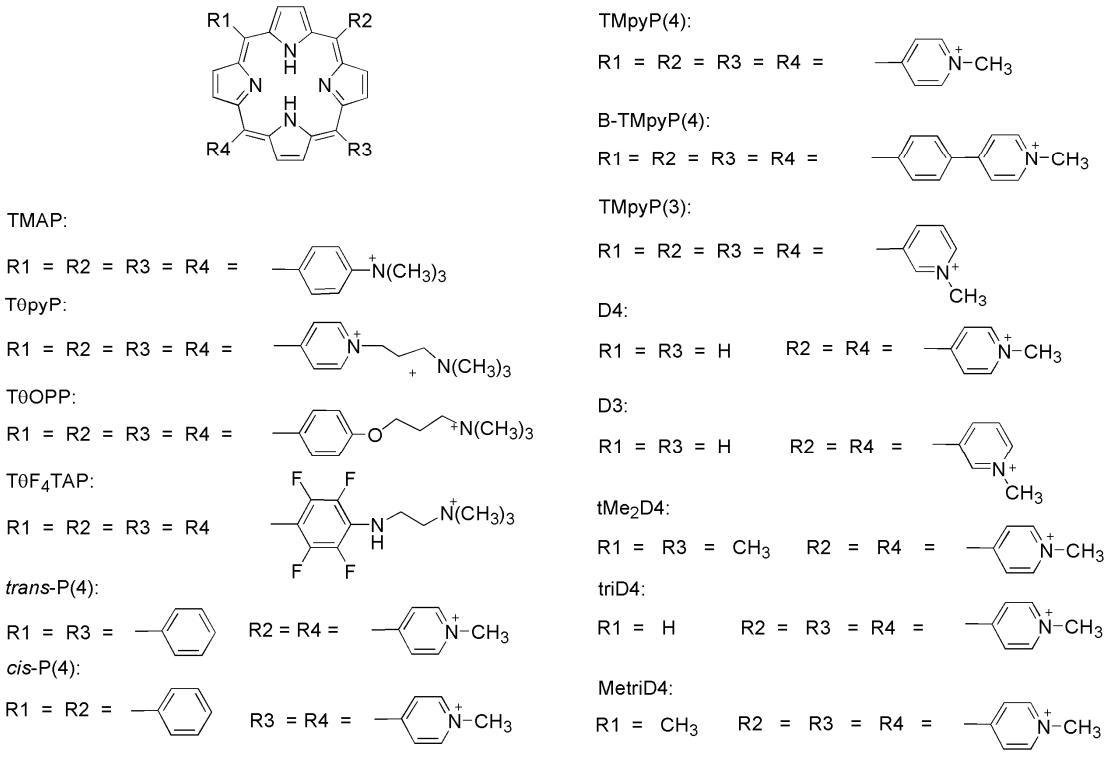

Figure 3.1. Structures of porphyrins mentioned in this study.

Several types of noncovalent interactions of cationic porphyrins with DNA have been found, including intercalative binding, simple outside binding, and outside binding with self-stacking (Figure 3.2).[5-7,19,20] The preferred binding mode and the distribution between modes are both highly dependent on the type of DNA and on the peripheral substituent groups on the porphyrin.[21,22] In order to achieve intercalation, the porphyrin core must have a limited thickness.[4,5,23] The metal-free porphyrin, TMpyP(4) (Figure 3.1), and its metal complexes constitute the porphyrin series most extensively studied for DNA binding; MTMpyP(4) with no axial ligands, such as Cu(II)TMpyP(4), generally intercalate into GC-rich DNA regions.[1,19,24] NMR spectral changes accompanying the binding of TMpyP(4) to oligodeoxyribonucleotides showed preferential insertion at the 5′-CG-3′ site.[25] An X-ray structure shows Cu(II)TMpyP(4) bound to $[d(CGATCG)]_2$ by intercalation between the C and the G of 5′-TCG-3′ accompanied by extrusion of the C of 5′-CGA-3′.[26] Metalloporphyrins possessing axial ligands, such as MTMpyP(4), with M = Fe(III), Co(III), and Zn(II), do not intercalate.[1,27] In general, these species bind preferentially to AT-rich DNA regions.[27] Water-soluble cobalt porphyrins containing a covalent axial methyl ligand synthesized in our laboratory were also found to be outside-binders with AT selectivity.[28]

In contrast to this clear understanding of how axial ligands influence intercalative vs. outside binding, the influences of the properties of the peripheral group and of the electronic properties of porphyrins with a thin core were not so well understood. Porphyrins that self-stack in aqueous solution (e.g., TMAP and *cis*- and *trans*-P4, Figure 3.1) are preferentially outside binders,[4,5,20,29,30] and porphyrins that have a low propensity to self-stack (such as TMpyP(4), Figure 3.1) are intercalators.[3,31]

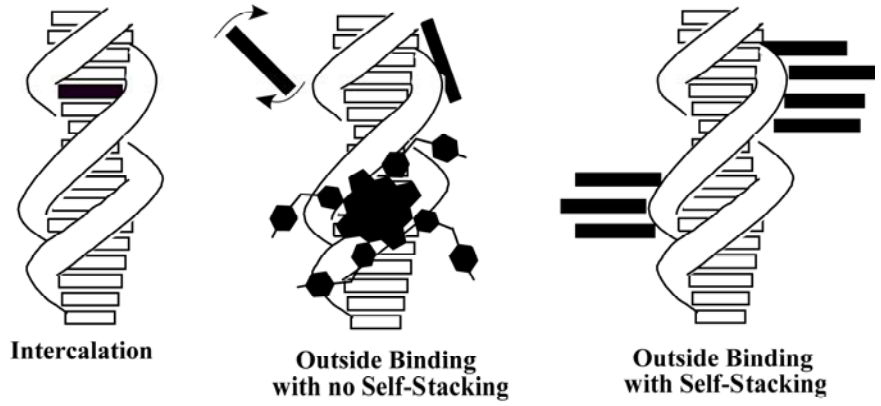

Figure 3.2. Binding modes of cationic porphyrins (represented by black bars in most cases). For outside binding without stacking, two subtypes are shown in the middle drawing. The upper left of this drawing illustrates how a tumbling porphyrin (shown side-on) such as TMpyP(2) might bind while its porphyrin core is maintained relatively far from the DNA. The other more commonly found subtype, shown both face-on (bottom) and side-on (upper right), allows the porphyrin core to approach the DNA more closely.

Thus, the electron-richness of the core could possibly stabilize the self-stacked, outside-bound porphyrin-DNA adduct, disfavoring intercalation.[32] To probe the influence of porphyrin properties on the DNA binding modes, we previously investigated the tentacle porphyrins depicted and defined in Figure 3.1. These studies revealed that only porphyrins possessing *N*-alkylated pyridinium groups, such as TθpyP, intercalate into GC-rich regions of DNA.[31] In contrast, TθF$_4$TAP and TθOPP, which are similar in size and shape to TθpyP but with no *N*-alkylated pyridinium groups, self-stacked along the DNA backbone and did not intercalate into DNA.[31-34] The studies with tentacle porphyrins thus indicated that, while the influence of porphyrin electron richness on the binding mode of relatively thin porphyrins was not important, pyridinium groups appear to be necessary for intercalation. Furthermore, bulk and thickness of the *N*-alkyl groups attached to the pyridinium groups but projecting away from the porphyrin core do not appear to prevent intercalation.

Taking a different tack, McMillin et al. have been synthesizing less sterically demanding porphyrins having less bulk at the periphery; these investigators have found that relatively small porphyrins such as D4 and D3 (Figure 3.1) intercalate into B-form DNA, regardless of the base composition.[35,36] In another study from the McMillin laboratory, the newly synthesized tMe_2D4 (Figure 3.1) was found to intercalate into DNA, in contrast to reports on *trans*-P(4), which binds externally, forming long-range stacked structures.[29,30,37] In a recent study of the binding modes of two tricationic porphyrins having different steric size, McMillin et al. found that triD4 (Figure 3.1) intercalates into $[poly(dA\text{-}dT)]_2$ ((poly dA-dT)-(poly dA-dT)), whereas the larger MetriD4 (Figure 3.1) binds externally, indicating that the presence of a fourth substituent destabilizes the intercalated form.[38] In summary, the size of porphyrins with *N*-alkylpyridinium groups influences the extent of intercalation in GC and AT regions.

In typical porphyrin intercalators, the *N*-alkylpyridinium group is attached to the porphyrin core, creating a common structural unit. This direct attachment allows the positive charges to delocalize onto the porphyrin ring[39] and also restricts the distances between the pyridinium groups. We now take an approach different from that of McMillin et al. and also from that we used previously. In particular, we expand the size of the pyridinium-containing porphyrins by placing a linking group between the porphyrin core and the pyridinium group. The larger but flexible porphyrins used here can assume conformations such that the separations between the charge-bearing nitrogens of the *N*-Mepy groups encompass the distances [~11 Å (*cis*) and ~16 Å (*trans*)] between these nitrogens in known intercalators. Specifically, we describe here the synthesis of new porphyrins ($[T(R^2R^1NSO_2Ar)P]X_{4/8}$) and metalloporphyrins ($[MT(R^2R^1NSO_2Ar)P]X_{4/8}$) bearing positively charged, peripheral *N*-Mepy or quaternary ammonium groups. These groups are linked to the 4-position of the phenylene group of the

porphyrin by secondary (-SO_2NHR) or tertiary (-SO_2NR_2) sulfonamide groups (Figure 3.3).[40] These porphyrins were designed for us to determine whether the new porphyrins containing *N*-Mepy groups would be intercalators and whether the new porphyrins lacking *N*-Mepy groups would allow us to gain some insight into factors that might influence outside binding interactions. The latter type of new porphyrins also serves as appropriate controls for comparison to the new porphyrins containing *N*-Mepy groups. We investigated the calf thymus (CT) DNA binding interactions of selected porphyrins by visible CD and other spectroscopic methods. We also assessed DNA binding of several new metalloporphyrins ([MT($R^2R^1NSO_2Ar$)P]$X_{4/8}$) by viscometric methods.

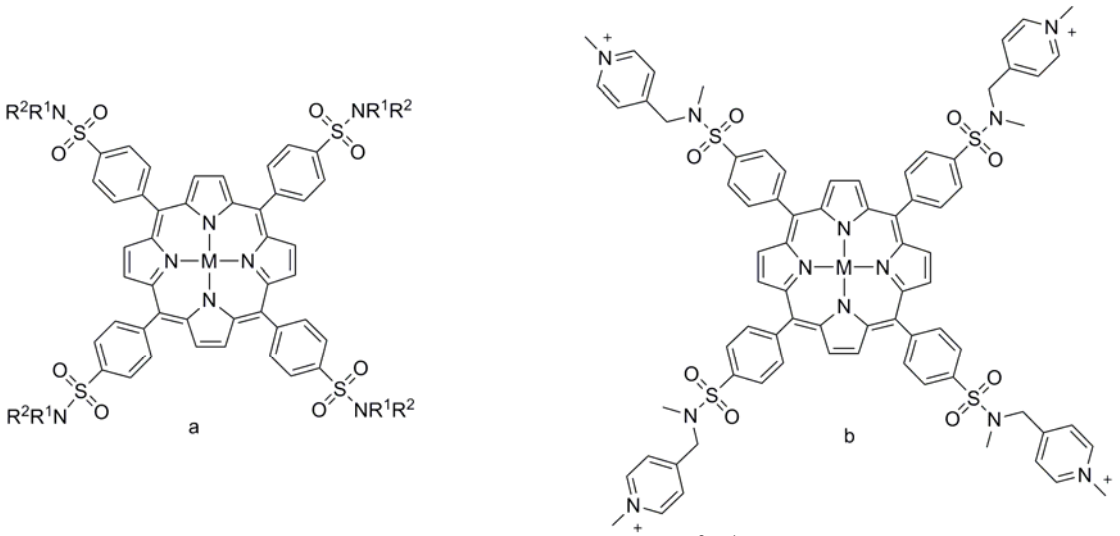

Figure 3.3. Structures of new porphyrins: (a) [MT($R^2R^1NSO_2Ar$)P]$X_{4/8}$ (in **1** to **3**, M = 2H and R^1 = H and R^2 = *N*-Mepy-n-CH_2, with n = 2, 3 or 4, respectively; in **4**, M = 2H and R^1 = H and R^2 = $Me_3NCH_2CH_2$; **5** differs from **1** in that R^1 = CH_3; in **7** and Cu(II)**7**, R^1 = R^2 = $Et_3NCH_2CH_2$ and M = 2H and Cu(II), respectively; and (b) [MT(*N*-Mepy-4-$CH_2(CH_3)NSO_2Ar$)P]Cl_4 (in **6**, M = 2H; in Cu(II)**6**, M = Cu(II); and in Zn(II)**6**, M = Zn(II)).

3.2 Experimental Section

3.2.1 Materials and Methods. All compounds and reagents used in the synthetic chemistry were purchased from Aldrich. The chloride salts of Cu(II)TMpyP(4) and Cu(II)TMAP were obtained from MidCentury. The syntheses of the non-alkylated porphyrin precursors are

described elsewhere.[40] The mean length of the DNA was ~5000 bp, established by gel electrophoresis on 1% agarose gel.[41] All CT DNA solutions were stored at -20 °C and were allowed to warm to RT before sample preparation. Stock solutions of CT DNA (GE Amersham) were prepared in 10 and 100 mM NaCl at pH 7.0. The CT DNA concentration in base pairs was determined by UV spectroscopy by using $\varepsilon_{260} = 1.32 \times 10^4$ $M^{-1}cm^{-1}$.[42] The porphyrin concentration was 7.5 μM in titration studies employing visible absorption, fluorescence, and CD spectroscopies.

All ^1H NMR spectra were recorded on either a 300 MHz or 400 MHz Bruker NMR spectrometer. Peak positions are relative to TMS or solvent residual peak, with TMS as reference. Visible absorption experiments were performed with a Cary 3 UV-visible spectrophotometer. CD spectra and titrations were recorded at 25 °C with a Jasco 710 spectrophotometer. Fluorescence studies were performed on a Fluorolog-3 spectrofluorimeter (Horiba Jobin Yvon) at 25 °C. Excitation wavelengths were 412 nm in the absence of DNA and 422 nm in the presence of DNA. Mass spectra for samples dissolved in methanol were obtained at the Mass Spectrometry Facility at LSU on a Hitachi MS-8000 3DQ LC-ion trap ESI mass spectrometer.

Solutions for visible spectroscopy were prepared by diluting a 25 μL aliquot of 1.5 mM porphyrin stock solution in 5.0 mL of a 10 or 100 mM NaCl solution. An aliquot of CT DNA was then added to such dilute porphyrin solutions to obtain the desired value of *R* ([porphyrin]/[DNA base pairs]). The pH of the solution was measured and readjusted to 7.0 with 0.01 M NaOH or 0.01 M HCl before recording spectra.

3.2.2 Viscosity Studies. Viscosity titrations were performed by using a Cannon-Ubbelohde semimicrodilution capillary viscometer in a circulating water bath maintained at 30.5 °C. Buffer

(1.0 mL of 100 mM NaCl at pH 7.0) was added to the viscometer, and the flow time was measured. Solution viscosity was determined by adding a small aliquot of CT DNA stock solution to a vial containing the buffer (~1 mL) to make the final concentration 75 μM in base pairs, and the pH was adjusted to 7.0. The flow time of the DNA solution was then obtained. An aliquot of the porphyrin stock solution (75 μM dissolved in CT DNA 75 μM) was then added to the viscometer in increments of 25 μL to give the desired value of *R*, while keeping the DNA concentration constant. Flow time measurements, obtained with a timer accurate to ±0.01 s, were recorded until three consecutive readings differed by less than ±0.1 s. The solution reduced viscosity (SRV) was presented as η/η_0 versus *R*, where $\eta/\eta_0 = t_c - t_0/t_D - t_0$ and t_0 is the flow time of the buffer, t_D is the flow time of the DNA in buffer, and t_c is the flow time of the DNA solution containing porphyrin.[43]

3.2.3 Competitive Binding Experiments. Solutions of Cu(II)TMpyP(4) (75 μM) and Cu(II)**6** (75 μM, Figure 3.3), both dissolved in 75 μM CT DNA, were prepared separately. Equal volumes of the two solutions were mixed and allowed to equilibrate for 1 h at room temperature. Aliquots of this 1:1 mixture were used as described above for viscosity measurements at different *R* values (where the porphyrin concentration equals the sum of the concentrations of the two Cu(II) porphyrins).

3.2.4 Sodium Dodecyl Sulfate (SDS) Studies. SDS solutions were prepared by adding surfactant in water (e.g., for 1 M SDS (2.89 g) in 10 mL) and stirring for 15 min, when the solution became clear. An aliquot of the desired porphyrin stock solution (1.5 mM) was added to make a 7.5 μM solution, the pH was adjusted to 7.0, and the visible spectral changes were monitored with time. In one experiment, an aliquot of the porphyrin stock solution was diluted with water to 15 μM. After ~10 min this solution was added to an equal volume of a 2 M SDS

solution such that the final concentrations were 1 M SDS and 7.5 μM porphyrin. The pH was quickly readjusted to 7.0 and the visible spectrum recorded.

3.2.5 General Synthesis for Alkylated [T($R^2R^1NSO_2Ar$)P]X_4 Porphyrins 1 to 6. Alkylation was carried out by suspending the parent porphyrin in an excess of CH_3I (10 mL) in a sealed flask and allowing the mixture to stir at RT overnight. The CH_3I that did not react was allowed to evaporate; the residue was dried under vacuum for 3 h to yield the iodide salt of the product porphyrin. To prepare the chloride salt of porphyrins **1** to **6**, a Dowex-1 (chloride form) anion-exchange resin column was prewashed with 0.1 N HCl and then washed with water until the eluate was at pH 7.0; a slurry of the compound in water was made with the resin and loaded onto a short column, and then eluted with water. The water was removed by rotary evaporation and the purplish solid residue dried under vacuum. The product was obtained as a purple powder by dissolving it in methanol and adding ethyl acetate. All compounds were isolated as chloride salts and analyzed by ^{1}H NMR spectroscopy and mass spectrometry.

[T(*N*-Mepy-2-CH_2(H)NSO_2Ar)P]Cl_4 (1). The general methylation method applied to the *non-alkylated* parent porphyrin (0.12 g, 0.092 mmol) afforded **1** as a brown precipitate (0.115 g, 84% yield). ^{1}H NMR (ppm) in DMSO-d_6: 8.90 (8H, s, β-pyrrole), 9.36 (4H, br, NH-sulfonamide), 9.12 (4H, d, pyH), 8.71 (4H, t, pyH), 8.49 (8H, d, ArH), 8.36 (8H, d, ArH), 8.31 (4H, d, pyH), 8.14 (4H, t, pyH), 4.87 (8H, d, CH_2), 4.44 (12H, s, CH_3) -2.95 (2H, br, NH). UV-vis (methanol) λ_{max} (ε) [nm ($M^{-1}cm^{-1}$)]: 416 (296,100), 512 (13,600), 546 (5300), 588 (4100), 642 (2300). ESI-MS(m/z): $[M+3H]^{3+}$ = 451.1344, $[M+4H]^{4+}$ = 338.6032, calcd. for $[M+3H]^{3+}$ = 451.1466, $[M+4H]^{4+}$ = 338.5996.

[T(*N*-Mepy-3-CH_2(H)NSO_2Ar)P]Cl_4 (2). The general method using the *non-alkylated* parent (0.12 g, 0.092 mmol) afforded **2** as a brown precipitate (0.13 g, 96% yield). ^{1}H NMR (ppm) in

DMSO-d_6: 8.87 (8H, s, β-pyrrole), 9.46 (4H, t, NH-sulfonamide), 9.30 (4H, s, pyH), 9.08 (4H, t, pyH), 8.72 (4H, d, pyH), 8.45 (8H, d, ArH), 8.32 (8H, d, ArH), 8.24 (4H, t, pyH), 4.57 (8H, d, CH_2), 4.42 (12H, s, CH_3) -2.96 (2H, br, NH). UV-vis (methanol) λ_{max} (ε) [nm ($M^{-1}cm^{-1}$)]: 416 (292,800), 512 (14,000), 546 (5800), 588 (4400), 642 (2300). ESI-MS(m/z): $[M+2H]^{2+}$ = 676.7088, $[M+3H]^{3+}$ = 451.1423, $[M+4H]^{4+}$ = 338.6103, calcd. for $[M+2H]^{2+}$ = 677.1994, $[M+3H]^{3+}$ = 451.1466, $[M+4H]^{4+}$ = 338.5996.

[T(*N*-Mepy-4-CH_2(H)NSO_2Ar)P]Cl_4 (3). The general method using the *non-alkylated* parent (0.12 g, 0.092 mmol) afforded **3** as a brown precipitate (0.12 g, 89% yield). ^{1}H NMR (ppm) in DMSO-d_6: 8.89 (8H, s, β-pyrrole), 9.20 (4H, br, NH-sulfonamide), 9.02 (8H, d, pyH), 8.49 (8H, d, ArH), 8.32 (8H, d, ArH), 8.20 (8H, d, pyH), 4.68 (8H, d, CH_2), 4.35 (12H, s, CH_3) -2.94 (2H, br, NH). UV-vis (methanol) λ_{max} (ε) [nm ($M^{-1}cm^{-1}$)], 416 (312,200), 512 (13,500), 546 (5200), 588 (4000), 642 (1700). ESI-MS(m/z): $[M+H]^+$ = 1354.4043, $[M+2H]^{2+}$ = 676.2131, $[M+3H]^{3+}$ = 451.14, $[M+4H]^{4+}$ = 338.6097, calcd. for $[M+H]^+$ = 1354.3987, $[M+2H]^{2+}$ = 677.1994, $[M+3H]^{3+}$ = 451.1466, $[M+4H]^{4+}$ = 338.5996.

[T($Me_3NCH_2CH_2$(H)NSO_2Ar)P]Cl_4 (4). The general method using the *non-alkylated* parent (0.12 g, 0.099 mmol) afforded **4** as a reddish precipitate (0.095 g, 69% yield). ^{1}H NMR (ppm) in DMSO-d_6: 8.88 (8H, s, β-pyrrole), 8.69 (4H, t, NH-sulfonamide), 8.48 (8H, d, ArH), 8.32 (8H, d, ArH), 3.63 (8H, d, CH_2), 3.58 (8H, t, CH_2), 3.23 (36H, s, CH_3), -2.94 (2H, br, NH). UV-vis (methanol) λ_{max} (ε) [nm ($M^{-1}cm^{-1}$)]: 416 (266,000), 512 (12,100), 546 (5000), 588 (3800), 642 (1800). ESI-MS(m/z): $[M+4H]^{4+}$ = 318.6365; calcd for $[M+4H]^{4+}$ = 318.6309.

[T(*N*-Mepy-2-CH_2(CH_3)NSO_2Ar)P]Cl_4 (5). The general method using the *non-alkylated* parent (0.116 g, 0.086 mmol) afforded **5** as a brown precipitate (0.125 g, 93% yield). ^{1}H NMR (ppm) in DMSO-d_6: 8.98 (8H, s, β-pyrrole), 9.18 (4H, d, pyH), 8.58 (8H, d, ArH), 8.42 (8H, d,

ArH), 8.74 (4H, t, pyH), 8.31 (4H, d, pyH), 8.16 (4H, t, pyH), 5.14 (8H, s, CH_2), 4.46 (12H, s, CH_3), 3.08 (12H, s CH_3), -2.81 (2H, br, NH). UV-vis (methanol) λ_{max} (ε) [nm ($M^{-1}cm^{-1}$)]: 416 (359,600), 512 (16,700), 546 (6900), 588 (6400), 642 (2500). ESI-MS(m/z): $[M + 4H]^{4+}$ = 352.6276; calcd for $[M+4H]^{4+}$ = 352.6177.

[T(*N*-Mepy-4-$CH_2(CH_3)NSO_2$Ar)P]Cl_4 (6). The general method using the *non-alkylated* parent (0.108 g, 0.079 mmol) afforded **6** as a brown precipitate (0.11 g, 88% yield). ^{1}H NMR (ppm) in DMSO-d_6: 8.88 (8H, s, β-pyrrole, 9.04 (8H, d, pyH), 8.56 (8H, d, ArH), 8.36 (8H, d, ArH), 8.19 (8H, d, pyH), 4.87 (8H, s, CH_2), 4.38 (12H, s, CH_3), 3.04 (12H, s, CH_3), -2.93 (2H, br, NH). UV-vis (methanol) λ_{max} (ε) [nm ($M^{-1}cm^{-1}$)]: 416 (302,100), 512 (14,500), 546 (6000), 588 (4400), 642 (2400). ESI-MS(m/z): $[M + 4H]^{+4}$ = 352.6199; calcd for $[M+4H]^{4+}$ = 352.6177.

[T($Et_3NCH_2CH_2)_2NSO_2$Ar)P]Cl_8 (7). Porphyrin **7** was synthesized from its *non-alkylated* precursor (synthesized by treating a suspension of $TPPSO_2Cl$ (0.22 g, 0.22 mmol) in acetonitrile (20 mL) with *N*,*N*,*N''*,*N''*-Et_4-dien (0.199 g, 0.93 mmol) in acetonitrile (10 mL) at RT). The resulting suspension became a solution when stirred overnight, and the solvent was then removed by rotary evaporation. The residue was recrystallized from dichloromethane and hexane as purple crystals (0.35 g, 93% yield). ^{1}H NMR (ppm) in $CDCl_3$: 8.79 (8H, s, β-pyrrole), 8.36 (8H, d, ArH), 8.28 (8H, d, ArH), 3.55 (16H, t, CH_2), 2.84 (16H, t, CH_2), 2.67 (32H, m. CH_2), 1.12 (48H, m, CH_3), -2.84 (2H, br, NH). The non-alkylated precursor (0.13 g) was alkylated by using iodoethane (5 mL) instead of iodomethane in the procedure above, and **7** was obtained as the chloride salt (0.115 g, 89% yield) as described above. ^{1}H NMR (ppm) in DMSO-d_6: 8.95 (8H, s, β-pyrrole), 8.51 (16H, d, ArH), 4.0 (16H, t, CH_2), 3.68 (16H, t, CH_2), 3.48 (48H, s. CH_2), 1.32 (72H, m, CH_3), -2.84 (2H, br, NH). UV-vis (methanol) λ_{max} (ε) [nm ($M^{-1}cm^{-1}$)]: 416 (320,000),

512 (15,500), 546 (6600), 588 (5100), 642 (2700). ESI-MS(m/z): $[M + 4H]^{+4}$ = 492.7939; calcd for $[M+4H]^{4+}$ = 492.8223.

[Cu(II)T(*N*-Mepy-4-$CH_2(CH_3)NSO_2Ar$)P]Cl_4 (Cu(II)6). A solution of **6** (0.05 g, 0.032 mmol) in methanol (10 mL) was treated with copper(II) acetate (0.64 mg, 0.032 mmol) in MeOH (5 mL). The solution was allowed to stir at RT for about 1 h. Completion of the reaction was indicated by UV/vis spectroscopy, with the four Q bands of the free base (λ = 512, 546, 588, 642 nm) collapsing to one peak (λ = 538 nm). The volume of the reaction mixture was reduced to ~1 mL, and acetone was added to precipitate the compound as a red powder (0.045 g, 88% yield). ^{1}H NMR (ppm) in DMSO-d_6: 8.99 (8H, br, pyH), 8.12 (8H, br, pyH), 4.80 (8H, br, CH_2), 4.35 (12H, s, CH_3), 2.95 (12H, br, CH_3). UV-vis (methanol) λ_{max} (ε) [nm ($M^{-1}cm^{-1}$)]: 414 (364,400), 538 (1740).

[Cu(II)T($Et_3NCH_2CH_2)_2NSO_2Ar$)P]Cl_8 (Cu(II)7). This compound was synthesized and isolated as for Cu(II)**6** above from (0.05 g, 0.022 mmol) of **7**; yield = 0.039 g (76%), UV-vis (methanol) λ_{max} (ε) [nm ($M^{-1}cm^{-1}$)]: 414 (449,000), 538 (21,600).

[Zn(II)T(*N*-Mepy-4-$CH_2(CH_3)NSO_2Ar$)P]Cl_4 (Zn(II)6). A solution of porphyrin **6** (0.05 g, 0.032 mmol) in dichloromethane (10 mL) was treated with a solution of zinc acetate (0.035 g, 0.16 mmol in methanol, 2 mL). The solution was stirred at RT for 2 h, after which a small sample of the reaction mixture that was analyzed by visible spectroscopy indicated that the metal insertion was complete, with the four Q bands of the free base (λ = 514, 549, 590, 643 nm) collapsing to two peaks (λ = 556, 596 nm). The dichloromethane was removed by rotary evaporation, and the purple precipitate that formed was collected on a filter and washed with methanol to remove the excess of zinc acetate, affording the zinc complex of the precursor of porphyrin **6** (0.033 g, 63% yield). ^{1}H NMR (ppm) in DMSO-d_6: 8.85 (8H, s, β-pyrrole, 8.64 (8H,

d, pyH), 8.46 (8H, d, ArH), 8.28 (8H, d, ArH), 7.46 (8H, d, pyH), 4.55 (8H, d, CH_2), 2.93 (12H, s, CH_3). The general method of alkylation described above afforded Zn(II)**6** as a purple powder (0.035 g, 93% yield). ^{1}H NMR (ppm) in DMSO-d_6: 8.85 (8H, s, β-pyrrole, 9.03 (8H, d, pyH), 8.50 (8H, d, ArH), 8.33 (8H, d, ArH), 8.20 (8H, d, pyH), 4.87 (8H, d, CH_2), 4.38 (12H, d, CH_3), 2.94 (12H, s, CH_3). UV-vis (methanol) λ_{max} (ε) [nm ($M^{-1}cm^{-1}$)]: 424 (388,100), 556 (14,600), 596 (5,900).

3.3 Results

3.3.1 Synthesis. The use of various metal salts to metallate porphyrins containing a secondary sulfonamide generally produced insoluble materials. The fact that sulfonamides are known to coordinate to metal ions through both the sulfonyl oxygen and the deprotonated sulfonamide nitrogen[44,45] led us to investigate the synthesis of the porphyrins containing a tertiary sulfonamide group. Utilizing the N-Me group in place of the dissociable NH group allowed us to prepare porphyrins that are very soluble in organic solvents; this property permitted successful alkylation and metallation of the porphyrins. The cationic porphyrins ([T($R^2R^1NSO_2Ar$)P]$X_{4/8}$) (Figure 3.3) were characterized by mass spectrometry (ESI), UV-vis (methanol), and ^{1}H NMR spectra (in DMSO-d_6).

The Cu(II) complexes of the cationic porphyrins (Figure 3.3) were characterized by visible spectroscopy, and the Zn(II) complexes were characterized by both ^{1}H NMR and visible spectroscopy. Upon Cu(II) insertion into [T(*N*-Mepy-4-$CH_2(CH_3)NSO_2Ar$)P]Cl_4 (**6**) to form [Cu(II)T(*N*-Mepy-4-$CH_2(CH_3)NSO_2Ar$)P]Cl_4 (Cu(II)**6**), the Soret band maximum (λ_{So}) was blue shifted by 3 nm for **6** and the number of Q bands decreased from four to one, results consistent with reported observations for other copper porphyrins, such as CuTMAP.[46,47] Zn(II) insertion into **6** to form [Zn(II)T(*N*-Mepy-4-$CH_2(CH_3)NSO_2Ar$)P]Cl_4 (Zn(II)**6**) produced a 10 nm red shift

of λ_{So}, and the number of Q bands decreased from four to two; both features have been observed previously with other zinc porphyrins.[47,48]

3.3.2 Solution Studies with No DNA Present. Values of λ_{So} and molar absorptivity at that wavelength (ε_{So}) are summarized for several new porphyrins and for Cu(II)TMAP in Table 3.1. All solution studies employed 7.5 μM porphyrin and pH 7.0, unless stated otherwise. Compared to the λ_{So} at 410 nm of an aqueous red solution of Cu(II)**6** (no added salt), λ_{So} was shifted slightly to 406 nm and 403 nm in 10 and 100 mM NaCl solutions, respectively, and ε_{So} decreased (Table 3.1). A similar comparison of aqueous Zn(II)**6** showed decreases in ε_{So}, but λ_{So} did not change with salt concentration (Table 3.1). The molar absorptivity of **6**, Cu(II)**6** and Zn(II)**6** in 10 mM NaCl increased with added methanol at least up to 50% methanol. This absorbance increase is attributable to the dissociation of porphyrin aggregates.

Table 3.1. Visible Spectroscopic Data for [T(*N*-Mepy-4-$CH_2(CH_3)NSO_2$Ar)P]Cl_4 (**6**), Cu(II)**6**, Zn(II)**6**, and Cu(II)TMAP

porphyrin [a]	λ_{So} [b] ($10^{-5} \times \varepsilon_{So}$) [c] in H_2O	λ_{So} [b] ($10^{-5} \times \varepsilon_{So}$) [c] in 10 mM NaCl	λ_{So} [b] ($10^{-5} \times \varepsilon_{So}$) [c] in 100 mM NaCl	λ_{So} [b] ($10^{-5} \times \varepsilon_{So}$) [c] in methanol
6	413 (1.5)	412 (1.1)	404 (0.9)	415 (3.0)
Cu(II)**6**	410 (2.0)	406 (1.6)	403 (1.1)	414 (3.6)
Zn(II)**6**	423 (2.9)	423 (1.8)	423 (1.5)	424 (3.9)
Cu(II)**7**	414 (3.1)	414 (2.3)	409 (2.2)	414 (4.4)
Cu(II)TMAP	411 (2.8)	411 (2.8)	411 (2.6)	412 (2.9)

[a] 7.5 μM porphyrin. [b] nm. [c] M^{-1} cm^{-1}.

The greater width and lower molar absorptivity of the Soret band of Cu(II)**6** compared to that of Cu(II)TMAP [Cu(II)**6**: 410 nm, full width at half-maximum (fwhm) = 22 nm, $\varepsilon_{So} = 2.0 \times 10^5$ $M^{-1}cm^{-1}$ vs. Cu(II)TMAP: 411 nm, fwhm = 16 nm, $\varepsilon_{So} = 2.8 \times 10^5$ $M^{-1}cm^{-1}$] in aqueous solution

indicate that Cu(II)**6** aggregates significantly. Likewise, Zn(II)**6** has fwhm = 14 nm and ε_{So} = 2.9 × 10^5 $M^{-1}cm^{-1}$, suggesting that the axial water on Zn as well as other effects of a five-coordinate geometry on the porphyrin structure disfavor stacking. These results suggest that the new cationic porphyrins, even at 7.5 μM, undergo appreciable aggregation and that the aggregated (stacked) Cu(II) porphyrins have relatively blue-shifted Soret bands.

3.3.3 SDS Studies. The λ_{So} and ε_{So} values of Cu(II)**6** in the presence and absence of SDS (Figure 3.4) are summarized in Table 3.2. During the first hour after a 1.5 mM stock solution of Cu(II)**6** was added to 1 M SDS to make a 7.5 μM solution, the spectra recorded with time (Figure 3.4) indicated that two forms of the porphyrin were present initially: one form with a blue-shifted λ_{So} at 399 nm and the other form with a red-shifted λ_{So} at 416 nm (when compared to λ_{So} at 410 nm in water). The facts that the 399 nm Soret band converted completely to the 416 nm Soret band after 12 h and that the intensity of this 416 nm band was high (Figure 3.4) indicate that Cu(II)**6** is stacked in water and slowly destacks in 1 M SDS.

To test this interpretation, the concentrated stock solution of Cu(II)**6** was diluted to 15 μM. Equal volumes of this dilute solution and a 2 M SDS solution were mixed, producing final concentrations of 1 M SDS and 7.5 μM Cu(II)**6**. The absorption spectrum recorded immediately shows only the red-shifted 416 nm band (Figure 3.4). This intense band is very similar to the band observed in the experiment described in the previous paragraph. These observations are consistent with a high degree of aggregation of Cu(II)**6** in water, especially at high concentrations, and with SDS causing disaggregation of Cu(II)**6**. (When the Cu(II)**6** is less stacked, the Soret band is red shifted.)

Table 3.2. Visible Spectroscopic Data for [Cu(II)T(*N*-Mepy-4-$CH_2(CH_3)NSO_2Ar$)P]Cl_4 (Cu(II)**6**) in H_2O and 1 M SDS at pH 7.0[a]

time	λ_{So}[b] ($10^{-5} \times \varepsilon_{So}$)[c] H_2O	λ_{So}[b] ($10^{-5} \times \varepsilon_{So}$)[c] 1 M SDS
5 min	410 (2.0)	416 (1.6), 399 (1.0)
10 min		416 (2.1), 399 (1.1)
30 min		416 (2.4), 399 (1.0)
1 h		416 (2.5), 399 (1.0)
12 h		416 (3.8)

[a] 7.5 μM porphyrin. [b] nm. [c] M^{-1} cm^{-1}.

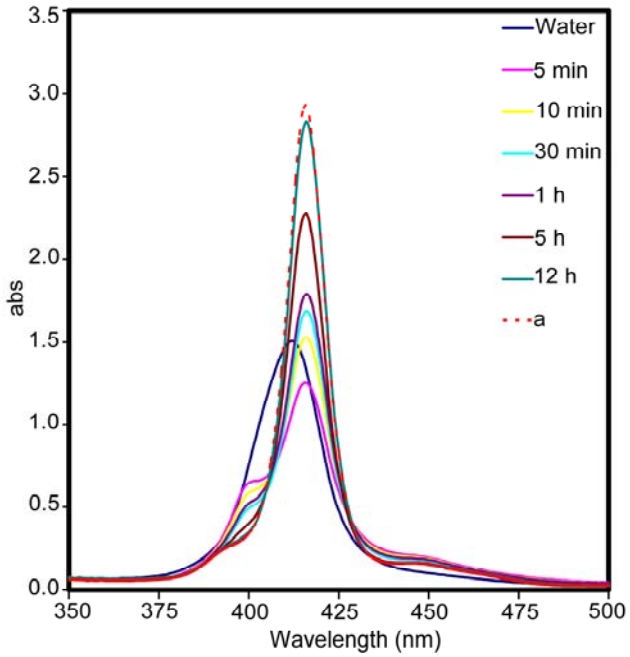

Figure 3.4. Visible spectrum monitored with time of 7.5 μM [Cu(II)T(*N*-Mepy-4-$CH_2(CH_3)NSO_2Ar$)P]Cl_4 (Cu(II)**6**) in 1 M SDS. Also shown are the spectrum in water and that in 1 M SDS but prepared with a dilute solution of the porphyrin (spectrum a, red dashed line).

When a 1.5 mM stock solution of Cu(II)**6** was added to 0.1 M SDS to make a 7.5 μM solution, the spectrum recorded with time (Supporting Information, Figure B.11) indicated that both the 399 nm and 416 nm bands were present, suggesting coexistence of two forms. The two bands

remained even after 12 h. This fact suggests that, in contrast to 1 M SDS, 0.1 M SDS does not cause complete disaggregation of the stacked positively charged porphyrin cation. SDS has negative charge, favoring stacking (aggregation) and hydrophobic character, favoring de-stacking. Evidently, the hydrophobic capacity of 0.1 M SDS is not sufficient to offset the effect of the negative charge.

3.3.4 DNA-Binding Studies. Several methods were used to evaluate DNA binding. We assessed how the Soret band position and intensity changed on DNA addition. Hypochromicity (%*H*) is defined here as $[(A_o - A_s)/A_o] \times 100\%$, where A_o and A_s are the absorbance values at λ_{So} in the absence and presence of CT DNA, respectively (a negative %*H* indicates *hyper*chromicity). Because both CT DNA and the free porphyrin have no CD band in the visible region, the only CD signal observed in this region is the induced CD signal of the bound porphyrins. Viscosity measurements are also useful because intercalation of a cation into DNA has a measurable effect on solution flow properties.[20] A fixed concentration (75 μM) of sonicated CT DNA was maintained as the concentration of several porphyrins in 100 mM NaCl was increased (Figure 3.5). The SRV increased with addition of the intercalating Cu(II)TMPyP(4). For Cu(II)TMAP the SRV first increased slightly at low *R*, but leveled off after *R* = 0.15. The addition of Cu(II)**6**, Zn(II)**6**, or Cu(II)**7** to CT DNA caused changes in SRV similar to those observed for the non-intercalating Cu(II)TMAP (Figures 3.5 and B.1). Viscosity experiments were used to determine if Cu(II)**6** binds DNA competitively with Cu(II)TMpyP(4). At different *R* values (0.025, 0.1, 0.2 and 0.3) with equimolar amounts of the two porphyrins, the SRV values found (1.08, 1.12, 1.25 and 1.35) were smaller than the respective values (1.16, 1.46, 1.62 and 1.74) for Cu(II)TMpyP(4) alone, Figures 3.5 and B.1.

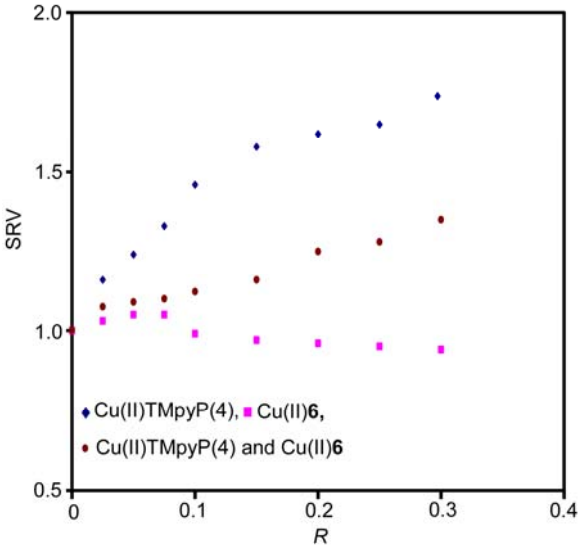

Figure 3.5. Plot of SRV vs. *R* for the addition of metalloporphyrins to solutions of CT DNA (75 μM, 100 mM NaCl, pH 7.0).

DNA Binding of [Cu(II)T(*N*-Mepy-4-$CH_2(CH_3)NSO_2Ar$)P]Cl_4 (Cu(II)6). The Cu(II)**6**–CT DNA visible studies are summarized in Table 3.3. After addition of CT DNA, the spectrum of Cu(II)**6** exhibited two Soret components. The red-shifted component (at 420 nm) in both 10 mM and 100 mM NaCl solutions (Table 3.3 and Figures 3.6 and B.2) is indicative of an unstacked bound form. As more CT DNA was added (as *R* changed from 0.25 to 0.005), the intensity of the long-wavelength component increased at the expense of the shorter-wavelength component. *Hyper*chromicity of the Soret band indicates unstacking of Cu(II)**6**.

The overall shape of the CD spectrum of Cu(II)**6** was independent of NaCl concentration. The binding of Cu(II)**6** to CT DNA for all *R* values induced a CD spectrum with a positive feature at ~415 nm (+exc) and a weak negative feature (-s) at ~433 nm (Table 3.4 and Figures 3.7 and B.3). The intensity of the positive band increased with increasing CT DNA concentration (decreasing *R*), while that of the negative feature decreased. At *R* = 0.005 in 10 mM NaCl the CD signal of Cu(II)**6** with CT DNA reached its maximum value (molar ellipticity ([Θ]) = 4.9 ×

10^4 deg cm^2 $dmol^{-1}$). These results and similar data for 100 mM NaCl are consistent with non-stacking or weakly stacking outside binding.

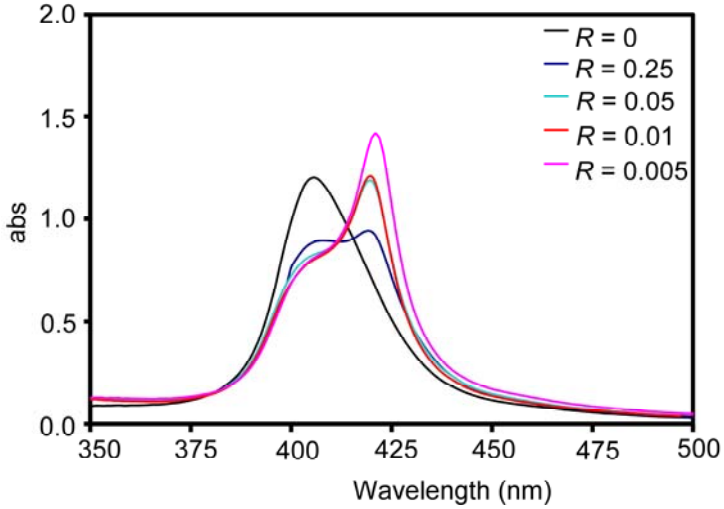

Figure 3.6. Effect of CT DNA on the visible spectrum of [Cu(II)T(*N*-Mepy-4-$CH_2(CH_3)NSO_2Ar$)P]Cl_4 (Cu(II)**6**, 7.5 μM) at various *R* values (10 mM NaCl, pH 7.0).

Table 3.3. Visible Spectroscopic Data for [Cu(II)T(*N*-Mepy-4-$CH_2(CH_3)NSO_2Ar$)P]Cl_4 (Cu(II)**6**) in the Presence of CT DNA at pH 7.0[a]

	10 mM NaCl			100 mM NaCl		
R	λ_{So}[b]	$10^{-5} \times \varepsilon_{So}$[c]	$\Delta\lambda$[b] (%*H*)	λ_{So}[b]	$10^{-5} \times \varepsilon_{So}$[c]	$\Delta\lambda$[b] (%*H*)
0	406	1.6		403	1.1	
0.25	404	1.2	-2 (25)	403	1.0	0 (9)
	420	1.3	14 (19)	420	1.2	17 (-9)
0.05	404	1.1	-2 (31)			
	420	1.6	14 (0)	420	1.4	17 (-27)
0.01	404	1.0	-2 (38)			
	420	1.6	14 (0)	420	2.2	17 (-100)
0.005	404	1.0	-2 (38)			
	420	1.8	14 (-13)	420	2.4	17 (-118)

[a] 7.5 μM porphyrin. [b] nm. [c] M^{-1} cm^{-1}.

Table 3.4. Effect of NaCl Concentration on the CD Spectrum of [Cu(II)T(*N*-Mepy-4-$CH_2(CH_3)NSO_2Ar$)P]Cl_4 (Cu(II)**6**) in the Presence of CT DNA at pH 7.0[a]

	10 mM NaCl				100 mM NaCl			
R	λ_{+exc}[b]	$10^{-4}\times[\Theta]_{+exc}$[c]	λ_{-s}[b]	$10^{-4}\times[\Theta]_{-s}$[c]	λ_{+exc}[b]	$10^{-4}\times[\Theta]_{+exc}$[c]	λ_{s}[b]	$10^{-4}\times[\Theta]_{-s}$[c]
0.25	413	2.3	433	–1.2	412	1.9	433	–0.5
0.05	414	3.2	433	–0.7	416	3.8	434	–0.2
0.01	415	3.6	433	–0.6	417	4.3	434	–0.5
0.005	416	4.9	433	–0.3	414	2.3	434	–0.2

[a] 7.5 μM porphyrin. [b] nm. [c] deg cm^2 $dmol^{-1}$.

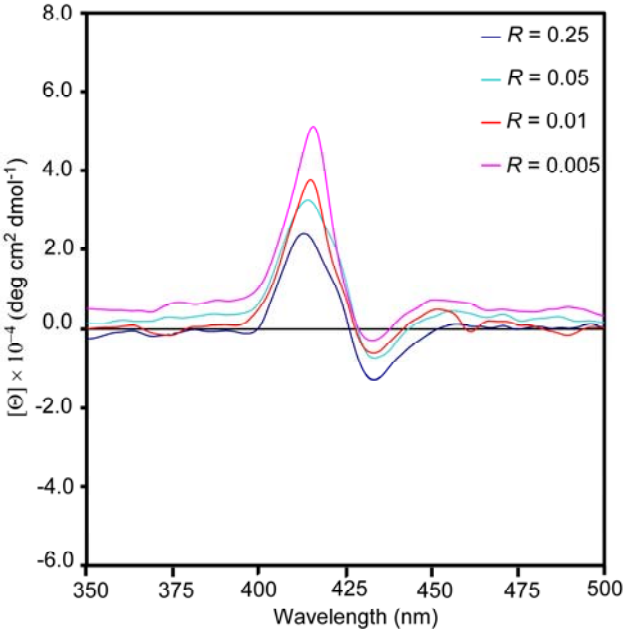

Figure 3.7. CT DNA-induced CD spectra of [Cu(II)T(*N*-Mepy-4-$CH_2(CH_3)NSO_2Ar$)P]Cl_4 (Cu(II)**6**, 7.5 μM) at various *R* values (10 mM NaCl, pH 7.0).

DNA Binding of [Zn(II)T(*N*-Mepy-4-$CH_2(CH_3)NSO_2Ar$)P]Cl_4 (Zn(II)6). Addition of CT DNA to a solution of Zn(II)**6** in 10 mM and 100 mM NaCl solutions caused a 3 nm red shift in λ_{So} at all *R* values (Table B.1). At the lowest DNA concentration, only small changes in Soret band intensity in both 10 mM and 100 mM NaCl solutions were observed (Table B.1 and Figures

B.6 and B.7). At the highest DNA concentration (R = 0.005), significant *hyper*chromicity was observed in 10 mM (%H = -61) and 100 mM (%H = -87) NaCl solutions (Table B.1 and Figures B.4 and B.5). At low R values, an induced CD signal (+exc at ~420 nm) was observed (Table B.2 and Figures B.6 and B.7). As for Cu(II)**6**, these results are consistent with non-stacking or weakly stacking outside binding.

DNA Binding of [Cu(II)T($Et_3NCH_2CH_2$)$_2$$NSO_2$Ar)P]$Cl_8$ (Cu(II)7). Addition of CT DNA to Cu(II)**7** caused 7 and 11 nm red shifts of λ_{So} in 10 mM and 100 mM NaCl solutions, respectively (Table 3.5). At the highest concentration of DNA (R = 0.005), *hyper*chromicity was observed (Table 3.5 and Figures B.8 and B.8). An induced CD signal (+exc at ~415 nm, -s at ~430 nm) was observed upon addition of CT DNA (Table 3.6). The intensity of these features generally decreased with an increase in DNA concentration (Table 3.6 and Figures 3.9 and B.9). As for Cu(II)**6**, these results are consistent with non-stacking or weakly stacking outside binding.

Table 3 5. Visible Spectroscopic Data for [Cu(II)T($Et_3NCH_2CH_2$)$_2$$NSO_2$Ar)P]$Cl_8$ (Cu(II)**7**) in the Presence of CT DNA at pH 7.0[a]

	10 mM NaCl			100 mM NaCl		
R	λ_{So}[b]	$10^{-5} \times \varepsilon_{So}$[c]	$\Delta\lambda$[b] (%H)	λ_{So}[b]	$10^{-5} \times \varepsilon_{So}$[c]	$\Delta\lambda$[b] (%H)
0	414	2.3		409	2.2	
0.25	421	2.0	7 (13)	420	2.4	11 (-9)
0.05	421	2.2	7 (4)	420	2.8	11 (-27)
0.01	421	2.4	7 (-4)	420	3.0	11 (-36)
0.005	421	2.7	7 (-17)	420	3.2	11 (-46)

[a] 7.5 μM porphyrin. [b] nm. [c] M^{-1} cm^{-1}.

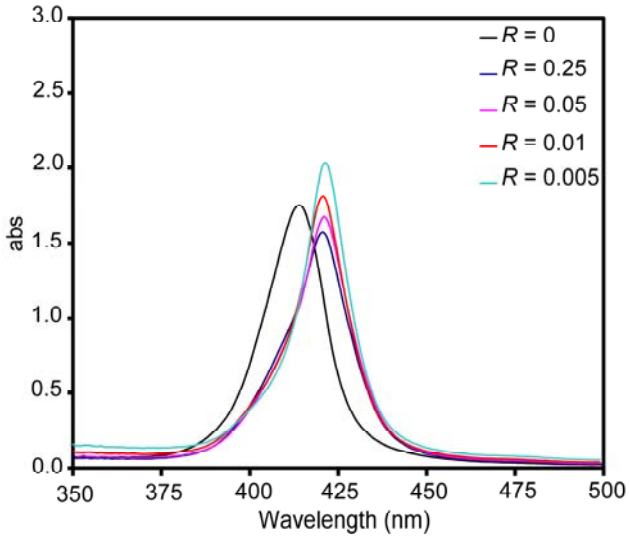

Figure 3.8. Effect of CT DNA on the visible spectrum of $[Cu(II)T(Et_3NCH_2CH_2)_2NSO_2Ar)P]Cl_8$ (Cu(II)**7**, **7**.5 μM) at various *R* values (10 mM NaCl, pH 7.0).

Table 3.6. Effect of NaCl Concentration on the CD Spectrum of $[Cu(II)T(Et_3NCH_2CH_2)_2NSO_2Ar)P]Cl_8$ (Cu(II)**7**) in the Presence of CT DNA at pH 7.0[a]

	10 mM NaCl				100 mM NaCl			
R	λ_{+exc}[b]	$10^{-4}\times[\Theta]_{+exc}$	λ_{-s}[b]	$10^{-4}\times[\Theta]_{-s}$[c]	λ_{+exc}[b]	$10^{-4}\times[\Theta]_{+exc}$	λ_{s}[b]	$10^{-4}\times[\Theta]_{-s}$[c]
0.25	414	3.9	428	–3.0	414	2.1	430	–1.5
0.05	415	2.6	430	–0.7	414	1.2	430	–0.7
0.01	415	1.8	429	–0.9	414	1.5	430	–0.5
0.005	415	1.6	429	–0.8	419	0.8	436	–0.5

[a] 7.5 μM porphyrin. [b] nm. [c] deg cm^2 $dmol^{-1}$.

DNA-Binding Studies of Porphyrins with Different Peripheral Groups. The λ_{So} of solutions of both **1** ($[T(N\text{-Mepy-2-}CH_2(H)NSO_2Ar)P]Cl_4$) and **5** ($[T(N\text{-Mepy-2-}CH_2(CH_3)NSO_2Ar)P]Cl_4$) in 10 mM NaCl was at 414 nm (Table B.3). The addition of CT DNA at a low DNA concentration (*R* = 0.25) to **1** and **5** led to red-shifted and blue-shifted (5 nm) bands and hypochromicity. At the higher DNA concentration (*R* = 0.005), the same two bands were observed (%*H* = 52 and 7 for **1** and %*H* = 54 and 15 for **5,** Table B.3). The binding of CT

DNA to both porphyrins induced a positive CD feature (Table B.4). As more CT DNA was added (as *R* changed from 0.25 to 0.005), the intensity of these positive features increased (Table B.4). Visible and CD spectral changes for **4** ([T($Me_3NCH_2CH_2$(H)NSO_2Ar)P]Cl_4) in 10 mM NaCl (Tables B.3 and B.4) were similar to those for **1** and **5**. The spectral features of the porphyrins described in this subsection are consistent with a combination of weakly stacked and unstacked outside binding rather than with intercalation.

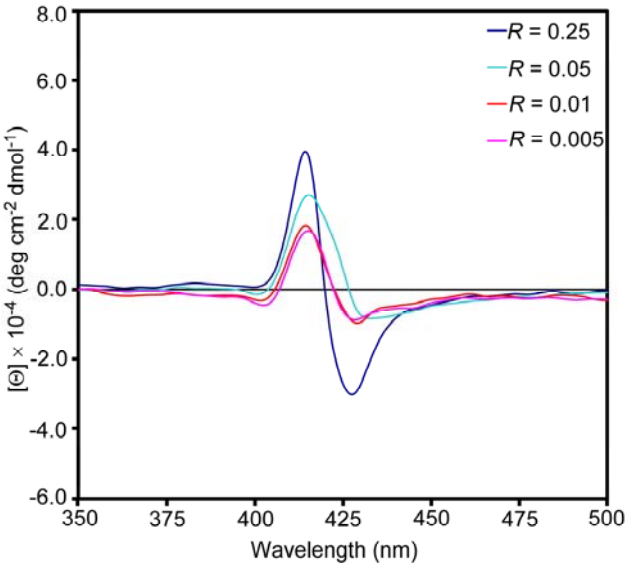

Figure 3.9. CT DNA-induced CD spectra of [Cu(II)T($Et_3NCH_2CH_2$)$_2NSO_2$Ar)P]Cl_8 (Cu(II)**7**, 7.5 μM) at various *R* values (10 mM NaCl, pH 7.0).

3.3.5 Fluorescence Spectroscopy. The fluorescence spectrum of the metal-free porphyrin, [T(*N*-Mepy-4-CH_2(CH_3)NSO_2Ar)P]Cl_4 (**6**), in 10 mM NaCl shows two emission maxima at 656 nm [Q(0,0) band] and at ~700 nm [Q(0,1) band] (Figure 3.10); the band assignment follows that used for other porphyrins.[49] The two bands shifted (656 nm band slightly, ~700 nm band significantly), and the intensity decreased significantly (by 34% and ~60%, respectively, Figure 3.10) upon the addition of a small amount of DNA (*R* = 0.25). The decrease in fluorescence

intensity of **6** is attributed to the proximity of the neighboring porphyrins, which are self-stacked when bound to DNA.[50] Further addition of CT DNA led to increases in intensity. The final value (R = 0.005) was ~1.2 times those found before DNA addition. We attribute these changes to conversion of the unbound porphyrin aggregates initially present first to bound aggregates (Figure 3.2, right) and then to the bound monomer form at high DNA concentration (Figure 3.2, middle).[50]

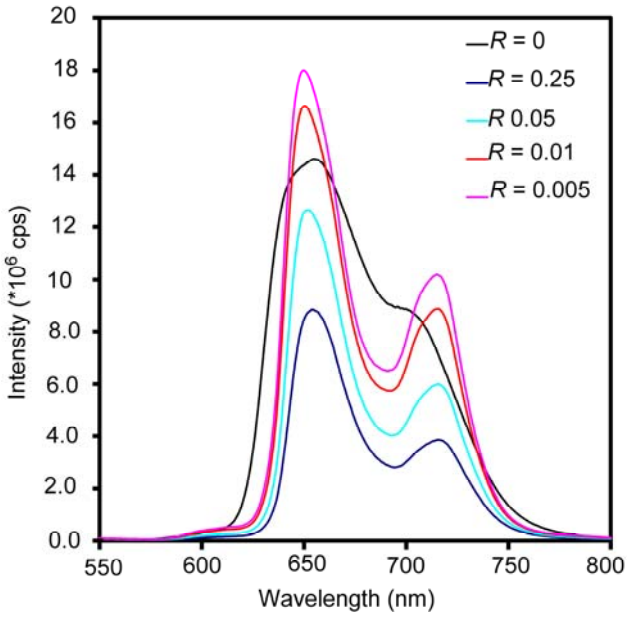

Figure 3.10. Effect of CT DNA on the fluorescence spectrum of [T(*N*-Mepy-4-$CH_2(CH_3)NSO_2Ar$)P]Cl_4 (6, 7.5 μM) at various R values (10 mM NaCl, pH 7.0).

3.4 Discussion

Our primary interests were to determine how the new water-soluble cationic porphyrins and metalloporphyrins prepared in this work bound to DNA, either as intercalators or outside-binders, and to use the results to gain further insight into important features that favor intercalation of cationic porphyrins. Experimental evidence useful for determining if a porphyrin intercalates and our evidence establishing that the new porphyrins do not intercalate will be discussed first. Next we discuss the factors that our work indicates are important for intercalation

of known porphyrin intercalators. Finally, we shall discuss briefly the nature of the DNA outside binding of the new porphyrins.

3.4.1 Experimental Criteria for Porphyrin Intercalation into DNA. Experimental observations indicating intercalative binding include changes in the Soret region of spectra, namely, a large red shift (~15 nm), a large hypochromicity (~30%) and a negative induced CD signal. These spectroscopic parameters tend to vary over a narrower range than those found for outside binders (see below). Perhaps the most characteristic spectral feature is the negative induced CD signal; typical magnitudes found are about -5×10^4 (deg cm^2/dmole).[5,31,37,38,51] However, perhaps the best procedure to assess DNA binding mode is to measure solution reduced viscosity (SRV). Porphyrins known to intercalate (e.g., Cu(II)TMpyP(4)[52]) increase the SRV of DNA solutions.[31]

3.4.2 Evidence That New Porphyrins Are Not Intercalators. No increase in DNA solution viscosity was observed for Cu(II)**6**, Zn(II)**6**, and Cu(II)**7** (Figures 3.5 and B.1). The SRV values of Cu(II)**6**, Zn(II)**6**, and Cu(II)**7** were comparable to that of Cu(II)TMAP, a non-intercalator.[53] The absence of an increase in SRV demonstrates that these new porphyrins are outside binders. At the same ratio of total Cu(II) porphyrin to DNA, lower SRV values were found in the presence of both [Cu(II)T(*N*-Mepy-4-$CH_2(CH_3)NSO_2$Ar)P]Cl_4 and Cu(II)TMpyP(4) than in the presence of Cu(II)TMpyP(4) alone (Figure 3.5). This finding indicates that [Cu(II)T(*N*-Mepy-4-$CH_2(CH_3)NSO_2$Ar)P]Cl_4 competes for DNA with Cu(II)TMpyP(4), which has a DNA binding constant of ~10^7 M^{-1}.[54] Therefore, because all the new porphyrins are similar, we expect that all are tight outside binders to DNA, and we turn our attention to comparing the features of the new porphyrins vs intercalating porphyrins in order to identify important features for intercalation.

3.4.3 Properties of Porphyrins Favoring Intercalation. On the basis of our past work and that of others,[1,19-21,29,52,55,56] we can conclude, as mentioned above, that the porphyrin peripheral groups should be N-alkyl pyridinium groups and that the porphyrin core of the metalloporphyrins with these groups need to lack axial ligands (e.g., Cu(II)TMpyP(4)) or have dissociable axial ligands (e.g., Ni(II)TMpyP(4)).[1,19,22,56] In general, the length of the *N*-alkyl group does not appear to be important;[22,31-34,57,58] however, the *N*-alkylpyridinium group must link to the porphyrin core via the 4- or 3- position of the pyridyl ring (not via the 2- position). This latter requirement has three implications: First, and most important, this requirement indictates that a relatively planar structural unit involving the pyridinium group and the adjacent portion of the porphyrin ring must be achieved. Second, the overall electronic nature of the directly attached pyridinium group and the porphyrin core appear to be important. Third, and less obvious, the separation between the charged nitrogens of the pyridinium groups may need to fall within a required range. These distances can be shorter (~6.5 Å) for TMpyP(2). The latter two aspects can be assessed with the results from our current work.

A recent paper contained a comparison of TMpyP(4) and its analogue with a 4-phenylene group inserted between the *N*-methylpyridinium group and the porphyrin core (B-TMpyP(4), Figure 3.1).[59] The latter compound does not intercalate. In TMpyP(4) the distances between the N's of the *N*-Mepy groups are 11 Å (cis) and 16 Å (trans), whereas for B-TMpyP(4) these distances between the N's of the 4-C_6H_4–*N*-Mepy groups are 19 Å (cis) and 27 Å (trans). This comparison suggests both that the separation between the charged nitrogens needs to be smaller and that, as mentioned above, the pyridinium group needs to be directly attached to the porphyrin core. The recent work of the McMillin laboratory showing that triD4 (Figure 3.1) intercalates indicates that a separation of 16 Å allows intercalation. This separation corresponds somewhat to

the cis distance in B-TMpyP(4). McMillin et al. showed that when bulk is present cis to the pyridinium groups (MetriD4), such larger porphyrins do not intercalate as well the original smaller porphyrin.[38] The 4-C_6H_4–*N*-Mepy group is large and projects out in a rigid manner. Other relatively large pyridinium porphyrins that intercalate have cis pyridinium groups with flexible N-alkyl substituents,[22,31] and this flexibility might allow the alkyl group to adopt an orientation that does not inhibit intercalation. In contrast, we believe that the rigid 4-C_6H_4–*N*-Mepy groups of B-TMpyP(4) do not allow the meso peripheral groups to avoid the steric clashes. Unlike B-TMpyP(4), the [T(*N*-Mepy-4-$CH_2(CH_3)NSO_2$Ar)P]Cl_4 porphyrins studied here are quite conformationally flexible. The various conformations can place the pyridinium groups in positions covering a range of distances from 9 Å (cis) to 25 Å (trans). These distances encompass those in pyridinium porphyrins for which intercalation has been found. However, the new porphyrins do not intercalate. This finding refines further the requirements for a porphyrin to be an intercalator and indicates that direct attachment of the pyridinium group to the porphyrin core is a very favorable and probably necessary feature for intercalation to occur. We believe the steric and electronic features of the combined pyridinium group and adjacent portions of the porphyrin core facilitate intercalation.

3.4.4 Stacking of Cationic Porphyrins under Aqueous Conditions. In the absence of DNA, many porphyrins undergo self-stacking in water.[39,60-64] The Soret bands of the face-to-face (H) and edge-to-edge (J) type stacked porphyrins are respectively blue shifted and red shifted.[60,63] The H-type stacking involves considerable overlap of the porphyrin cores, whereas J-type stacking can be viewed as a slippage of the porphyrin cores so that there is less overlap.[60] The electronic spectra are also influenced by the way the porphyrins align with respect to each other because alignment influences the relative orientation of the transition moments.[63] It was not our

objective to analyze in depth this very complicated stacking process. Rather, our goal was to determine qualitatively the relative importance of stacking for the unbound porphyrin because stacking influences the electronic spectra, and understanding this influence is useful in assessing spectral changes accompanying binding.

For types of cationic porphyrins usually studied, self-stacking upon DNA binding is normally accompanied by hypochromicity, broadening, and/or a shift in λ_{So}.[4-7,20,29,33] Self-aggregation of cationic porphyrins is believed to be responsible for the large hypochromicities (50-65%) observed in high salt concentrations.[29,33,39] From data in previous studies[29,61] the spectral changes indicate that TMAP and *trans*-P(4) in the presence of salt exist as H- and J-type aggregates, respectively.

3.4.5 Properties of the New Cationic Porphyrins in the Absence of DNA. We investigated the behavior of selected new porphyrins under aqueous conditions. The addition of NaCl to a solution of [Cu(II)T(*N*-Mepy-4-$CH_2(CH_3)NSO_2$Ar)P]Cl_4 (Cu(II)**6**) affected the Soret band, causing a blue shift, a broadening, and a decrease in the intensity (%*H* = 70 at 3.0 M NaCl, Figure B.10). These changes in the visible spectrum indicate that Cu(II)**6** undergoes substantial self-stacking and that the aggregates are of the H-type. Even in water, Cu(II)**6** gives evidence for stacking and the stacking increases under the low salt conditions used here. The literature indicates TMpyP(4) exists as the monomer in water even in the presence of inorganic salts.[24,65] Indeed, we compared aqueous and 200 mM NaCl solutions of TMpyP(4) and found that the Soret band (421 nm) did not shift and there was little change in intensity (%*H* = 3). In the same type of experiment but with Cu(II)**6** the Soret band showed a blue shift (9 nm) and %*H* = 45. Thus, Cu(II)**6** has a greater propensity to stack than TMpyP(4).

Addition of SDS to a solution of Cu(II)**6** produced a visible spectrum with two Soret bands at 399 nm and 416 nm. At low SDS concentration (0.1 M) the two bands were observed even after 12 h (Figure B.11). After 12 h in a 1 M solution of SDS the blue-shifted Soret band at 399 nm converted completely to the 416 nm band (red-shifted by 4 nm, an indication of a J-type aggregate). The intensity of this band increased with time (%*H* = -90 after 12 h, Figure 3.4). For TMpyP(4) at neutral pH, SDS produced no spectral shifts and thus the aggregate type could not be assigned as H- or J-type.[62]

The Soret band of octacationic [Cu(II)T($Et_3NCH_2CH_2$)$_2NSO_2$Ar)P]Cl_8 (Cu(II)**7**) in water (λ_{So} = 414 nm) was much sharper than that of Cu(II)**6**, indicating that Cu(II)**7** is less aggregated than Cu(II)**6** in water. Upon addition of salt, the Soret band of Cu(II)**7** became less intense and broader, and these effects increased with increasing salt (Figure B.12). These characteristics indicate that Cu(II)**7** undergoes self-stacking with an increase in salt concentration. At 3.0 M NaCl, the %*H* value of 57 is less than that of Cu(II)**6**. All results indicate that (because of its high charge) stacking of Cu(II)**7** is lower than that of Cu(II)**6**.

In aqueous 10 and 100 mM NaCl, the solution conditions used here for DNA binding studies, the Soret band of Cu(II)**6**, Cu(II)**7** and also Zn(II)**6 (**Figure 3.3**)** gave evidence for aggregation (Table 3.1). Upon DNA addition (see below), the Soret bands of these porphyrins shifted to the red and sharpened. The significant *hyper*chromicity and the red shift of the Soret bands are indicative of porphyrin binding to DNA as non-self-stacking outside binders.[21,28,31,66] Such changes must be assessed in the context of the degree of aggregation with stacking of the unbound porphyrin. For example, the extent of the *hyper*chromicity on DNA binding is less for Cu(II)**7** than for Cu(II)**6** because Cu(II)**7** is already less self-stacked than Cu(II)**6** prior to DNA binding. Thus, the DNA-bound Cu(II)**7** is not stacked (see below).

3.4.6 Outside Binding to DNA by Porphyrins. Porphyrins that induce no increase in the SRV of linear DNA are outside binders. The type of outside binding can be evaluated by observation of features of the induced CD signal. In addition, the Soret region of the visible spectrum undergoes changes. Because outside binding depends on a number of variables such as salt, ratio of porphyrin to the DNA, DNA base pair composition, etc., and because there can be combinations of co-existing outside binding modes, simple spectral signatures are difficult to define and categorize. In addition, because self-stacking often occurs and the self-stacking can itself change with the various conditions, it is not a simple matter to define precisely the binding. To illustrate the effects on CD and Soret spectra on porphyrin outside binding to DNA, we consider three limiting cases (Figure 3.2, middle and right), namely no self-stacking with the porphyrin core close to the DNA, no self-stacking with the core somewhat further and tumbling anisotropically, and extensive self-stacking.

Each of the three cases gives a distinct induced CD signal. A relatively unstacked outside-bound porphyrin will typically have a non-conservative positive CD signal with an intensity for $[\Theta] = \sim 1 \times 10^5$ deg cm^2 dmol^{-1}.[21,31] One system with this type of binding is TMpyP(4)–[poly(dA-dT)]$_2$.[21,31] We believe that TMpyP(2) is an example of a porphyrin that exhibits tumbling anisotropically. No appreciable induced CD signal was observed.[21] Conservative CD signals (in some cases strong) are indicative of outside binding with self-stacking.[4,5,30,33,35-37,67] Although the negative and positive features for the conservative signal detected are often not much stronger than the single prominent feature of an unstacked porphyrin, porphyrins with tentacle arms (e.g., TθOPP) offer an example of extensive self-stacking on DNA with both positive and negative features [Θ] having an absolute magnitude ten times greater than normal, with values of $\sim 10^6$ deg cm^2 dmol^{-1}.[33]

The Soret band is also useful for assessing stacking. As mentioned above, hyperchromicity is most reliably indicative of outside-bound unstacked porphyrins. Previously studied porphyrins (Mn(III)TMpyP(4) and Co(III)TMpyP(4)) showed small red shifts (5 nm) of the Soret band and significant *hyper*chromicity with CT DNA (-30% and -27%, respectively).[21] Outside binding with porphyrin stacking produces variable effects on the Soret band. A moderate (9 nm) red shift of λ_{So}, along with less than 30% hypochromicity[4,5] has been observed, but a large (25-30 nm) red shift[29] with large (~60%) hypochromicity has also been observed.[29,30,33,34,67]

[Cu(II)T(*N*-Mepy-4-$CH_2(CH_3)NSO_2Ar$)P]Cl_4 (Cu(II)6) and [Zn(II)T(*N*-Mepy-4-$CH_2(CH_3)NSO_2Ar$)P]Cl_4 (Zn(II)6). Visible and CD spectroscopic results for Cu(II)**6** and Zn(II)**6** are consistent with both being non-stacking outside binders. After addition of CT DNA to Cu(II)**6** and Zn(II)**6**, a red-shifted Soret band component was evident. Large *hyper*chromicities (Table 3.3) of up to -118% for Cu(II)**6** were observed. At all *R* values, a positive induced CD band (Figures 3.7 and B.3) for Cu(II)**6** was observed at ~416 nm, indicative of outside binding. Likewise, Zn(II)**6** exhibited a positive CD band (Figures 3.6 and 3.7), a red shift (3 nm) and *hyper*chromicity (%*H* as large as -87) of the Soret band (Table 3.1). We conclude that both Cu(II)**6** and Zn(II)**6** are non-stacking outside binders.

Another method for assessing binding mode is fluorescence. Porphyrins exhibit reduced fluorescence intensity at high *R* followed by increase in fluorescence intensity as *R* decreases. However, Cu(II)**6** does not have usable fluorescence intensity. Because the metal-free porphyrin, [T(*N*-Mepy-4-$CH_2(CH_3)NSO_2Ar$)P]Cl_4 (**6**), exhibits spectral features on addition of CT DNA similar to those found for Cu(II)**6**, we studied **6**. The fluorescence intensity of **6** first decreased and then increased as *R* decreased (Figure 3.10), another finding indicating that non-stacking outside binding at low *R*.[33,50] In view of the similar structures and visible spectral behavior of **6**

and Cu(II)**6**, the fluorescence data support the other results indicating that Cu(II)**6** is a non-self-stacking outside binder.

[Cu(II)T(Et$_3$NCH$_2$CH$_2$)$_2$NSO$_2$Ar)P]Cl$_8$ (Cu(II)7). Cu(II)**7** is also a non-stacking outside binder as evidenced a small red shift (7–11 nm) and (except at high *R* and low salt) *hyper*chromicity of the Soret band (Table 3.5 and Figures 3.8 and B.8). The highest *hyper*chromicity observed for Cu(II)**7** (%*H* = -46) was much lower than that of Cu(II)**6** and Zn(II)**6** because the unbound Cu(II)**7** is not significantly self-stacked. For the Cu(II)**7**-DNA adduct at *R* = 0.005 (100 mM), the magnitude of ε_{So} (3.2×10^5 M^{-1} cm^{-1}) is typical of a non-stacking outside binder.

Other Porphyrins. [T(*N*-Mepy-2-CH$_2$(H)NSO$_2$Ar)P]Cl$_4$ (**1**) and [T(*N*-Mepy-2-CH$_2$(CH$_3$)NSO$_2$Ar)P]Cl$_4$ (**5**) have *N*-Mepy groups similar to those in TMpyP(2), but unlike TMpyP(2), their interaction with CT DNA led to a red shift (8 nm) of the Soret band, *hyper*chromicity, and a positive CD feature (Tables B.3 and B.4). These results indicate that **1** and **5** are non-stacking outside binders. The Soret band of TMpyP(2) was unaffected by interaction with CT DNA, and no *hyper*chromicity or CD signal was observed.[21] Because the *N*-Mepy groups of TMpyP(2) are close to the porphyrin core, steric hindrance between the *N*-Me group and the pyrrole protons prevents the pyridinium group from rotating to become coplanar with the porphyrin core, thus hindering intercalation.[21] However, we suggest that another effect of the *N*-Mepy groups linked via the 2- position in TMpyP(2) is to keep the porphyrin core from interacting tightly with DNA. In this situation, we believe that the porphyrin is tumbling anisotropically (Figure 3.2). Compared to TMpyP(2), the *N*-Mepy groups of [T(*N*-Mepy-2-CH$_2$(H)NSO$_2$Ar)P]Cl$_4$ and [T(*N*-Mepy-2-CH$_2$(CH$_3$)NSO$_2$Ar)P]Cl$_4$ are far from the porphyrin

core and thus do not inhibit the porphyrin core from approaching the DNA closely. We propose proximity is needed for a CD signal to be induced.

3.5 Conclusions

[Cu(II)T(*N*-Mepy-4-$CH_2(CH_3)NSO_2Ar$)P]Cl_4 (Cu(II)**6**), [Zn(II)T(*N*-Mepy-4-$CH_2(CH_3)NSO_2Ar$)P]Cl_4 (Zn(II)**6**), and [Cu(II)T($Et_3NCH_2CH_2)_2NSO_2Ar$)P]Cl_8 (Cu(II)**7**) are non-stacking outside binders with CT DNA, as shown by viscometric studies and by the positive induced CD band and *hyper*chromicity in the Soret region. The decrease in SRV in the competitive viscosity studies reveals that [Cu(II)T(*N*-Mepy-4-$CH_2(CH_3)NSO_2Ar$)P]Cl_4 competes with CuTMpyP(4) in DNA binding. In general, the outside-binding mode is similar in both 10 and 100 mM NaCl. Furthermore, the metal does not influence binding mode, and **6** binds to CT DNA in a similar fashion as Cu(II)**6**.

Most of these new porphyrins contain the same 4-substituted *N*-Mepy group as in TMpyP(4) and in several other known intercalating porphyrins. However, the *N*-Mepy group in the new porphyrins is not directly attached to the porphyrin ring. The lack of such direct attachment means that the porphyrin ring is more electron rich than that of TMpyP(4), but studies with TθF_4TAP have shown that electron-poor porphyrin rings do not lead to intercalation.[32] Our results on new porphyrins having 4-substituted *N*-Mepy groups that can have separations similar to those in intercalating porphyrins indicate that spacing is not the deciding factor. This finding, along with results on porphyrins with *N*-Mepy groups linked at the 2-position, let us conclude that direct attachment of the *N*-alkylpyridinium groups to the porphyrin ring in such a way that the *N*-alkylpyridinium group can become nearly coplanar with the porphyrin ring is necessary for intercalation to occur.

Our current results with [T(*N*-Mepy-4-$CH_2(CH_3)NSO_2Ar$)P]Cl_4 and its derivatives showing that these are outside binders without self-stacking indicate that their behavior is unlike that of TθOPP (another porphyrin with an electron-rich core). TθOPP is an outside binder to DNA exhibiting substantial self stacking.[33] We attribute the difference in stacking propensity (which we view as a matter of degree, differing in the relative abundance of stacked vs unstacked bound porphyrin) to subtle differences involving the interaction of the charged groups with the DNA and also perhaps other interactions such as hydrogen bonding. We note, however, that the new porphyrins with secondary and tertiary sulfonamide groups bind to DNA in a similar manner. Thus, any role of the sulfonamide in hydrogen bonding would be as an H-bond acceptor by the sulfonamide oxygen atoms.

These new porphyrins have various charged groups, but the differences do not affect binding mode. When TMpyP(4) interacts with AT rich regions of DNA as an a non-stacking outside binder, its fluorescence behavior (decrease at high R and increase at low R) is similar to that of **6**. Thus the porphyrin rings of these two rather different porphyrins probably are positioned relative to DNA in a very similar manner.

The same characteristic binding and spectral changes found for new porphyrins with 4-substituted *N*-Mepy groups were also found for [T(*N*-Mepy-2-$CH_2(H)NSO_2Ar$)P]Cl_4 and [T(*N*-Mepy-2-$CH_2(CH_3)NSO_2Ar$)P]Cl_4. These latter contain *N*-Mepy groups attached at the 2-position as in TMpyP(2), a porphyrin that does not exhibit spectral changes upon DNA binding.[21] Our findings indicate that the porphyrin ring of the new porphyrins is close to the DNA when bound in a non-stacking manner, as shown in Figure 3.2. In turn, we conclude that TMpyP(2) tumbles anisotropically, with the porphyrin ring on average farther from the DNA than the porphyrin ring of other porphyrins when these bind outside of DNA (Figure 3.2).

3.6 References

1. Marzilli, L. G. *New J. Chem.* **1990**, *14*, 409-420.

2. Ishikawa, Y.; Yamakawa, N.; Uno, T. *Biorg. Med. Chem.* **2007**, *15*, 5230-5238.

3. Fiel, R. J.; Howard, J. C.; Mark, E. H.; Dattagupta, N. *Nucleic Acids Res.* **1979**, *6*, 3093-3118.

4. Carvlin, M. J.; Dattagupta, N.; Fiel, R. J. *Biochem. Biophys. Res. Commun.* **1982**, *108*, 66-73.

5. Carvlin, M. J.; Fiel, R. J. *Nucleic Acids Res.* **1983**, *11*, 6121-6139.

6. Carvlin, M. J.; Mark, E.; Fiel, R.; Howard, J. C. *Nucleic Acids Res.* **1983**, *11*, 6141-6154.

7. Fiel, R. J. *J. Biomol. Struct. Dyn.* **1989**, *6*, 1259-1275.

8. Fiel, R. J.; Munson, B. R. *Nucleic Acids Res.* **1980**, *8*, 2835-2842.

9. Dixon, D. W.; Schinazi, R.; Marzilli, L. G. *Ann. N.Y. Acad. Sci.* **1990**, *616*, 511-513.

10. Bristow, C.-A.; Hudson, R.; Paget, T. A.; Boyle, R. W. *Photodiagn. Photodyn. Ther.* **2006**, *3*, 162-167.

11. Engelmann, F. M.; Mayer, I.; Gabrielli, D. S.; Toma, H. E.; Kowaltowski, A. J.; Araki, K.; Baptista, M. S. *J. Bioenerg. Biomembr.* **2007**, *39*, 175-185.

12. Kessel, D.; Luguya, R.; Vicente, M. G. H. *Photochem. Photobiol.* **2003**, *78*, 431-435.

13. Munson, B. R.; Fiel, R. J. *Nucleic Acids Res.* **1992**, *20*, 1315-1319.

14. Groves, J. T.; Farrell, T. P. *J. Am. Chem. Soc.* **1989**, *111*, 4998-5000.

15. Han, F. X.; Wheelhouse, R. T.; Hurley, L. H. *J. Am. Chem. Soc.* **1999**, *121*, 3561-3570.

16. Vicente, M. G. H. *Curr. Med. Chem.: Anti-Cancer Agents* **2001**, *1*, 175-194.

17. Ding, L.; Etemad-Moghadam, G.; Cros, S.; Auclair, C.; Meunier, B. *J. Med. Chem.* **1991**, *34*, 900-906.

18. Izbicka, E.; Wheelhouse, R. T.; Raymond, E.; Davidson, K. K.; Lawrence, R. A.; Sun, D. Y.; Windle, B. E.; Hurley, L. H.; Von Hoff, D. D. *Cancer Research* **1999**, *59*, 639-644.

19. Strickland, J. A.; Banville, D. L.; Wilson, W. D.; Marzilli, L. G. *Inorg. Chem.* **1987**, *26*, 3398-3406.

20. Banville, D. L.; Marzilli, L. G.; Strickland, J. A.; Wilson, W. D. *Biopolymers* **1986**, *25*, 1837-1858.

21. Pasternack, R. F.; Gibbs, E. J.; Villafranca, J. J. *Biochemistry* **1983**, *22*, 2406-2414.

22. Gray, T. A.; Yue, K. T.; Marzilli, L. G. *J. Inorg. Biochem.* **1991**, *41*, 205-219.

23. Pasternack, R. F.; Gibbs, E. J.; Villafranca, J. J. *Biochemistry* **1983**, *22*, 5409-5417.

24. Pasternack, R. F.; Gibbs, E. J.; Gaudemer, A.; Antebi, A.; Bassner, S.; Depoy, L.; Turner, D. H.; Williams, A.; Laplace, F.; Lansard, M. H.; Merienne, C.; Perreefauvet, M. *J. Am. Chem. Soc.* **1985**, *107*, 8179-8186.

25. Marzilli, L. G.; Banville, D. L.; Zon, G.; Wilson, W. D. *J. Am. Chem. Soc.* **1986**, *108*, 4188-4192.

26. Lipscomb, L. A.; Zhou, F. X.; Presnell, S. R.; Woo, R. J.; Peek, M. E.; Plaskon, R. R.; Williams, L. D. *Biochemistry* **1996**, *35*, 2818-2823.

27. Ward, B.; Skorobogaty, A.; Dabrowiak, J. C. *Biochemistry* **1986**, *25*, 7827-7833.

28. Trommel, J. S.; Marzilli, L. G. *Inorg. Chem.* **2001**, *40*, 4374-4383.

29. Gibbs, E. J.; Tinoco, I.; Maestre, M. F.; Ellinas, P. A.; Pasternack, R. F. *Biochem. Biophys. Res. Commun.* **1988**, *157*, 350-358.

30. Pasternack, R. F.; Bustamante, C.; Collings, P. J.; Giannetto, A.; Gibbs, E. J. *J. Am. Chem. Soc.* **1993**, *115*, 5393-5399.

31. Marzilli, L. G.; Petho, G.; Lin, M. F.; Kim, M. S.; Dixon, D. W. *J. Am. Chem. Soc.* **1992**, *114*, 7575-7577.

32. McClure, J. E.; Baudouin, L.; Mansuy, D.; Marzilli, L. G. *Biopolymers* **1997**, *42*, 203-217.

33. Mukundan, N. E.; Petho, G.; Dixon, D. W.; Kim, M. S.; Marzilli, L. G. *Inorg. Chem.* **1994**, *33*, 4676-4687.

34. Mukundan, N. E.; Petho, G.; Dixon, D. W.; Marzilli, L. G. *Inorg. Chem.* **1995**, *34*, 3677-3687.

35. Bejune, S. A.; Shelton, A. H.; McMillin, D. R. *Inorg. Chem.* **2003**, *42*, 8465-8475.

36. Wall, R. K.; Shelton, A. H.; Bonaccorsi, L. C.; Bejune, S. A.; Dube, D.; McMillin, D. R. *J. Am. Chem. Soc.* **2001**, *123*, 11480-11481.

37. Shelton, A. H.; Rodger, A.; McMillin, D. R. *Biochemistry* **2007**, *46*, 9143-9154.

38. Andrews, K.; McMillin, D. R. *Biochemistry* **2008**, *47*, 1117-1125.

39. Kano, K.; Minamizono, H.; Kitae, T.; Negi, S. *J. Phys. Chem. A* **1997**, *101*, 6118-6124.

40. Manono, J.; Marzilli, P. A.; Marzilli, L. G., Manuscript in Preparation.

41. Schaffer, H. E.; Sederoff, R. R. *Anal. Biochem.* **1982**, *115*, 113-122.

42. Wells, R. D.; Larson, J. E.; Grant, R. C.; Shortle, B. E.; Cantor, C. R. *J. Mol. Biol.* **1970**, *54*, 465-497.

43. Satyanarayana, S.; Dabrowiak, J. C.; Chaires, J. B. *Biochemistry* **1992**, *31*, 9319-9324.

44. Christoforou, A. M.; Fronczek, F. R.; Marzilli, P. A.; Marzilli, L. G. *Inorg. Chem.* **2007**, *46*, 6942-6949.

45. Saladini, M.; Iacopino, D.; Menabue, L. *J. Inorg. Biochem.* **2000**, *78*, 355-361.

46. Butje, K.; Nakamoto, K. *Inorg. Chim. Acta* **1990**, *167*, 97-108.

47. Spellane, P. J.; Gouterman, M.; Antipas, A.; Kim, S.; Liu, Y. C. *Inorg. Chem.* **1980**, *19*, 386-391.

48. Kalyanasundaram, K. *Inorg. Chem.* **1984**, *23*, 2453-2459.

49. Kano, K.; Takei, M.; Hashimoto, S. *J. Phys. Chem.* **1990**, *94*, 2181-2187.

50. Nyarko, E.; Hanada, N.; Habib, A.; Tabata, M. *Inorg. Chim. Acta* **2004**, *357*, 739-745.

51. McMillin, D. R.; Shelton, A. H.; Bejune, S. A.; Fanwick, P. E.; Wall, R. K. *Coord. Chem. Rev.* **2005**, *249*, 1451-1459.

52. Strickland, J. A.; Marzilli, L. G.; Wilson, W. D. *Biopolymers* **1990**, *29*, 1307-1323.

53. Pasternack, R. F.; Ewen, S.; Rao, A.; Meyer, A. S.; Freedman, M. A.; Collings, P. J.; Frey, S. L.; Ranen, M. C.; de Paula, J. C. *Inorg. Chim. Acta* **2001**, *317*, 59-71.

54. Strickland, J. A.; Marzilli, L. G.; Gay, K. M.; Wilson, W. D. *Biochemistry* **1988**, *27*, 8870-8878.

55. Pasternack, R. F.; Brigandi, R. A.; Abrams, M. J.; Williams, A. P.; Gibbs, E. J. *Inorg. Chem.* **1990**, *29*, 4483-4486.

56. Strickland, J. A.; Marzilli, L. G.; Wilson, W. D.; Zon, G. *Inorg. Chem.* **1989**, *28*, 4191-4198.

57. Yue, K. T.; Lin, M. F.; Gray, T. A.; Marzilli, L. G. *Inorg. Chem.* **1991**, *30*, 3214-3222.

58. Bordbar, A. K.; Mohammadi, K.; Keshavarz, M.; Dezhampanah, H. *Acta Chim. Slov.* **2007**, *54*, 336-340.

59. Lee, M. J.; Jin, B.; Lee, H. M.; Jung, M. J.; Kim, S. K.; Kim, J. M. *Bull. Korean Chem. Soc.* **2008**, *29*, 1533-1538.

60. de Miguel, G.; Perez-Morales, M.; Martin-Romero, M. T.; Munoz, E.; Richardson, T. H.; Camacho, L. *Langmuir* **2007**, *23*, 3794-3801.

61. Dixon, D. W.; Steullet, V. *J. Inorg. Biochem.* **1998**, *69*, 25-32.

62. Maiti, N. C.; Mazumdar, S.; Periasamy, N. *J. Phys. Chem. B* **1998**, *102*, 1528-1538.

63. Wang, Y. T.; Jin, W. J. *Spectrochim. Acta, Part A* **2008**, *70*, 871-877.

64. Martin, M. T.; Prieto, I.; Camacho, L.; Mobius, D. *Langmuir* **1996**, *12*, 6554-6560.

65. Pasternack, R. F.; Centuro, G. C.; Boyd, P.; Hinds, L. D.; Huber, P. R.; Francesconi, L.; Fasella, P.; Engasser, G.; Gibbs, E. *J. Am. Chem. Soc.* **1972**, *94*, 4511-4517.

66. Lugo-Ponce, P.; McMillin, D. R. *Coord. Chem. Rev.* **2000**, *208*, 169-191.

67. Hudson, B. P.; Sou, J.; Berger, D. J.; McMillin, D. R. *J. Am. Chem. Soc.* **1992**, *114*, 8997-9002.

CHAPTER 4. NEW PORPHYRINS BEARING NEGATIVELY CHARGED PERIPHERAL GROUPS LINKED BY SULFONAMIDE BOND TO THE PHENYL GROUP OF TETRA PHENYL PORPHYRIN CORE FOR VIRUCIDAL ACTIVITY

4.1 Introduction

The human immunodeficiency virus (HIV) epidemic continues to have enormous human health consequences. Every 6 seconds, a new person is infected by the virus and every 10 seconds another person dies as a result of AIDS or associated opportunistic infection. [1] Recent studies toward vaccine development have yielded promising results, but a vaccine capable of preventing HIV-1 and HIV- 2 infections is not yet available. The complexity inherent to the viral life cycle and the added problem of a high mutation rate, which leads to the development of resistance to antiviral drugs, warrant a greater effort toward the discovery and development of alternative methods to prevent HIV transmission. Sexual transmission plays a predominant role in the spread of HIV infection, and approaches to prevent such transmission are urgently needed.

One promising approach receiving increasing attention is the development of microbicides which, when applied topically, can prevent viral infection. These compounds could directly interact with HIV virions to decrease or prevent infectivity, thus providing a defense against sexual transmission of the virus. Current clinical trials with the most promising anti-HIV microbicides employ mostly polymeric sulfonates.[2] A number of retroviral agents are already on the market, but these are expensive and studies have shown the virus is resistant to them and have toxic effect. [3] These factors prompted our research group to focus on small molecules that will inhibit entry of the virus into the cell. There have been a number of reports on the antiviral activity of phthalocyanines (**1)** against HIV.[4,5] The photoinactivation of viruses by diamagnetic porphyrins and phthalocyanines has been studied by Horowitz.[6] Photoactivation involves

absorption of light by a compound with resulting production of free radicals and singlet oxygen. Porphyrins and metalloporphyrins have also been shown to have antiviral activity against HIV.

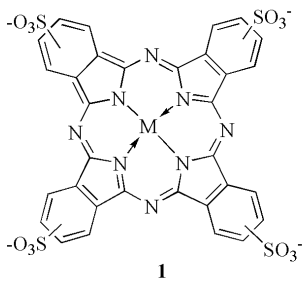

1
PcS

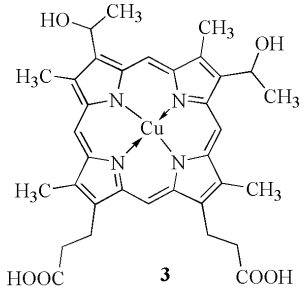

3
CuHPIX

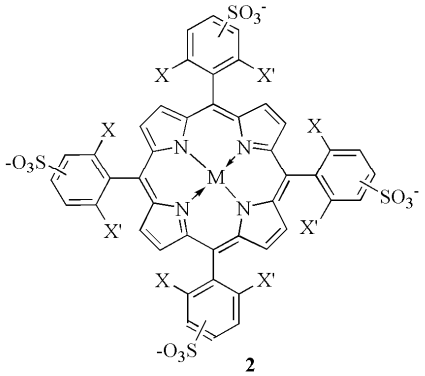

2

TPP(2, 6-F_2)S,Co(III): X = X' = F, M = Co
TPP_2FS: X = F, X' = H, M = H_2
TPP_2ClS: X = Cl, X' = H, M = H_2

Previous studies indicated that some porphyrins inhibit the interaction between the virus envelope protein and its receptors.[2] We have shown[4,7] also that porphyrins block infection by HIV-1 and that this activity appears to be a result of an interaction with the envelope protein. Most of these compounds that were active in blocking HIV-1 were sulfonated. In other studies[8] sulfonated porphyrins (**2)** and some natural porphyrins (**3)** were found to be active against pox virus. The sulfonamide –SO_2NH– group occurs in numerous biologically active compounds, which include antimicrobial drugs, saluretics, carbonic anhydrase inhibitors, insulin-releasing sulfonamides, antithyroid agents and a number of other agents with biological activities.[9]

Amprenavir is an example of a sulfonamide compound that was introduced in the market in 1999 as an HIV protease inhibitor, in spite of the success of this drug it has some shortcomings, including gastrointestinal side effects and long term metabolic disturbances.[10] The aim of my research is to introduce one or more sulfonamide group into different porphyrin derivatives.

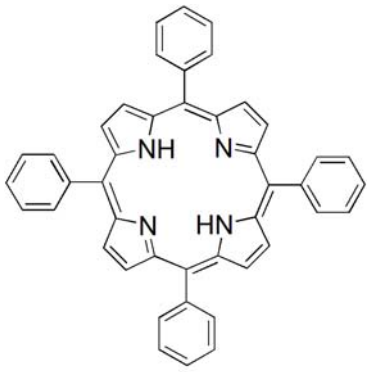

4

5,10,15,20-tetraphenylporphyrin (H_2TPP)

Porphyrins are readily synthesized from pyrrole and aromatic aldehyde derivatives. This porphyrin H_2TPP (**4)** have aromatic groups at the *meso* position, hydrogen substituents on the pyrrole rings, the central N have NH and are organic soluble. Water- soluble porphyrins based in sulphonic groups have been prepared by direct sulfonation with strong sulfuric acid [11,12] Formation of the sulfonic acid derivative limits us from adding other groups to these porphyrins because the only way to form the sulfonamide is by first making the sulfonyl chloride of the porphyrin. Recently Gonsalves et al.[13] synthesized a 5,10,15,20-tetra(4-chlorosulfonylphenyl)porphyrin (**5**) from the parent compound 5,10, 15,20-tetraphenylporphyrin (**4)** by using chlorosulfonic acid. The chlorosulfonyl compound **5** may be converted into derivatives with a variety of nucleophiles so as to give, for example, the free sulfonic acid, a sulfonamide, or a sulfonate ester.[14] The work described here involves preparation of the

chlorosulfonyl porphyrins **5** and **7**, and condensation of different amines with **5** to form sulfonamide derivatives of the porphyrin and some metal complexes.

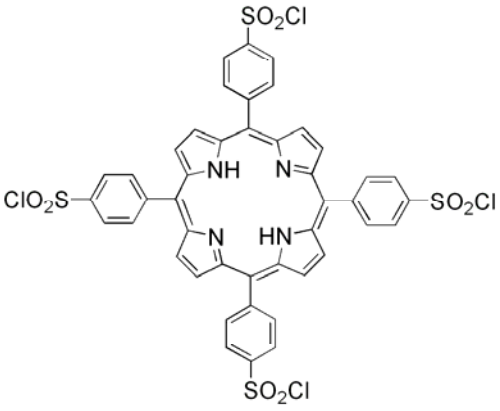

5

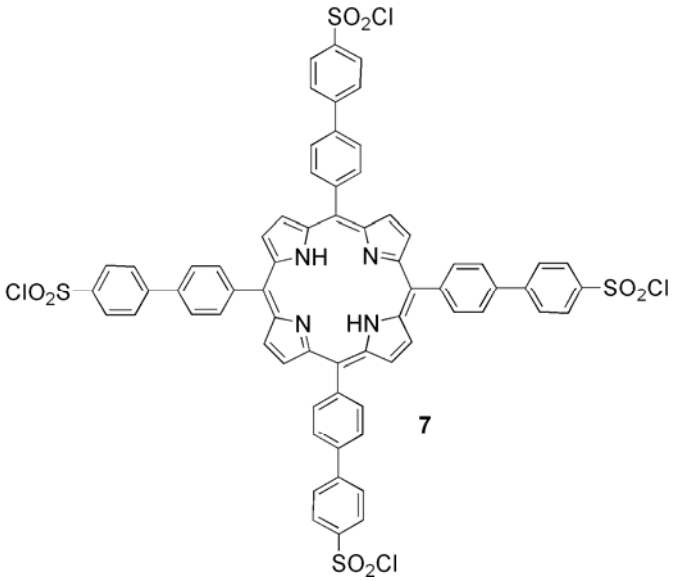

7

4.2 Experimental Section

4.2.1 Materials and Methods. All compounds used in the synthetic chemistry were purchased from Aldrich. 5,10,15,20-tetra(4-chlorosulfonylphenyl)porphyrin ($TClSO_2PP$, **5**) was synthesized by a known method, and the chemical shifts of the NMR spectrum in $CDCl_3$ matched the reported values.[13]

All ^1H NMR spectra were recorded on either a 300 MHz or a 400 MHz Bruker NMR spectrometer. Peak positions are relative to TMS or solvent residual peak, with TMS as reference. Mass spectra for samples dissolved in methanol were obtained at the Mass Spectrometry Facility at LSU on a Hitachi MS-8000 3DQ LC-ion trap ESI mass spectrometer.

Electronic absorption spectra were recorded with a Cary 3 spectrophotometer. ^1H NMR spectra were recorded for DMSO-d_6 and $CDCl_3$ solutions on a Bruker 300 MHz or 400 MHz

spectrometer. Peak positions are relative to TMS. All NMR data were processed using the XWINNMR and Mestre-C softwares.

4.2.2 Sulfonation of the Benzylamine Derivatives. (a) Benzylamine (0.046 mmol, 5 mL) was placed into a 250 mL round-bottomed flask; the flask was placed in an ice bath, and fuming H_2SO_4 (12.5 mL, 0.242 mmol) was added very slowly.[12] The mixture was left stirring for 6 h in a steam water bath, then removed and left stirring at room temperature overnight. HPLC water (50 mL) was added cautiously to the reaction mixture, and immediately a white precipitate formed, which was vacuum filtered and washed several times with absolute alcohol and dried under vacuum to yield 4-(aminomethyl)benzenesulfonic acid (**15**); yield, 87.5 mg, ~ 90%. The purity of the compound was checked by NMR spectroscopy. ^{1}H NMR (ppm) in D_2O: 7.8 (2H, d, ArH); 7.64 (2H, d, ArH); 4.20 (2H, s, CH_2).

(b) Trifluoroacetic acid anhydride (TFAA) (30 mL, 0.21mol) was added to conc. H_2SO_4 (10 g, 0.1 mol) with cooling (ice water) in a dry atmosphere and stirred for 3 h, after which complete dissolution of H_2SO_4 was achieved; the solution was light brown. 3-iodobenzylamine (0.1 mol, 23.3g) was added dropwise to the cooled solution, and this solution was heated at reflux for 10 min.[15] Water was added dropwise with cooling (ice water).The yellowish precipitate was washed with absolute ethanol several times to remove trifluoroacetic acid (TFA),filtered and dried under vacuum to yield 4-(aminomethyl)-2-iodobenzenesulfonic acid (**16**) yield, 45 mg, ~ 62%. The purity of the compound was checked by NMR spectroscopy. ^{1}H NMR (ppm) in DMSO-d_6: 8.99 (8H, s, β-pyrrole), 8.56 (8H, d, ArH); 8.37 (8H, d, ArH); 7.72 (8H, d, ArH; 7.48 (8H, d, ArH); 4.40 (8H, s, CH_2); -2.87 (s, 2H, NH).

5,10,15,20-tetra(4-sulfonamidophenyl)porphyrin (8): Ammonia (conc. 35% w/V; 25 mL) was added to **5**; (100 mg, 0.099 mmol) in dichloromethane (25 mL) and stirred for 1 h at

room temperature The precipitate formed was collected by filtration to give the crude sulfonamide. This solid was washed with dichloromethane, crystallized from acetone/dichloromethane (1:1) and dried under vacuum to give the solid 5,10,15,20-tetra(4-sulfonamidophenyl)porphyrin (**8**), yield 45 mg, 48.8%. The purity of **8** was checked by NMR spectroscopy. ^{1}H NMR (ppm) in DMSO-d_6): δ 8.83 (8H, s,β-pyrrole), 8.41 (8H, d, ArH); 8.27 (8H, d, ArH); 7.51 (4H, br, NH); -2.97 (s, 2H, NH).

5,10,15,20-tetra(4-isopropylsulfonamidophenyl)porphyrin (9): Isopropylamine (28.96 mg, 0.49mmol) was added to **5** (100 mg, 0.099 mmol) in chloroform (25 mL); the mixture was left stirring at room temperature for 48 h. The solution was evaporated to dryness and the compound was recrystallized from $CHCl_3$/MeOH (90:10); yield, 65 mg, 60%. The purity of 5,10,15,20-tetra(4-isopropylsulfonamidophenyl)porphyrin (**9**) was checked by NMR spectroscopy. ^{1}H NMR (ppm) in DMSO-d_6: 8.804 (8H, s,β-pyrrole), 8.42 (8H, d J = 8.1 Hz, ArH); 8.22 (8H, d J = 8.4 Hz, ArH); 3.56(4H, m CH); 1.14(24H, d, J = 6.6Hz, CH_3); -2.97 (s 2H, NH).

5,10,15,20-tetra(4-phenylsulfonamidophenyl)porphyrin (10): Aniline (46.09 mg, 0.495mmol) was added **5** (100 mg, 0.099 mmol) in chloroform (25 mL) The reaction mixture was left stirring at room temperature for 4 h and was then concentrated by rotary evaporation. With dichloromethane as the eluent, the resulting solid was passed through a silica gel column. The collected fraction was concentrated and the solution treated with n-hexane to induce recrystallization; yield, 37 mg, 30%. The purity of 5,10,15,20-tetra(4-phenylsulfonamidophenyl)porphyrin (**10)** was checked by NMR spectroscopy. ^{1}H NMR (ppm) in DMSO-d_6: 10.50 (4H,br,NH); 8.65 (8H, s, β-pyrrole), 8.35 (8H, d, ArH), 8.14 (8H, d, ArH), 7.44 (20H, m, ArH), -3.09 (s, 2H, NH).

5,10,15,20-tetra(4-toluinylsulfonamidophenyl)porphyrin (11): p-toluidine (158 mg, 1.47 mmol) was added to **5** (100 mg, 0.099 mmol) in chloroform (25 mL), pyridine (10 mL) was also added and the resulting solution heated at reflux for 24 h. After it had cooled to room temperature, the solution was washed with 10% HCl. The organic layer was separated and washed with cold distilled water until the pH of the washing water was neutral. The organic phase was dried over anhydrous sodium sulfate and evaporated to dryness. The final product that precipitated from chloroform, was vacuum filtered and vacuum dried; Yield, 30mg, ~24% The purity of 5,10,15,20-tetra(4-toluinylsulfonamidophenyl)porphyrin (**11)** was checked by NMR spectroscopy. ^{1}H NMR (ppm) in $CDCl_3$: 8.63 (8H, s, β-pyrrole), 8.19 (8H, d, ArH), 8.13 (8H, d, ArH), 7.27 (8H, d, ArH), 7.16 (8H, d, ArH), -2.97 (s, 2H, NH).

5,10,15,20-tetra(4-{3'-iodobenzyl}sulfonylamidophenyl)porphyrin (12): 3-Iodobenzylamine (230.64 mg, 0.99 mmol) was added to **5** (100 mg, 0.099 mmol) in dry acetonitrile (25 mL). The reaction mixture was left stirring at room temperature for 4h. The suspension was filtered, and the residue was washed several times (3 x 15 mL) with ethyl acetate and left in the filter to dry; yield, 120 mg, 67%. The purity of the compound 5,10,15,20-tetra(4-{3′-iodobenzyl}sulfonylamidophenyl)porphyrin (**12**) was checked by NMR spectroscopy. ^{1}H NMR (ppm) in DMSO-d_6: 8.65 (8H, s, β-pyrrole), 8.63 (4H,b,NH), 8.40 (8H, d, ArH), 8.21 (8H, d, ArH), 7.81 (4H, s, ArH), 7.72 (4H, d, ArH), 7.45(4H, d, ArH), 7.23 (4H, m, ArH), 4.34 (8H, s, CH_2), -2.98 (s, 2H, NH).

5,10,15,20-tetra(4-{3'-fluorobenzyl}sulfonylamidophenyl)porphyrin (13): 3-Fluorobenzylamine (227.7 mg, 0.99 mmol) was added to **5** (100 mg, 0.099 mmol) in dry acetonitrile (25 mL). The reaction mixture was left stirring at room temperature for 4 h. There were some precipitate at the end of the reaction which was filtered, washed with ethyl acetate

and the residue was left in the filter to dry; yield, 95 mg, 71%. The purity of 5,10,15,20-tetra(4-{3′-fluorobenzyl}sulfonylamidophenyl)porphyrin (**13**) was checked by NMR spectroscopy. ^{1}H NMR (ppm) in DMSO-d_6: δ 8.79 (8H, s β-pyrrole), 8.65 (4H, b, NH), 8.38 (8H, d, ArH), 8.19 (8H, d, ArH), 7.44 (4H, d, ArH), 7.26(12H, m, ArH), 4.40 (8H, s, CH_2), -3.0 (s, 2H, NH).

5,10,15,20-tetra(4-benzylsulfonamidophenyl)porphyrin (14): Benzylamine (42.4 mg, 0.395 mmol) was added to **5** (50 mg, 0.049 mmol) in dry acetonitrile (25 mL). The reaction mixture was left stirring at room temperature for 4 h. The reaction mixture was filtered, and the residue washed with ethyl acetate. The filtrate was evaporated to dryness; yield, 38 mg, 76%. The purity of **14** was checked by NMR spectroscopy. ^{1}H NMR (ppm) in DMSO-d_6: 8.81 (8H, s, β-pyrrole), 8.63 (4H, br, NH), 8.37 (8H, d, ArH), 8.19 (8H, d, ArH), 7.40 (20H, m, ArH), 4.35 (8H, s, CH_2), -3.00 (s, 2H, NH).

5,10,15,20-tetra(4-{p-sulfonbenzyl}sulfonylamidophenyl)porphyrin (15): 4-(aminomethyl)benzenesulfonic acid (65.5 mg, 0.35 mmol) was added to **5** (70 mg, 0.069 mmol) in dry acetonitrile (5 mL), and anhydrous K_2CO_3 (70 mg, 0.5 mmol) Anhydrous methanol (1 mL) was also added, and the mixture was sealed and left stirring at room temperature for 12 h. The reaction mixture was filtered to give a reddish powder. The red powder was left to dry on the filter paper before purifying as follows: small amount of the residue was dissolved in a minimal volume of HPLC water and passed through a Sephadex LH20 column. With methanol as an eluant, a red fraction was collected, concentrated and acetone added to recrystallize; Yield, 45 mg, 62%. The purity of 5,10,15,20-tetra(4-{*p*-sulfonbenzyl}sulfonylamidophenyl)porphyrin (**15)** was checked by NMR spectroscopy. ^{1}H NMR (DMSO-d_6): δ 8.91 (8H, s, β-pyrrole), 8.48 (8H, d, ArH); 8.29 (8H, d, ArH); 7.64 (8H, d, ArH; 7.40 (8H, d, ArH); 4.32 (8H, s, CH_2); -2.87 (s, 2H, NH). ESI-MS(m/z): $[M-4H]^{4-}$ = 401.53. Calcd for $[M - H]^{4-}$ = 401.94.

5,10,15,20-tetra(4-{3′-iodosulfonbenzyl}sulfonylamidophenyl)porphyrin 16: 4-(aminomethyl)-3-iodobenzenesulfonic acid (82.1 mg, 0.245 mmol) was added to **5** (50 mg, 0.049 mmol) in dry acetonitrile (5 mL), and anhydrous K_2CO_3 (33.8 mg, 0.245 mmol). Anhydrous methanol (1 mL) was also added and the mixture was sealed and left stirring at room temperature for 12 h. The reaction mixture was filtered and the residue was left to dry on the filter paper and then further purification of the residue was carried out as follows:

A small amount of the residue was dissolved in a minimal volume of HPLC water and passed through a Sephadex LH20 column. With methanol as an eluant, the red fraction was collected, concentrated, and treated with acetone to induce crystallization; yield, 71.6 mg, 67%. The purity of 5,10,15,20-tetra(4-{3′-iodosulfonbenzyl}sulfonylamidophenyl)porphyrin **16** was checked by NMR spectroscopy and ^{1}H NMR (ppm) in DMSO-d_6: 8.82 (8H, s, β-pyrrole), 8.38 (12H, d, ArH and NH), 8.17 (8H, d, ArH), 7.83 (4H, s, ArH), 7.75 (4H, d, ArH), 7.59 (4H, d, ArH), 4.79 (8H, s, CH_2), -2.98 (s, 2H, NH).

5,10,15,20-tetra(4-{3′-fluorosulfonbenzyl}sulfonylamidophenyl)porphyrin 17: 4-(aminomethyl)-3′-fluorobenzenesulfonic acid (55.6 mg, 0.245 mmol) was added to **5** (50 mg, 0.049 mmol) in dry acetonitrile (5 mL), and anhydrous K_2CO_3 (33.8 mg, 0.245 mmol). Anhydrous methanol (1 mL) was also added and the mixture was sealed and left stirring at room temperature for 12 h. The reaction mixture was filtered and the residue was left to dry on the filter paper and then further purification of the residue was carried out as follows:

A small amount of the residue was dissolved in a minimal volume of HPLC water and passed through a Sephadex LH20 column. With methanol as an eluant, the red fraction was collected, concentrated, and treated with acetone to induce crystallization; yield, 51.2 mg, 61%. The purity of 5,10,15,20-tetra(4-{3′-fluorosulfonbenzyl}sulfonylamidophenyl)porphyrin **17** was

checked by NMR spectroscopy and ^{1}H NMR (ppm) in DMSO-d_6): δ 8.79 (8H, s, β-pyrrole), 8.50(4H, t, NH), 8.47 (8H, d, ArH), 8.18 (8H, d, ArH), 7.24 (4H, s, ArH), 7.17(4H, m, ArH), 4.82 (8H, s, CH_2), -2.98 (s, 2H, NH). ESI-MS(m/z): $[M-4H]^{4-}$ = 419.52. Calcd for $[M - H]^{4-}$ = 419.93.

5,10,15,20-tetra(4-{1′sulfonaphthalene-N-5′-amino-ethyl}sulfonamidophenyl)porphyrin (18): 5-(2-aminoethylaminonaphthalene sulfonic acid (148.2 mg, 0.49 mmol) was added to **5** (100 mg, 0.098 mmol) in dry acetonitrile (5 mL), and anhydrous K_2CO_3 (68 mg, 0.49 mmol) Anhydrous methanol (1 mL) was also added and the mixture was sealed in a pressure proof flask and left stirring at room temperature for 12 h. The reaction mixture was filtered to give a brown solid that was dried before purifying. The brown residue was dissolved in a minimal volume of HPLC water and passed through a Sephadex LH20 column. With methanol as an eluant, the red fraction was collected, concentrated and treated with acetone to induce recrystallization; yield, 73 mg, ~ 70%. The purity of 5,10,15,20-tetra(4-{1′sulfonaphthalene-*N*-5′-amino-ethyl}sulfonamidophenyl)porphyrin (**17**) was checked by NMR spectroscopy. ^{1}H NMR (ppm) in DMSO-d_6: 8.82 (8H, s, β -pyrrole), 8.46 (8H, ArH), 8.31 (8H, d, ArH), 8.26 (4H,b,NH), 8.20 (8H, dd, ArH), 7.94 (4H, d, ArH), 7.32 (8H, dd, ArH), 6.56 (4H, d, ArH), 6.16 (s, 2H, NH), 3.40 (16H, s, CH_2), -2.99 (s, 2H, NH). ESI-MS(m/z): $[M-4H]^{4-}$ = 480.58. Calcd for $[M - H]^{4-}$ = 480.04.

Cu(II)-5,10,15,20-tetra(4-{p-sulfonylbenzyl}sulfonylamidophenyl)porphyrin: 5,10,15,20-tetra(4-{*p*-sulfonylbenzyl}sulfonylamidophenyl)porphyrin (**15**) (100 mg, 0.058 mmol) was dissolved in water (5 mL) and treated with 0.11 mmol of CuO; the reaction mixture was left stirring at room temperature for 12 h. The reaction was followed b y UV-vis spectroscopy and stopped after the Q band had shifted from 515 nm to 539 nm.(Figure 3.6) The

solution was filtered through 20 μm filter and the filtrate concentrated by rotary evaporation and passed through a cationic exchange column (Na^+ form to remove excess copper). The fraction collected was evaporated to dryness and the compound dried under vacuum.

5,10,15,20-tetra(4-{p-sulfonbenzyl}sulfonamidophenyl)porphyrinPd(II): 5,10,15,20-tetra(4-{*p*-sulfonbenzyl}sulfonamidophenyl)porphyrin **(15)**(50 mg, 0.029 mmol) was suspended in an acetate buffer (pH 4 – 5) solution containing potassium tetrachloropalladate (47.33 mg, 0.145 mmol) and the solution was heated at reflux for 1 to 2 h until the green solution changed color to orange. The solution was concentrated using a rotary evaporator. Ethanol was added and the solution was filtered to remove sodium acetate. The solution was evaporated to dryness and a small amount of water added to dissolve the residue; this solution was then passed through a cationic exchange column (Na^+) to exchange the potassium ions with sodium ions. The solution was evaporated to dryness to yield the Pd^{2+} derivative of porphyrin. UV-vis spectroscopy in water (Soret band at 408 nm and Q-band at 523 nm). The purity of the Pd(II) 5,10,15,20-tetra(4-{*p*-sulfonbenzyl}sulfonamidophenyl) porphyrin was checked by NMR spectroscopy. ^{1}H NMR (ppm) in DMSO-d_6: 8.86 (8H, s, β-pyrrole), 8.43 (8H, d, ArH), 8.27 (8H, ArH), 7.64 (8H, ArH), 7.40 (8H, d, ArH), 4.32 (8H, s, CH_2).

4.3 Results and Discussion

Chlorosulfonic acid in Scheme 4.1 readily protonates the porphyrin ring of 5,10,15,20-tetraphenylporphyrin **(4)**, thereby deactivating the pyrrolic positions and directing electrophilic substitution to any *meso* aryl groups which may be present. The advantage of chlorosulfonation over sulfonation using concentrated sulfuric acid is that the initially formed chlorosulfonyl compounds are easily isolated from the reaction medium because they are insoluble in water but soluble in organic solvents. The chlorosulfonyl group can easily be hydrolyzed to its water

soluble by-product by heating 5,10,15,20-tetra(4-chlorosulfonylphenyl)porphyrin (**5)** at reflux in water for 12 h.

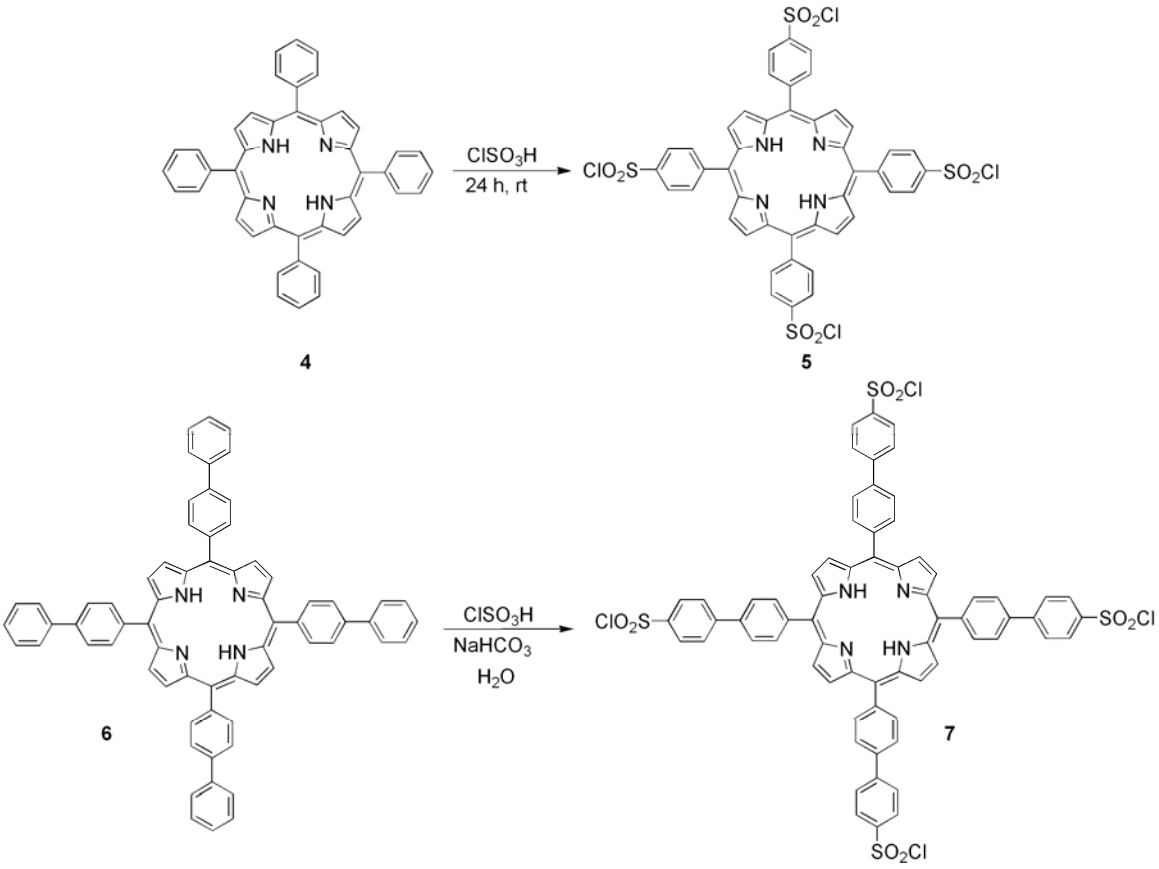

Scheme 4.1. Chlorosulfonation of 5,10,15,20-tetraphenylporphyrin (**4**) and 5,10,15,20-tetrabiphenylporphyrin (**6**).

The ^{1}H NMR spectrum of the parent compound **4** in DMSO-d_6 (Figure 4.1) has four peaks assigned to the pyrrolic protons, the *m*-, *p*-, and *o*- protons and the inner NH protons. There was a downfield shift of the chlorosulfonyl phenyl group compared to the signals in the parent compound **4** (~0.19ppm) and an upfield shift of the *m*-proton.(~0.05ppm) In addition, the *p*-H signal was missing, as expected from chlorosulfonation at the para position of the parent **4**. ^{1}H NMR spectroscopy of **5** (Figure 4.2) in DMSO-d_6 showed clearly that the compound was successfully synthesized. Because the porphyrin is symmetric, it should have only three peaks, a

singlet assigned to eight pyrrolic protons and two doublets, each assigned to the *meso* aryl group eight *ortho* protons and eight *meta* protons.

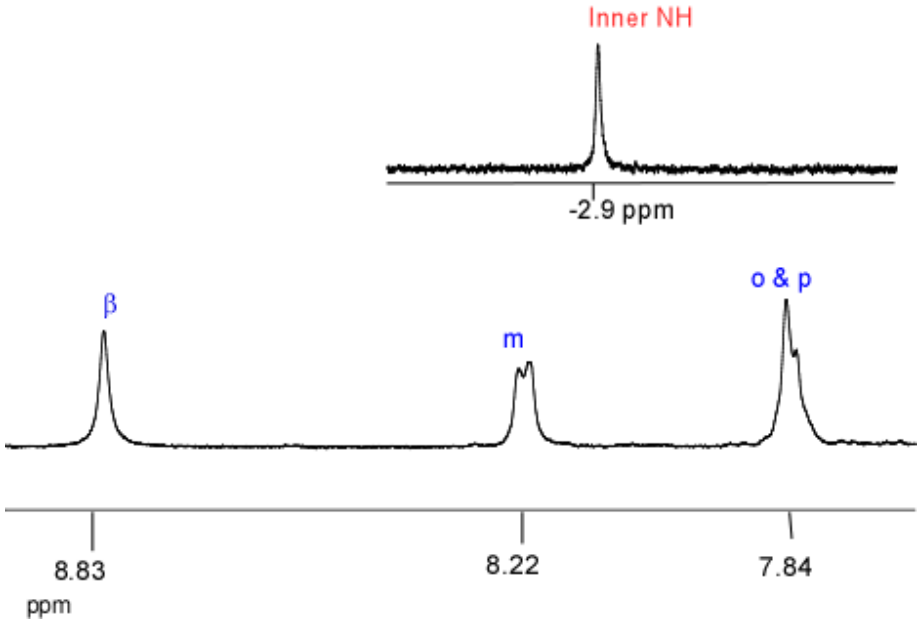

Figure 4.1. ^{1}H NMR spectrum for 5,10,15,20-tetraphenylporphyrin (**4**).

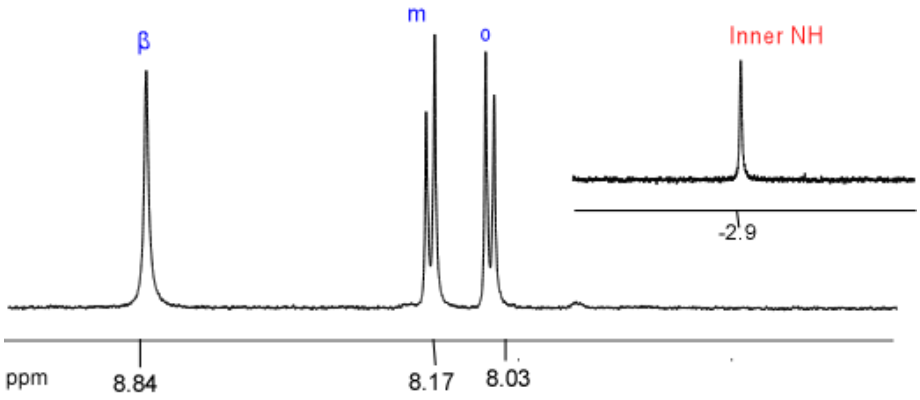

Figure 4 .2. ^{1}H NMR, spectrum for 5,10,15,20-tetra(4-chlorosulfonylphenyl)porphyrin (**5**).

The chlorosulfonyl compound **5** was reacted with a series of amines, to give the sulfonamide derivative of the porphyrin. Scheme 4.2 depicts the porphyrin sulfonamide derivatives synthesized.

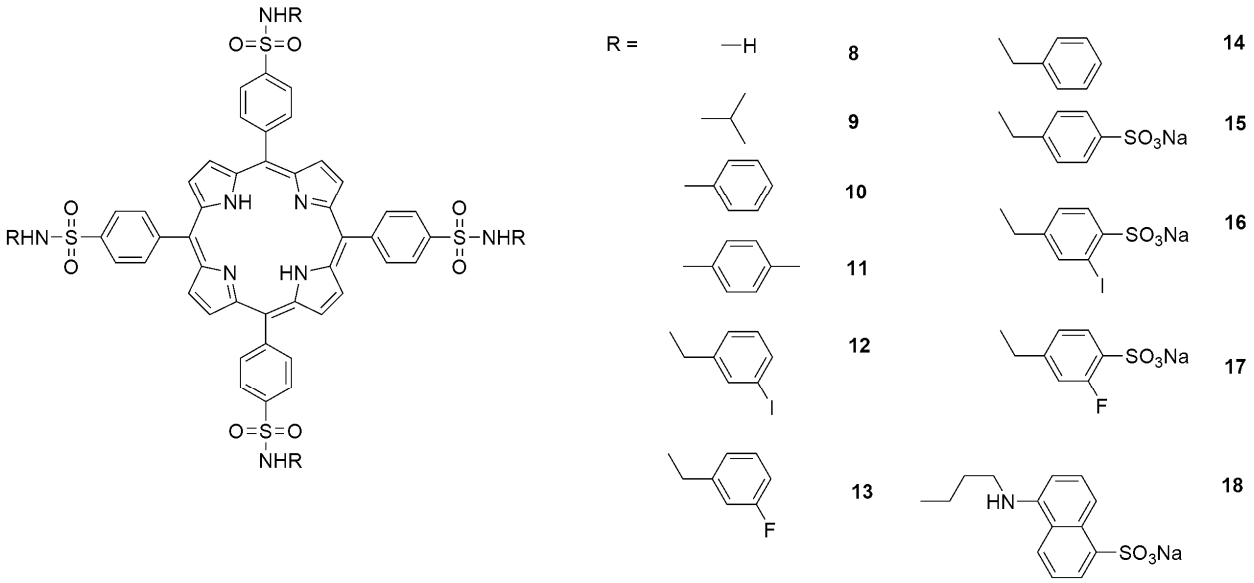

Scheme 4.2. porphyrin sulfonamide derivatives synthesized

The products of the reaction of the chlorosulfonyl compound **5** with amines (Scheme 4.2) were assessed by ^{1}H NMR spectra in different solvents. The reaction of **5** with aqueous ammonia hydroxide (35%) was used as a model for the synthesis of the rest of the sulfonamides. The reaction was successful and it yielded~90% of the 5,10,15,20-tetra(4-sulfonamidophenyl)porphyrin (**15**) and ~10% of the hydrolyzed derivative of compound (**5**). This was confirmed by ^{1}H NMR spectra (Figure 4.3) of the product in DMSO-d_6, which had a set of two peaks for the phenyl protons corresponding to the two compounds formed. The chemical shift of the pyrrolic protons was not affected by the sulfonamide group, but there was a downfield shift (~0.24ppm) of the phenyl signal (*o*- and *m*-) due the electron-withdrawing effect of the sulfonamide group compared to the phenyl signals of compound **5** (Figure 4.3).

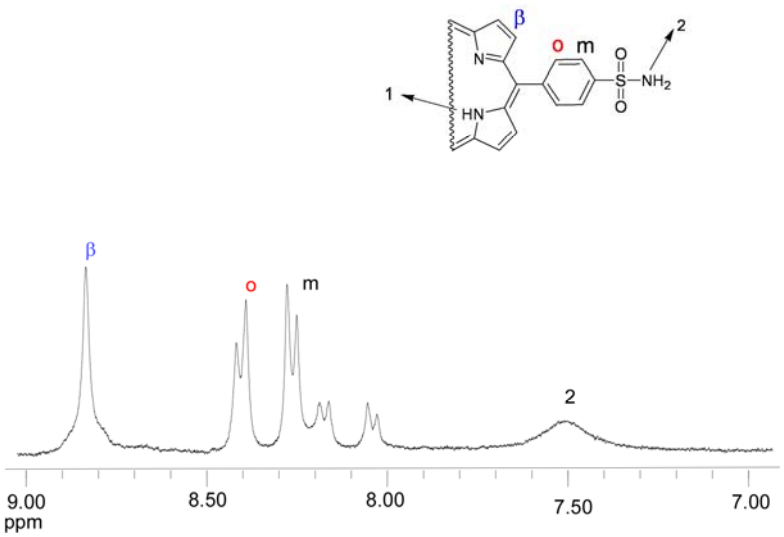

Figure 4.3. ^{1}H NMR, spectrum for 5,10,15,20-tetra(4-sulfonamidophenyl)porphyrin (**15**).

For all the compounds synthesized the porphyrin peaks and the NH signal of the sulfonamide had approximately the same chemical shifts (pyrrolic signals ~8.82 ppm, phenyl signals ~8.40 ppm and 8.21 ppm and the sulfonamide NH signal at ~8.63 ppm) which were characteristic and aided in confirming the synthesis of the sulfonamide compound.

Attempts to chlorosulfonate the sulfonamide derivative **14** at different temperatures (-10 to 10 ^{o}C) failed and led to cleavage of the sulfonamide bond.[16]

Reaction of compound **5** with amines with electron-withdrawing groups was not successful and resulted mainly in hydrolysis of the porphyrin to its sulfonic acid derivative. The electron-withdrawing groups especially at the *o*- and *p*- position of the aryl amines decrease the basicity of the amine. However, the conditions of the reaction of the chlorosulfonyl compound, **5**, with benzylamine derivatives with sulfonic acid groups were optimized. In particular, 4-(aminomethyl)benzenesulfonic acid and **5** reacted to give the 5,10,15,20-tetra(4-{*p*-sulfobenzyl}sulfonylamidophenyl)porphyrin. (**15**) Figure 4.4 shows the ^{1}H NMR spectrum of the compound.

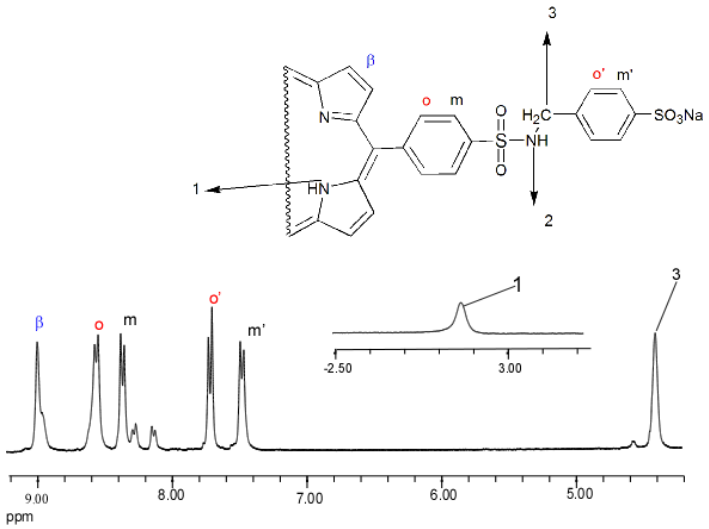

Figure 4.4. [1]H NMR, spectra for 5,10,15,20-tetra(4-{*p*-sulfobenzyl}sulfonylamidophenyl)porphyrin.

Metallation of the 5,10,15,20-tetra(4-{*p*-sulfobenzyl}sulfonylamidophenyl) porphyrin (**15)** with potassium tetrachloropalladate was confirmed by both NMR spectroscopy and UV-vis spectroscopy. [1]H NMR spectra showed that the inner NH signals of the porphyrin were missing, as the NH's were replaced by the metal ion (Figure 4.5); UV-vis spectra showed that the Soret 414 nm band of **15** had shifted to 408 nm, while the Q-bands typical of free base porphyrin (515 nm, 530 nm, 582 nm, 637 nm) had collapsed to one band at 523 nm(Figure 4.6).

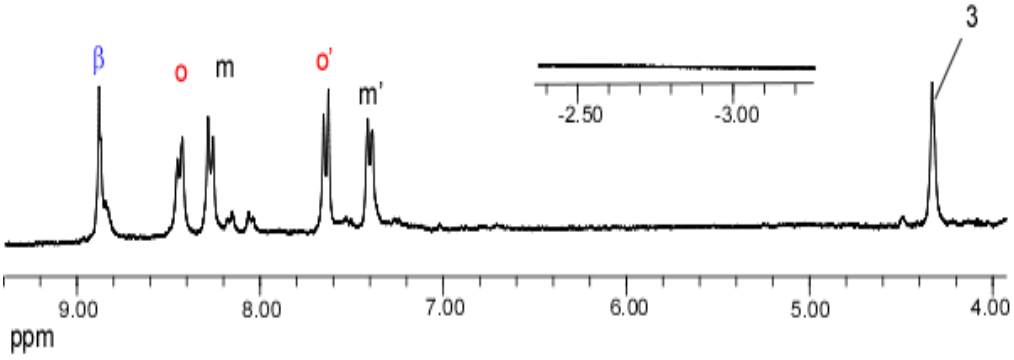

Figure 4.5. [1]H NMR, spectra for 5,10,15,20-tetra(4-{*p*-sulfobenzyl}sulfonylamidophenyl)porphyrin Pd(II).

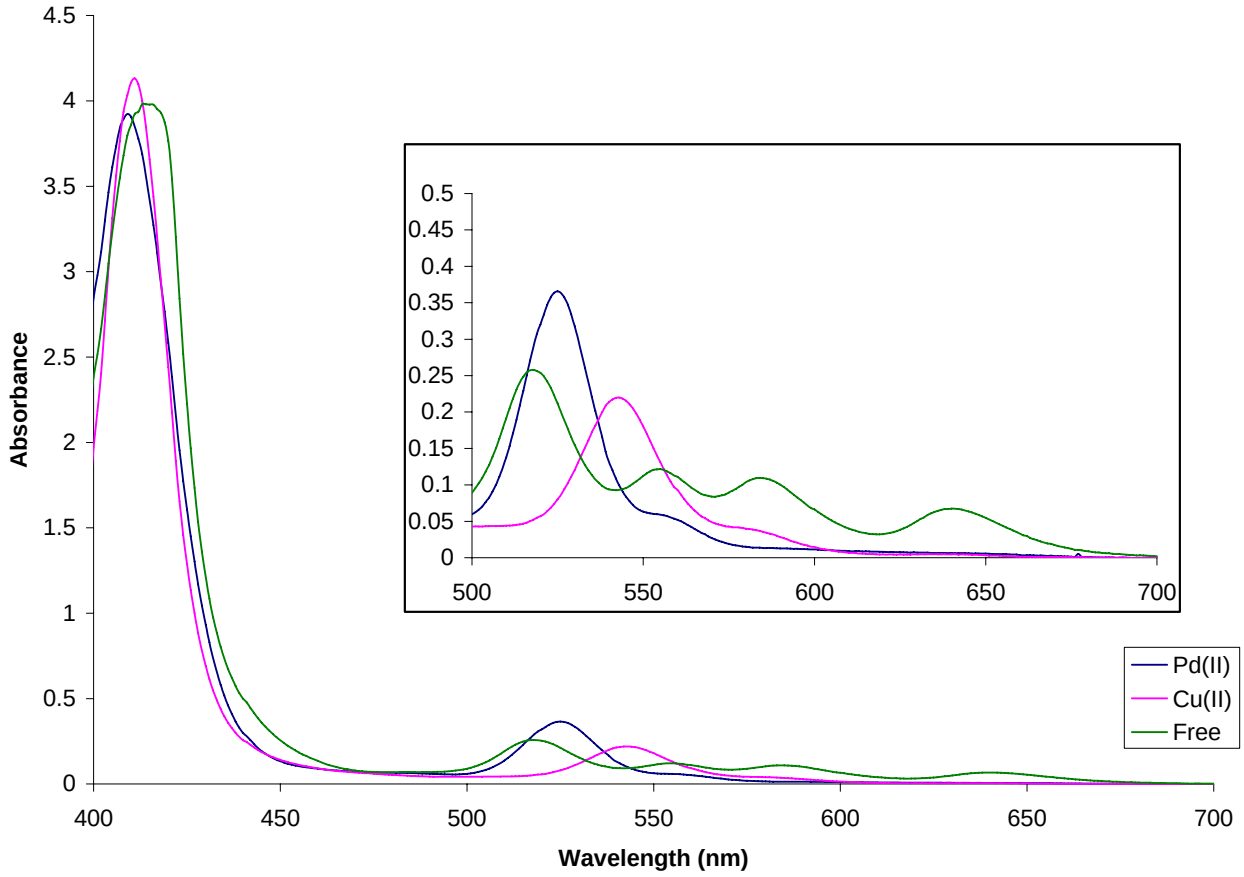

Figure 4.6. Absorption spectrum of 5,10,15,20-tetra(4-{*p*-sulfobenzyl}sulfonylamidophenyl)porphyrin Free base (green), Pd(II) (blue) and Cu(II) (pink), derivative.

Also, copper metallation was successfully carried under the same conditions Figure 4.6 shows the UV-spectrum of the 5,10,15,20-tetra(4-{*p*-sulfobenzyl}sulfonylamidophenyl)porphyrin Cu(II). Also the tetra(4-sulfonatobiphenyl)porphyrin was metallated to its copper (II) compound. Figure 4.7 shows the UV-spectrum of the Cu(II) compound.

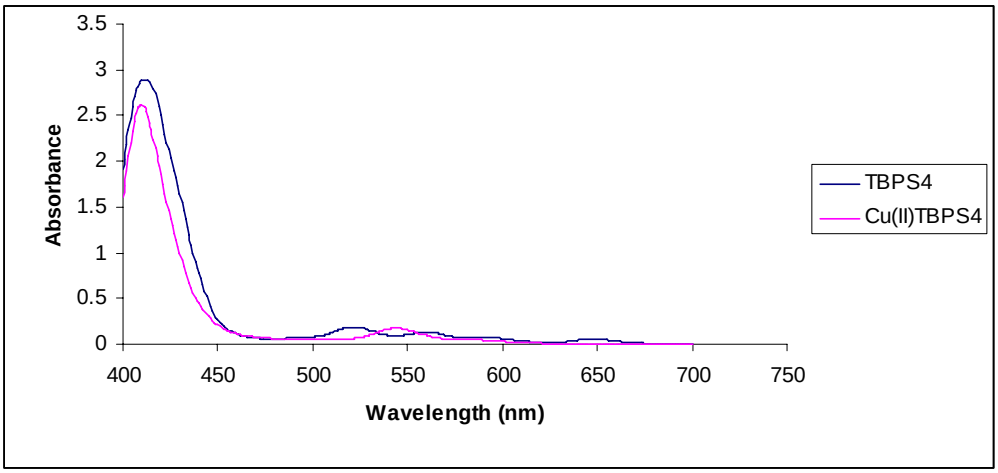

Figure 4.7. Absorption spectra of tetra(4-sulfonatobiphenyl)porphyrin ($TBPS_4$) and its copper derivative, showing both the Soret band and the Q-bands.

The antiviral activity against Equine Herpesvirus Type 1 of 5,10,15,20-tetra(4-{*p*-sulfobenzyl}sulfonylamidophenyl) porphyrin Cu(II) is under study.

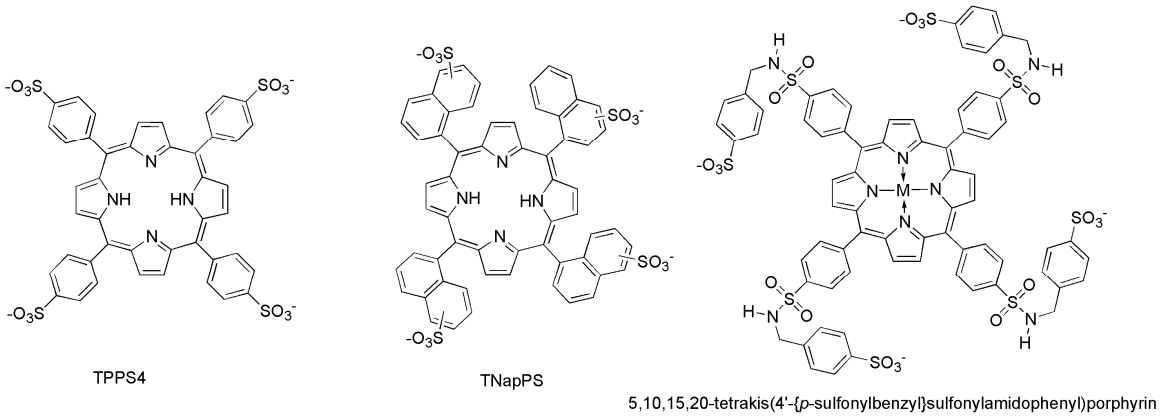

Figure 4 8. Structures of porphyrins studied and porphyrin synthesized**.**

Previous studies have shown that certain porphyrins show antiviral activity against HIV and in some cases virucidal activity. Among these porphyrins the natural porphyrin (Protophyrin, hematoporphyrin) and metallloporphyrins have been shown to have acitivity aginst HIV in the micromolar range in such antiviral assays. Also other synthetic porphyrins namely the sulfonated derivatives of the tetraphenylporphyrin have also been shown to be active against HIV-1, HSV-1 and HSV-2. In other studies the metalloderivatives without axial ligands (TPPS4 and its Cu

chelate) had the highest activity against HIV-1 (Figure 4.8). Sulfonated derivatives of TPP with halogen groups at different position (2, 6-difluoro-meso-tetraphenylporphine and its copper chelate, and sulfonated porphyrin with one chloro at the fourth position were shown to inhibit the HIV virus. Sulfonated tetranaphthyl porphyrin (TNaPS) and tetra-anthracenyl porphyrin (TAnthPS) were also found to be very active against HIV-1 virus. TNaPS (Figure 4.8) was showed higher activity against pox virus and HIV-1 virus.[8],[7] This suggests that modified porphyrins with extended structure would be more active against the different viruses.Another class of compounds which is related to the porphyrins are the sulfonated pthalocyanines and its copper chelate which previously have shown activity against HIV-1.[4,7]

For virucidal activity one important characteristic is that the agent should be not phototoxic. Previous studies have shown that the different porphyrins with paramagnetic metals [Cu(II), Fe(III)] in its core had the highest activity against HIV-1. Porphyrins synthesized in this proposal are expected to have better virucidal activity against HIV-1 and other related viruses since they are related structurally to the already studied porphyrin compounds. The porphyrin synthesized has more advantages over the already studied ones since it has a sulfonamide group in addition to the sulfonic acid groups which is found in numerous biologically active compounds, which includes antimicrobial drugs and also its an extended molecule.. Amprenavir is an example of a sulfonamide compound that was introduced in the market in 1999 as a HIV protease inhibitor.[10]

4.4 Conclusion

Reaction of the 5,10,15,20-tetra(4-chlorosulfonylphenyl)porphyrin (**5**) with a series of amines was successful and confirmed by ^{1}H NMR spectroscopy. From ^{1}H NMR spectra of all the compounds synthesized it was observed that at least 90% of the target compounds were present

while 10% was the product of hydrolysis of compound **5**. Attempts to separate the hydrolysis compound from the target compound failed. Conditions for coupling amines with sulfonic acid groups at different positions were optimized. Metallation of the sulfonamide porphyrin derivatives with Cu^{2+}, Pd^{2+} was successful and afforded excellent yields.

4.5 Current and Future Work

Current work involves the purification of the sulfonamide porphyrin derivatives since from the ^{1}H NMR spectroscopy the compound contains 10% of the hydrolyzed compound. More reactions of 5,10,15,20-tetra(4-chlorosulfonylphenyl)porphyrin (**5**) with amines with different substituents especially electron withdrawing groups preferably halogenated groups at different positions will be carried. Also conjugation of 5,10,15,20-tetra(4-chlorosulfonylbiphenyl)porphyrin (**7**) with different amines will be done. Other porphyrins such as acyl chloride derivative of 5,10,15,20-tetraphenylporphyrin will be synthesized and its conjugations with different amines studied. All the compounds synthesized will be provided to virologist for testing against several viruses.

4.6 References

1. Warner, C. G. *Nat. Immunol.* **2004**, *5*, 867-871.

2. Song, R.; Witvrouw, M.; Schols, D.; Robert, A.; Balzarini, J.; De Clercq, E.; Bernadou, J.; Meunier, B. *Antiviral Chem. Chemother.* **1997**, *8*, 85-97.

3. Asim, K. D.; Shibo, J.; Nathan, S.; Kang, L.; Paul, H.; Robert, N. *J. Med. Chem.* **1994**, *37*, 1099-1108.

4. Vzorov, A. N.; Marzilli, L. G.; Compans, R. W.; Dixon, D. W. *Antiviral Res.* **2003**, *59*, 99-109.

5. Neurath, A. R.; Strick, N.; Haberfield, P.; Jiang, S. *Antiviral Chem. Chemother.* **1992**, *3*, 55-63.

6. Horowitz, B.; Rywkin, S.; Prince, A. M.; Pascual, D.; Geacintov, N. E.; Valinsky, J. *Blood cells* **1991**, *18*, 141-150.

7. Vzorov, A. N.; Dixon, D. W.; Trommel, J. S.; Marzilli, L. G.; Compans, R. W. *Antimicrob. Agents Chemother.* **2002**, *46*, 3917-3925.

8. Chen-Collins, A. R. M.; Dixon, D. W.; Vzorov, A. N.; Marzilli, L. G.; Compans, R. W. *BMC Infect. Dis.* **2003**, *3*.

9. Remko, M. *J. Phys. Chem. A* **2003**, *107*, 720-725.

10. Miller, F. J.; Furfine, S. E.; Hanlon, H. M. H.; R.J Ray, A. J. R., L. ; Samano, V.; Spaltenstein, A. *Bioorg. Med. Chem. Lett.* **2004**, *14*, 959-963.

11. Fleischer, E. B.; Palmer, J. M.; Srivastava, T. S.; Chatterjee, J. *J. Am. Chem. Soc.* **1971**, *93*, 3162-3167.

12. Busby, C. A.; DiNello, R. K.; Dolphin, D. *Canadian Journal of Chemistry* **1975**, *53*, 1554-1555.

13. Gonsalves, A. M. R.; Johnstone, R. A. W.; Pereira, M. M.; de SantAna, A. M. P.; Serra, A. C.; Sobral, A. J. F. N.; Stocks, P. A. *Heterocycles* **1996**, *43*, 829-838.

14. Sobral, A. J. F. N.; Eleouet, S.; Rousset, N.; Gonsalves, A. M. d. A. R.; Le Meur, O.; Bourre, L.; Patrice, T. *J. Porphyrins Phthalocyanines* **2002**, *6*, 456-462.

15. Corby, B. W.; Gray, A. D.; Meaney, P. J.; Falvey, M. J.; Lawrence, G. P.; Smyth, T. P. *J. Chem. Res., Synop.* **2002**, 326-327.

16. Cremlyn, J. R.; Swinbourne, J. F.; Devlukia, P.; Shode, O. *Indian J. Chem., Sect. B* **1984**, *23B*, 249-253.

CHAPTER 5. SYNTHESIS OF PORPHYRIN DERIVATIVES WITH APPENDED PLATINUM MOIETIES

5.1 Introduction

Cis-dichlorodiammineplatinum(II) (cisplatin) remains one of the most widely used anticancer drugs for treatment of testicular and ovarian cancer.[1] Platinum drugs, such as cisplatin and carboplatin, nonselectively penetrate fast-growing tissues, leading to severe side effects (e.g. nausea, myelosuppression, nephrotoxicity and ototoxicity) that limit the dose that can be applied to patients.[2,3] These strong side effects may be reduced by selective delivery of cisplatin in the tumor tissue compared to the normal tissue.[4] It is also known that the effectiveness of Pt(II) antitumor drugs can be improved by linking the reactive platinum functionality to DNA binding agents, such as acridine,[5-8] anthraquinones,[9,10] and other intercalators.[11-13]

Selective delivery of the anti-tumor drug to the tumor tissue may be achieved by incorporating a carrier group that can target tumor cells with high specificity. Porphyrins are known to have the ability to localize selectively in a wide variety of tumors.[14,15] Porphyrin-based compounds possess good photochemical, photophysical, and biological properties that make them highly desirable for medical applications.[16] Porphyrins have also been used widely for photodynamic therapy and fluorescence imaging, which are based on the preferential uptake and retention of the porphyrins by tumor tissues.[17-21] Promising results have been published by Brunner et al., who synthesized porphyrin-platinum conjugates by utilizing carboxylic acid groups on the natural porphyrin as ligands for the platinum moiety. The antitumor activity of these compounds revealed a double therapeutic effect on inhibition of cell growth by the cytotoxic platinum effect and the phototoxic porphyrin effect.[22-26]

Conjugating a platinum moiety onto a porphyrin can possibly lead to selective delivery of the drug into tumor tissues. Furthermore, the photoactivity of the porphyrin can be applied as in photodynamic therapy. Studies have identified a cationic 5,10,15-tri(*N*-methyl-4-pyridiniumyl)porphyrin-platinum conjugate with greater antitumor activity than cisplatin and with a greater tumor-localizing effect (tumor/muscle ratio > 2) than carboplatin.[27]

Simple dinuclear compounds that are cationic and which can exist as both *cis* and *trans* isomers have displayed anti-tumor activity.[28] Farrell and co-workers have reported that dinuclear cationic *trans* complexes (which utilize as linkers the naturally available polyamines, spermine and spermidine) are very active substances that overcome cisplatin resistance in L1210 murine leukemia cells in vitro.[29] The additional positive charges assure a high affinity for DNA. A trinuclear platinum complex, BBR 3464, is in phase II clinical trials as a chemotherapeutic drug for treatment of ovarian and lung cancer.[30,31] Recently, five tetrapyridylporphyrin areneruthenium (II) derivatives and a *p*-cymeneosmium and two pentamethylcyclopentadienyliridium and rhodium analogues were analyzed as potential photosensitizing chemotherapeutic agents by Schmitt and co-workers.[32] The ruthenium analogues were found to exhibit excellent phototoxicity towards melanoma cells when exposed to laser light.[32] Cellular uptake and localization microsocopy studies revealed that the ruthenium and the rhodium analogues accumulated in the melanoma cell cytoplasm in granular structures different from lysosomes.[32]

We describe here the synthesis of a new family of Pt(II) complexes of tetraphenylporphyrin derivatives bearing polyamine ligands linked to the para position of the phenyl group through a sulfonamide group to bind Pt(II) moiety. The porphyrin ligands used (Scheme 5.1) in this study are 5,10,15,20-tetra(4-

[aminoethylaminoethylsulfonamidophenyl])porphyrin (Porphyrin-4(SO_2NHdien)) and 5,10,15,20-tetra(4-[diaminodiethylaminoethylsulfonamidophenyl])porphyrin (Porphyrin-4(SO_2NHtren). Porphyrin-4(SO_2NHdien) afforded 5,10,15,20-tetra(4-[dichloroPt(II)aminoethylaminoethyl)sulfonamidophenyl])porphyrin (Porphyrin-4((SO_2NHdien)Pt(II)Cl_2)**,** complex whereas Porphyrin-4(SO_2NHtren) gave 5,10,15,20-tetra(4-[chloroPt(II)diaminodiethylaminoethyl)sulfonamidophenyl])porphyrin Chloride ([Porphyrin-4((SO_2NHtren)Pt(II)Cl)]4Cl**) (**Figures 5.1 and 5.2)**.**

Scheme 5.1. Synthesis of [2-(2-amino-ethylamino)ethyl]carbamic acid tert-butyl ester (dien mono Boc) and {2-[(2-aminoethyl)-(2-tert-butoxycarbonylaminoethyl)amino]ethyl}-carbamic acid *tert*-butyl ester (tren bis Boc)

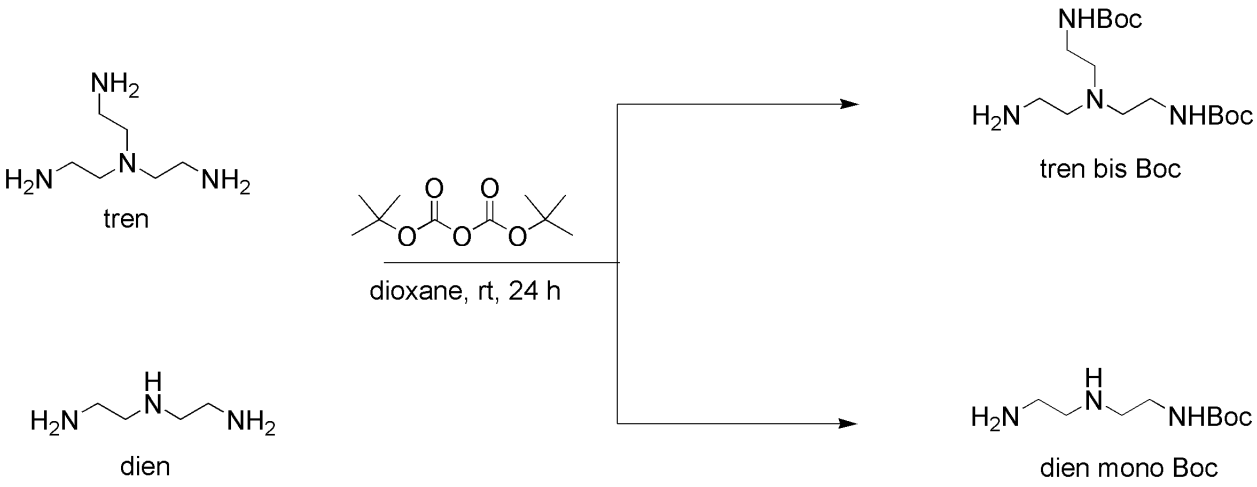

5.2 Experimental Section

5.2.1 Materials and Methods. Diethylenetriamine (dien), tris(2-aminoethyl)amine (tren) and Di-*tert*-butyl dicarbonate (Boc_2O) were obtained from Aldrich (Scheme 5.1). 5,10,15,20-tetra(4-chlorosulfonylphenyl)porphyrin ($TPPSO_2Cl$ (**1**), Scheme 5.2) was synthesized by a known method and the chemical shift of the ^{1}H NMR spectrum in $CDCl_3$ matched the reported value.[33] *Cis*-Pt(Me_2SO)$_2Cl_2$ was prepared as described in the literature.[34]

All ^{1}H NMR spectra were recorded on either a 300 MHz or a 400 MHz Bruker NMR spectrometer. Peak positions are relative to TMS or solvent residual peak, with TMS as reference. All NMR data were processed with *Mestre-C* software.

Mass spectra were obtained at the Mass Spectrometry Facility at Louisiana State University, Baton Rouge, LA, on a Bruker ProFlex III MALDI-TOF and Hitach M8000 ESI mass spectrometer. The compounds were dissolved in dichloromethane or chloroform using dithranol as the matrix and in methanol for ESI MS.

5.2.2 Synthesis of [2-(2-Aminoethylamino)ethyl]carbamic Acid tert-Butyl Ester (dien mono Boc) and {2-[(2-Aminoethyl)-(2-tert-butoxycarbonylaminoethyl)amino]ethyl}-carbamic Acid tert-Butyl Ester (tren bis Boc). Dien mono Boc and tren bis Boc were synthesized by a slight modification of Krapcho's method (Scheme 5.1).[35] A solution of Boc_2O (5 mmol, 50 mL of dioxane) was added dropwise over the course of about 2 h to a solution of dien or tren (20 mmol, 50 mL of dioxane). The reaction mixture was stirred at RT for 24 h. The dioxane was completely removed under vacuum, and water (50 mL) was added. The product was extracted into CH_2Cl_2 (3 × 50 mL), and the solvent was removed under rotary evaporation.

[2-(2-Aminoethylamino)ethyl]carbamic Acid *tert*-Butyl Ester (dien mono Boc). The general method described above with dien (2.1 g, 20 mmol) yielded dien mono Boc (3.9 g, 56%). ^{1}H NMR (ppm) in $CDCl_3$: 4.48 (1H, br, NHBoc), 3.35 (2H, d, CH_2), 2.18-3.28 (6H, m, CH_2), 1.43 (9H, s, t-butyl).

{2-[(2-Aminoethyl)-(2-tert-butoxycarbonylaminoethyl)amino]ethyl}-carbamic Acid *tert*-Butyl Ester (tren bis Boc). The general method described above with tren (2.9 g, 20 mmol) yielded tren bis Boc (1.75 g, 43%).^{1}H NMR (ppm) in $CDCl_3$: 5.28 (2H, br, NHBoc), 3.18 (2H, d, CH_2), 2.73 (2H, t, CH_2), 2.46-2.58 (6H, m, CH_2), 1.45 (18H, s, t-butyl).

The oils thus obtained were used to synthesis the porphyrin ligands as in Scheme 5.2.

Scheme 5.2. Porphyrin ligands synthesized in this study

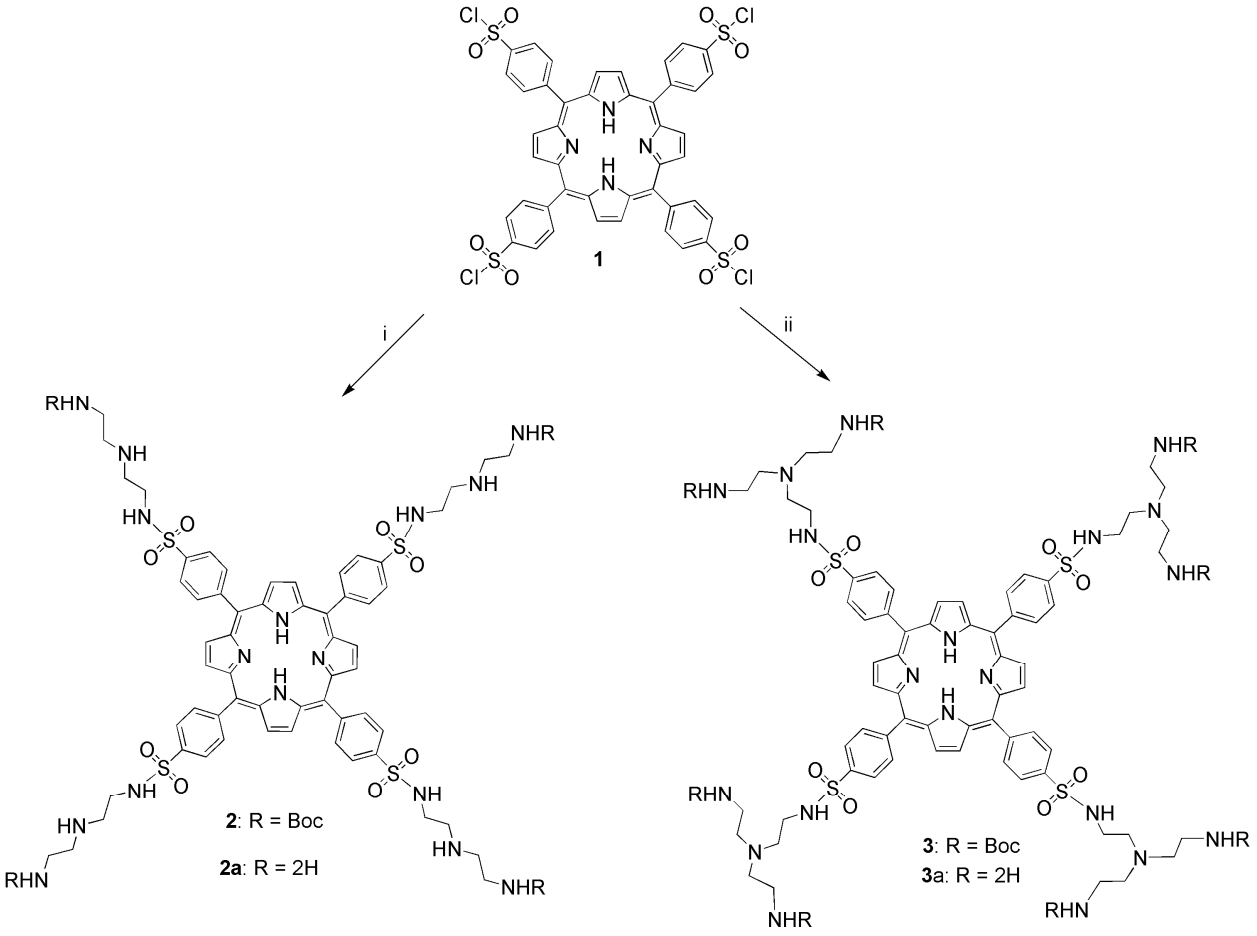

5.2.3 Synthesis of 5,10,15,20-tetra(4-[N-tert-butyloxycarbonyldiethylenetriaminylsulfonamido]phenyl)porphyrin (2) and 5,10,15,20-tetra(4-[N-bistert-butyloxycarbonyldiaminodiethylaminoethylsulfonamidophenyl]porphyrin (3). To a solution of porphyrin 1 (Scheme 5.2, 0.1 g, 0.1 mmol) in anhydrous dichloromethane (20 mL) was added a solution of dien mono Boc or tren bis Boc (0.5 mmol, 10 mL of dichloromethane). The reaction mixture was stirred at room temperature for 12 h. The reaction mixture was washed with water

(3 × 10 mL) to remove the unreacted amine. The organic phase was dried over anhydrous Na2SO4 and the solvent was removed under vacuum. The final compounds were precipitated from dichloromethane/hexane.

5,10,15,20-tetra(4-[*N-tert*-butyloxycarbonyldiethylenetriaminylsulfonamido]phenyl)porphyrin (**2**): The general method described in Scheme 5.2 with dien mono Boc (0.1 g) produced porphyrin **2 (**0.18 g, 81%). ^{1}H NMR (ppm) in DMSO-d_6: 8.85 (8H, s, β-pyrrole), 8.45 (8H, d, ArH), 8.24 (8H, d, ArH), 6.75 (8H, br, NHBoc), 3.12 (8H, t, CH_2), 3.01 (8H, q, CH_2), 2.70 (8H, t, CH_2), 2.57 (8H, q, CH_2), 1.31 (36H, s, t-butyl), -2.96 (2H, br, NH).

5,10,15,20-tetra(4-[*N*-bis*tert*-butyloxycarbonyldiaminodiethylaminoethylsulfonamidophenyl])porphyrin (3): The general method described above with tren bis Boc (0.17 g) yielded porphyrin **3,** Scheme 5.2 (0.16 g, 95%) ^{1}H NMR (ppm) in DMSO-d_6: 8.85 (8H, s, β-pyrrole), 8.44 (8H, d, ArH), 8.26 (8H, d, ArH), 7.83 (4H, br, NH-sulfonamide), 6.79(8H, br, NHBoc), 3.15 (8H, t, CH_2), 2.96 (16H, q, CH_2), 2.59 (8H, t, CH_2), 2.50 (8H, t, CH_2), 1.32(72H, s, t-butyl), -2.96 (2H, br, NH).

5.2.4 General Procedure for Removal of the Boc-protecting Group

Method A: Following a published procedure,[36] TFA (2 mL) was added to porphyrin **2** or **3** and the final solution was stirred at room temperature for 5 min. TFA was evaporated under reduced pressure; the residue was triturated and washed with ethyl acetate (3 × 5 mL) to give a green powder.

Method B: A suspension of porphyrin **2** or **3** in HCl/dioxane (4 M, 5 mL) was stirred at room temperature for 30 min. The reaction mixture was dried under vacuum. The residue (green solid) was then washed with diethyl ether, collected on a filter paper and dried under vacuum.

5,10,15,20-tetra(4-[aminoethylaminoethylsulfonamidophenyl])porphyrin (2a): Method B with 0.05 g of porphyrin **2** yielded a green precipitate of porphyrin **2a,** Scheme 5.2 (0.068 g, 88% yield). ^{1}H NMR (ppm) in DMSO-d_6: 8.85 (8H, s, β-pyrrole), 8.45 (8H, d, ArH), 8.25 (8H, d, ArH), 7.97 (4H, br, NH-sulfonamide), 7.79 (24H, br, NH_3^+), 3.32 (8H, t, CH_2), 2.94 (16H, t, CH_2), 2.73 (24H, t, CH_2), -2.95 (2H, br, NH).

5,10,15,20-tetra(4-[diaminodiethylaminoethylsulfonamidophenyl])porphyrin (3a): Method B with 0.05 g of porphyrin **3** yielded a green precipitate of porphyrin **3a**, Scheme 5.2 (0.041 g, 87% yield). ^{1}H NMR (ppm) in DMSO-d_6: 8.89 (8H, s, β-pyrrole), 8.49 (8H, d, ArH), 8.41 (4H, br, NH-sulfonamide), 8.29 (20H, ArH and NH_3^+) 3.34 (16H, t, CH_2), 3.29 (16H, t, CH_2), -2.97 (2H, br, NH).

5.2.5 Synthesis of Porphyrin-Platinum(II) Complexes

Synthesis of Porphyrin-4((SO_2NHdien)Pt(II)Cl_2) (4, Figure 5.1**):** A suspension of *cis*-Pt($Me_2SO)_2Cl_2$ (0.148 g, 0.352 mmol) in methanol (10 mL) was treated with porphyrin **2a** (0.11 g, 0.070 mmol) in methanol (10 mL), and the reaction mixture was stirred at 50 ^{o}C overnight. The brown solid that precipitated was collected on a filter, washed with diethyl ether and dried under vacuum; yield, 0.05 g, (31%). ^{1}H NMR (ppm) in DMSO-d_6: 8.87 (8H, s, β-pyrrole), 8.47 (8H, d, ArH), 8.27 (12H, d, ArH and NH), 7.11(4H, br, NH), 6.17 (8H, br, NH_2), 3.3 (32H, br, CH_2), -2.97 (2H, br, NH).

Synthesis of [Porphyrin-4((SO_2NHtren)Pt(II)Cl)]4Cl (5, Figure 5.2**):** A suspension of *cis*-Pt($Me_2SO)_2Cl_2$ (0.06 g, 0.144 mmol) in methanol (10 mL) was treated with porphyrin **3a** (0.05 g, 0.029 mmol) in methanol (10 mL), and the reaction mixture was stirred at 50 ^{o}C overnight. The brown solid that precipitated was collected on a filter, washed with diethyl ether and dried under vacuum; yield, 0.045 g (62.5%). ^{1}H NMR (ppm) in DMSO-d_6: 8.88 (8H, s, β-

pyrrole), 8.48 (8H, d, ArH), 8.41(4H, t, NH-sulfonamide), 8.32 (8H, d, ArH), 5.75 (8H, br, NH_2), 5.47 (8H, br, NH_2), 3.69(8H, t, CH_2), 3.43 (8H, t, CH_2), 3.31 (16H, br, CH_2), 2.96 (8H, t, CH_2), -2.96 (2H, br, NH).

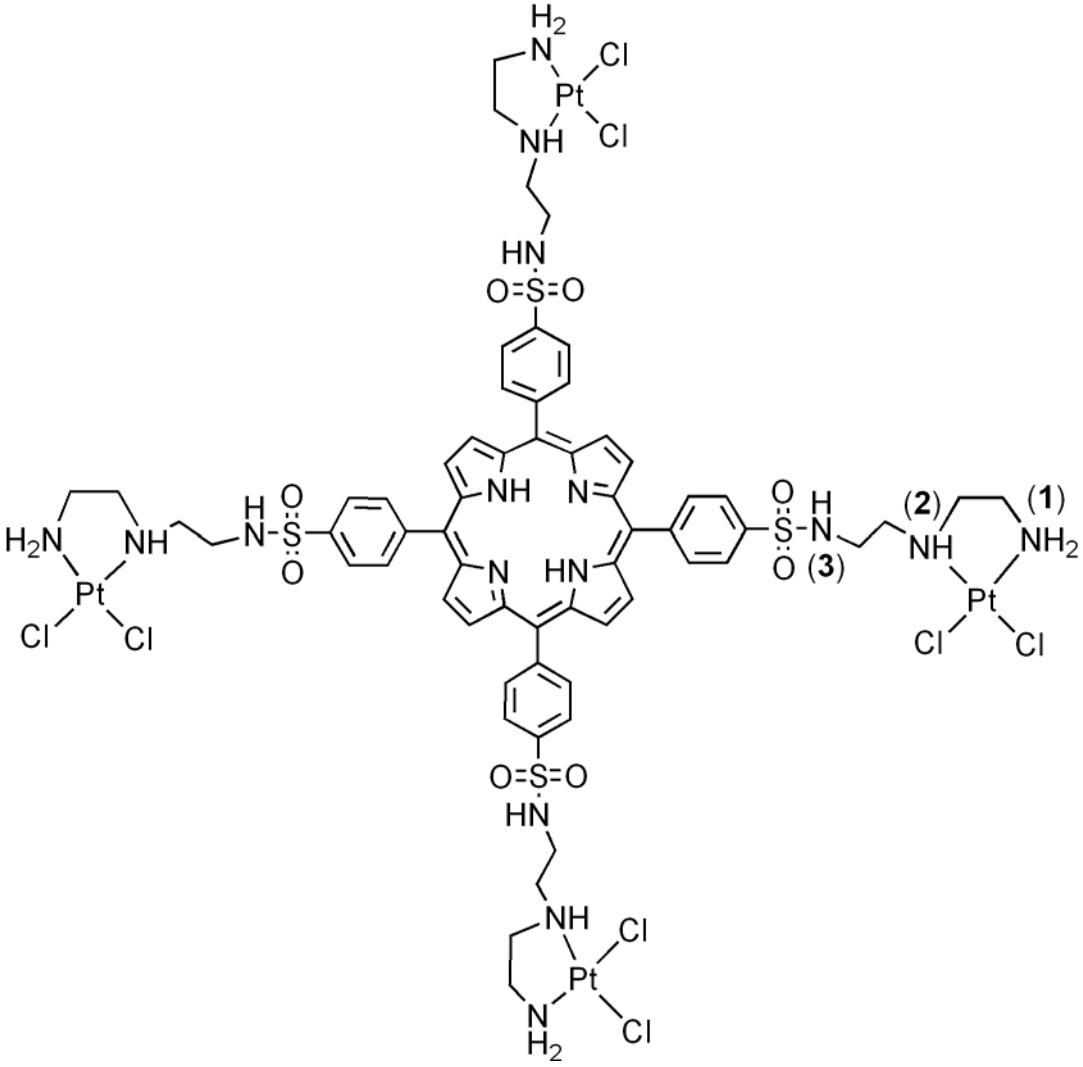

Figure 5.1. Porphyrin-4((SO_2NHdien)Pt(II)Cl_2) (4).

5.3 Results and Discussion

Starting from the easily synthesized 5,10,15,20-tetra(4-chlorosulfonylphenyl)porphyrin[33] and reaction of different polyamines that were Boc-protected (Scheme 5.1), new porphyrins

containing sulfonamide groups with multidentate ligands (Scheme 5.2) were synthesized. The Boc-protected amines were obtained following previously published procedures[35] (Scheme 5.1), and their ^{1}H NMR spectra in $CDCl_3$ are shown in Figures 5.3 and 5.4.

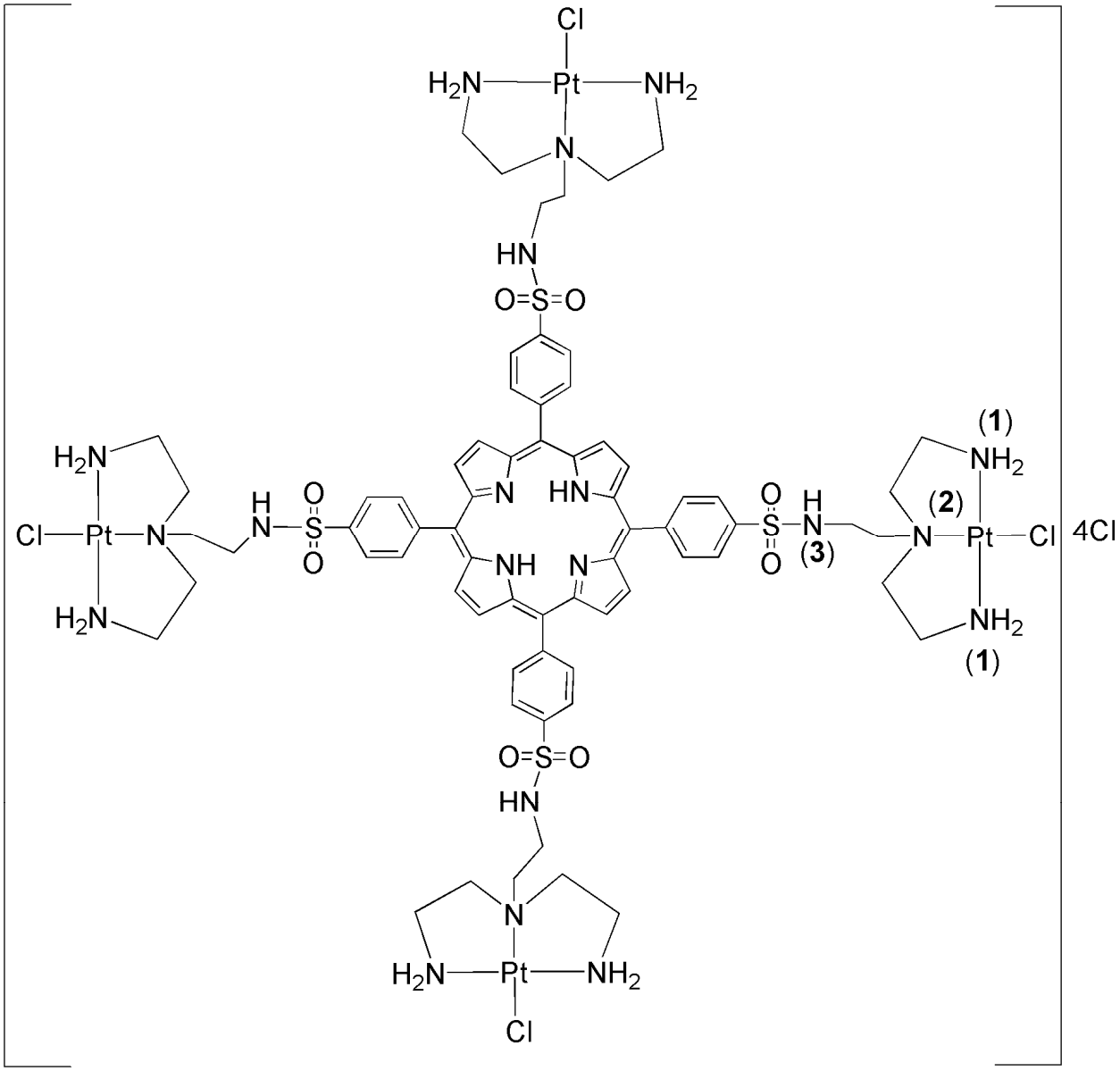

Figure 5.2. [Porphyrin-4((SO$_2$NHtren)Pt(II)Cl)]4Cl (**5**).

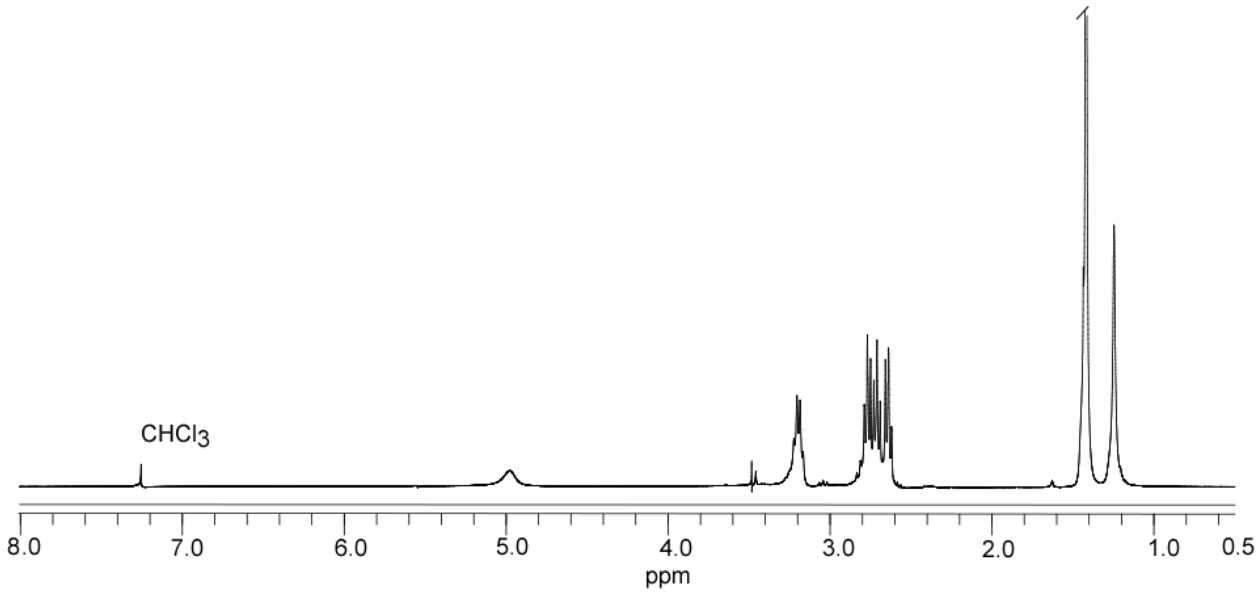

Figure 5.3. ^{1}H NMR spectrum of **dien mono Boc** in $CDCl_3$.

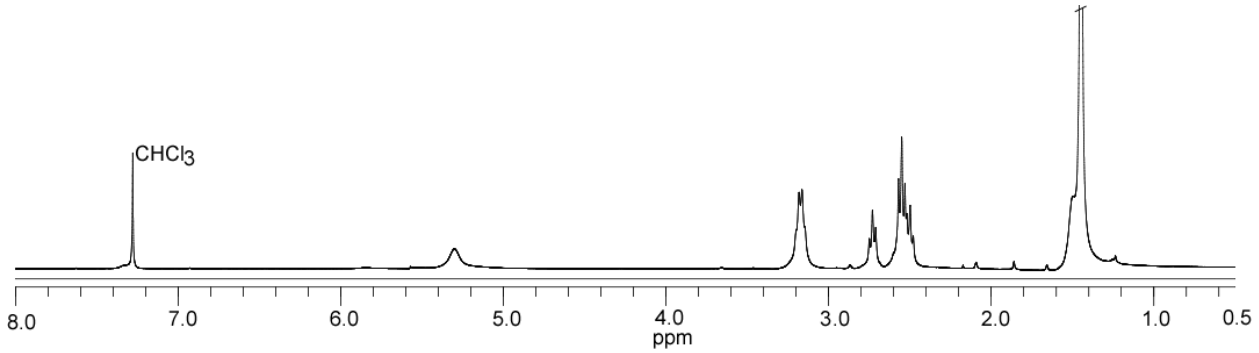

Figure 5.4. ^{1}H NMR spectrum of **tren bis Boc** in $CDCl_3$.

The porphyrin Boc-protected compounds synthesized (**2** and **3,** Scheme 5.2) are soluble in organic solvents (chloroform, dichloromethane) and the Boc groups are easily cleaved in quantitative yield by using TFA at room temperature.[36] The deprotected porphyrin conjugates, **2a** and **3a,** were soluble in water, methanol and DMSO. The porphyrin-ligands were analyzed by ^{1}H NMR spectroscopy in DMSO-d_6 (Figures 5.5 and 5.6). The ^{1}H NMR spectra of the protected porphyrin-ligand showed the resonance of the sulfonamide NH protons (7-8.5 ppm) and of the

amide NH of the Boc-protected groups at ~6.8 ppm (Figures 5.5 and 5.6). The signal of the methyl groups of the *tert*-butyl group observed at ~1.3 ppm confirmed the synthesis of the protected porphyrin ligands. Removal of the protecting group of **2** and **3** was confirmed by ^{1}H NMR spectroscopy; the disappearance of the methyl signal of the *tert*-butyl group and appearance of a broad peak at ~7.5 ppm for the protonated primary amine groups confirmed the cleavage of the *tert*-butyl groups. Further confirmation was obtained by addition of D_2O to the NMR sample of the deprotected porphyrin ligands, whereupon the broad signal of the primary amines disappeared because of exchange with D_2O.

5.3.1 ^{1}H NMR Characterization of Porphyrin-Pt(II) Complexes

Porphyrin-Pt(II) conjugates (Figures 5.1 and 5.2) were prepared by treating the deprotected porphyrin ligands (Porphyrin-4(SO_2NHdien) and Porphyrin-4(SO_2NHtren)) dissolved in methanol with *cis*-Pt($Me_2SO)_2Cl_2$ at 50 °C for 12 h. The porphyrin-Pt(II) conjugates precipitated, and the precipitate was washed with methanol to remove the excess of *cis*-Pt($Me_2SO)_2Cl_2$ and the unchanged porphyrin ligand. All the porphyrin-Pt(II) conjugates were soluble only in DMSO and were analyzed by ^{1}H NMR spectroscopy in DMSO-d_6 (Figures 5.5 and 5.6).

Porphyrin-4((SO_2NHdien)Pt(II)Cl_2) (4). Soon after Porphyrin-4((SO_2NHdien)Pt(II)Cl_2) (Figure 5.1) was dissolved in DMSO-d_6, one major and one minor set of NH signals were observed, and only one set of the porphyrin signals was observed. The minor set of signals (upfield) disappeared after ~5 min. One set of the NH signals (upfield) belongs to Porphyrin-4((SO_2NHdien)Pt(II)Cl_2) while the major set (downfield) belongs to the solvated species [Porphyrin-(4((SO_2NHdien)Pt(II)(Me_2SO)Cl]$^{4+}$. The minor set did not appear upon addition of [Et_4N]Cl. Similar results were observed with Pt(DNSH-dienH)Cl_2 (DNSH-dienH =

N-(2-((2-aminoethyl)amino)ethyl)-5-(dimethylamino)naphthalene-1-sulfonamide).[37] The ^{1}H NMR signals of **4** compared to those of the deprotected porphyrin derivative (**2a**) are not significantly affected upon platinum binding to the Porphyrin-4(SO_2NHdien (**2a**), indicating that the porphyrin moiety is far from the platinum. The presence of the sulfonamide N3H signal (Figure 5.5) is an indication that N1 and N2 participate in the binding to Pt(II) but N3 does not.

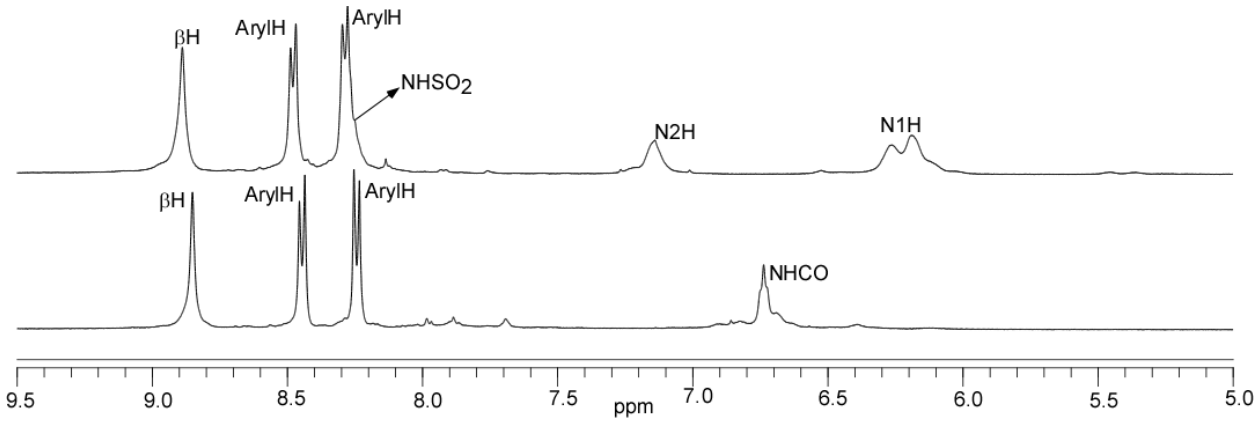

Figure 5.5. Selected region of the ^{1}H NMR spectrum of the protected porphyrin-ligand (**2**) (bottom) and of Porphyrin-4((SO_2NHdien)Pt(II)Cl_2) (**4**) (top) in DMSO-d_6.

The presence of the sulfonamide N3 signal in the ^{1}H NMR spectrum of **4** is an indication that the Porphyrin-4(SO_2NHdien) ligand acts as a bidentate ligand (central N2 and terminal N1) (Figure 5.1). There are two signals of the terminal amino groups (N1H) of **4** (5.36-5.47 ppm), and they are comparable to the shifts of Pt(DNSH-dienH)Cl_2 (5.23-5.34 ppm) observed previously.[37] The shift (6.57 ppm) of N2H in **4** is comparable to that of Pt(DNSH-dienH)Cl_2 (6.27 ppm) reported previously.[37] The sulfonamide N3H signal of **4** (8.26 ppm) is comparable (8.22 ppm) to that of Pt(DNSH-dienH)Cl_2.[37] In general all the NH signals were slightly downfield (~ 0.05 ppm) as compared to the NH shifts of the previously reported (Pt(DNSH-dienH)Cl_2)[37] arising from the electron-withdrawing effect of the porphyrin.

[Porphyrin-4(SO_2NHtren)Pt(II)Cl)]4Cl (5). [Porphyrin-4(SO_2NHtren)Pt(II)Cl)]4Cl (Figure 5.2) was prepared by treating *cis*-Pt($Me_2SO)_2Cl_2$ with porphyrin **3a**. In DMSO-d_6 the ^{1}H NMR signals of the porphyrin are not significantly affected by Pt binding (Figure 5.6). Upon dissolution of **5** in DMSO-d_6 one major and one minor set of NH signals were observed (Figure 5.6). The minor set of the NH signals (downfield shifted) was for the solvated species [Porphyrin-4((SO_2NHtren)Pt(II)(Me_2SO-d_6)]$^{8+}$ and only 10% of this solvated species was formed; the major set arises from the unsolvated species ([Porphyrin-4((SO_2NHtren)Pt(II)Cl)]4Cl). The presence of the sulfonamide N3H signal confirmed that the desired structure formed. Similar results were observed with [Pt(DNSH-tren)Cl]Cl, which can be used as a model of **5**.[37] Previous studies from our laboratory revealed that the presence of the alkyl group on the central N2 decreases DMSO solvolysis.

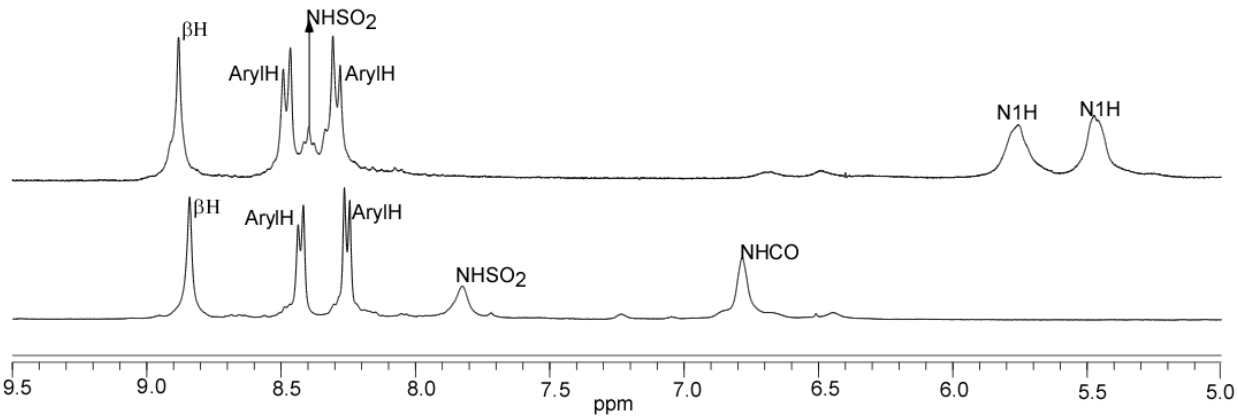

Figure 5.6. Selected region of the ^{1}H NMR spectrum of the protected porphyrin-ligand (**3**) bottom) and [Porphyrin-4((SO_2NHtren)Pt(II)Cl)]4Cl (**5**) (top) in DMSO-d_6.

5.4 Conclusions and Future Work

The Porphyrin-4(SO_2NHdien) and Porphyrin-4(SO_2NHtren) ligands act as bidentate and tridentate ligands for platinum (II) complexes, respectively. The sulfonamide NH signal was found to be diagnostic in confirming the synthesis of the porphyrin-platinum conjugates. The

synthesized compounds will be submitted for testing for anticancer activity. Derivatives of the compounds can be prepared in order to improve their solubility in water.

5.5 References

1. Pratt, B. W.; Ruddon, W. R.; Ensigminger, J.; Maybaum, J.; 2nd ed.; Oxford University Press: New York, 1994, pp 133-168.

2. Keppler, K. B. *Metal Complexes in Cancer Therapy*; Wiley-VCH Verlag GmbH: Weinheim, 1993.

3. Vonhoff, D. D.; Schilsky, R.; Reichert, C. M.; Reddick, R. L.; Rozencweig, M.; Young, R. C.; Muggia, F. M. *Canc Treat. Rep.* **1979**, *63*, 1527-1531.

4. Song, R.; Kim, Y. S.; Sohn, Y. S. *J. Inorg. Biochem.* **2002**, *89*, 83-88.

5. Brow, J. M.; Pleatman, C. R.; Bierbach, U. *Bioorg. Med. Chem. Lett.* **2002**, *12*, 2953-2955.

6. Holmes, R. J.; McKeage, M. J.; Murray, V.; Denny, W. A.; McFadyen, W. D. *J. Inorg. Biochem.* **2001**, *85*, 209-217.

7. Temple, M. D.; McFadyen, W. D.; Holmes, R. J.; Denny, W. A.; Murray, V. *Biochemistry* **2000**, *39*, 5593-5599.

8. Temple, M. D.; Recabarren, P.; McFadyen, W. D.; Holmes, R. J.; Denny, W. A.; Murray, V. *Biochim. Biophys. Acta - Gene Struct. Express* **2002**, *1574*, 223-230.

9. Gibson, D.; Binyamin, I.; Haj, M.; Ringel, I.; Ramu, A.; Katzhendler, J. *Eur. J. Med. Chem.* **1997**, *32*, 823-831.

10. Gibson, D.; Gean, K. F.; Benshoshan, R.; Ramu, A.; Ringel, I.; Katzhendler, J. *J. Med. Chem.* **1991**, *34*, 414-420.

11. Gude, L.; Fernandez, M. J.; Grant, K. B.; Lorente, A. *Bioorg. Med. Chem. Lett.* **2002**, *12*, 3135-3139.

12. Gude, L.; Fernandez, M. J.; Grant, K. B.; Lorente, A. *Tetrahedron Lett.* **2002**, *43*, 4723-4727.

13. Perez, J. M.; Lopez-Solera, I.; Montero, E. I.; Brana, M. F.; Alonso, C.; Robinson, S. P.; Navarro-Ranninger, C. *J. Med. Chem.* **1999**, *42*, 5482-5486.

14. Barrett, A. J.; Kennedy, J. C.; Jones, R. A.; Nadeau, P.; Pottier, R. H. *J. Photochem. Photobiol., B* **1990**, *6*, 309-323.

15. Cohen, L.; Schwartz, S. *Cancer Research* **1966**, *26*, 1769-1773.

16. Vicente, M. G. *Curr. Med. Chem. Anti-Cancer Agents* **2001**, *1*, 175-194.

17. Campbell, D. L.; Gudgin-Dickson, E. F.; Forkert, P. G.; Pottler, R. H.; Kennedy, J. C. *Photochem. Photobiol.* **1996**, *64*, 676-682.

18. Hebeda, K. M.; Wolbers, J. G.; Sterenborg, H. J. C. M.; Kamphorst, W.; van Gemert, M. J. C.; van Alphen, H. A. M. *J. Photochem. Photobiol., B* **1995**, *27*, 85-92.

19. Mang, T. S.; McGinnis, C.; Liebow, C.; Nseyo, U. O.; David H. Crean, D. H.; Dougherty, T. J. *Cancer* **1993**, *71*, 269-276.

20. Trepte, O.; Rokahr, I.; Anderssonengels, S.; Carlsson, K. *J. Microsc.* **1994**, *176*, 238-244.

21. Wang, I.; Pais Clemente, L.; Pratas, R. M. G.; Cardoso, E.; Pais Clemente, M.; Montán, S.; Svanberg, S.; Svanberg, K. *Cancer Lett.* **1998**, *135*, 11-19.

22. Brunner, H.; Arndt, M. R.; Treittinger, B. *Inorg. Chim. Acta* **2004**, *357*, 1649-1669.

23. Brunner, H.; Obermeier, H. *Angew. Chem. Int. Ed.* **1994**, *33*, 2214-2215.

24. Brunner, H.; Schellerer, K. M.; Treittinger, B. *Inorg. Chim. Acta* **1997**, *264*, 67-79.

25. Brunner, H.; Schellerer, K. M. *Z. Naturforsch., B: Chem. Sci.* **2002**, *57*, 751-756.

26. Brunner, H.; Schellerer, K. M. *Inorg. Chim. Acta* **2003**, *350*, 39-48.

27. Song, R.; Kim, Y.-S.; Lee, C. O.; Sohn, Y. S. *Tetrahedron Lett.* **2003**, *44*, 1537-1540.

28. Oehlsen, M. E.; Hegmans, A.; Qu, Y.; Farrell, N. *J. Biol. Inorg. Chem.* **2005**, *10*, 433-442.

29. Rauter, H.; Di Domenico, R.; Menta, E.; Oliva, A.; Qu, Y.; Farrell, N. *Inorg. Chem.* **1997**, *36*, 3919-3927.

30. Harris, A. L.; Yang, X.; Hegmans, A.; Povirk, L.; Ryan, J. J.; Kelland, L.; Farrell, N. P. *Inorg. Chem.* **2005**, *44*, 9598-9600.

31. Harris, A. L.; Ryan, J. J.; Farrell, N. *Mol. Pharmacol.* **2006**, *69*, 666-672.

32. Schmitt, F.; Govindaswamy, P.; Suss-Fink, G.; Ang, W.; Dyson, P. J.; Juillerat-Jeanneret, L.; Therrien, B. *J. Med. Chem.* **2008**, *51*, 1811-1816.

33. Gonsalves, A. M. R.; Johnstone, R. A. W.; Pereira, M. M.; de SantAna, A. M. P.; Serra, A. C.; Sobral, A. J. F. N.; Stocks, P. A. *Heterocycles* **1996**, *43*, 829-838.

34. Price, J. H.; Schramm, R. F.; Wayland, B. B.; Williamson, A. N. *Inorg. Chem.* **1972**, *11*, 1280-1284.

35. Krapcho, A. P.; Kuell, C. S. *Synth. Commun.* **1990**, *20*, 2559-2564.

36. Sibrian-Vazquez, M.; Jensen, T. J.; Fronczek, F. R.; Hammer, R. P.; Vicente, M. G. H. *Bioconjugate Chem.* **2005**, *16*, 852-863.

37. Christoforou, A. M.; Marzilli, P. A.; Marzilli, L. G. *Inorg. Chem.* **2006**, *45*, 6771-6781.

CHAPTER 6. SYNTHESIS OF PROTOPORPHYRIN IX POLYAMINE CONJUGATES APPENDED WITH PLATINUM MOIETIES

6.1 Introduction

Cis-dichlorodiammineplatinum(II) (cisplatin), as one of the leading metal-based drugs, is widely used in the treatment of various forms of cancer.[1] However, its clinical usefulness has been limited by severe side effects, such as nephrotoxicity, gastrointenstinal toxicity, ototoxicity and neurotoxicity.[2,3] Extensive efforts have been made to overcome the drawbacks of cisplatin to develop cisplatin analogues having equivalent or better antitumor activity and less toxicity. One of the strategies for designing new platinum antitumor compounds is to combine the chemotherapeutic agent (platinum compounds) with proper carrier groups that target selectively the tumor cells.

Porphyrins have been used effectively in the photodynamic treatment of tumors over a decade and play an important role in fluorescence imaging, both based on the preferential uptake and retention of the porphyrins in tumor tissues.[4-7] Porphyrins are known to accumulate selectively in tumor tissues, while platinum complexes such as cisplatin and carboplatin penetrate unselectively into all fast-growing tissues, giving rise to the known side effects.[8,9] Studies dealing with the combination of the useful properties of the platinum containing preparations and porphyrins resulted in the synthesis of a number of compounds representing platinum complexes (covalent conjugates) with protoporphyrin, hematoporphyrin, tetraphenyl porphyrin derivatives and with zinc phthalocyanines.[10-18] A study of the effect of the conjugates to the living cells showed an additive effect of the porphyrin photodynamic activity and platinum cytotoxic acitivity.[10,19,20] Porphyrin platinum conjugates already synthesized are of the natural porphyrin (hematoporphyrin), in which the platinum(II) moiety is attached to the propionic acid

side chains out of the porphyrin macrocycle. In previous studies involving conjugation of the carboxylic acid side chains of hematoporphyrin with the platinum compounds, only one platinum compound per porphyrin was synthesized. Herein, we describe a different approach to the synthesis of Pt(II) complexes. In this study the carboxylic acid groups of protoporphyrin (IX) were conjugated with different amines, which acted as ligands for platinum(II) compounds. As a result, in our system each protoporphyrin ligand synthesized contains two platinum compounds.

6.2 Experimental Section

6.2.1 Materials and Methods. 2,18-dipropionic-3,8,13,17-tetramethyl-7,12-divinylporphyrin (PP, **1**) (Frontier), 1–hydroxybenzonitrile (HOBt), 2-(1H-benzonitriazole-1-yl)-1,1,3,3-tetramethyluronium tetrafluoroborate (TBTU), N,N-diisopropylethylamine (DIEA) and *N,N*– dimethylformide (DMF) from Aldrich, [2-(2-Amino-ethylamino)-ethyl]-carbamic acid *tert*-butyl ester (dien mono Boc) and {2-[(2-Amino-ethyl)-(2-tert-butoxycarbonylamino-ethyl)-amino]-ethyl}-carbamic acid *tert*-butyl ester (tren bis Boc) were synthesized as described in Chapter 4, and the chemical shifts of the ^{1}H NMR spectra in $CDCl_3$ matched the reported values. *cis*-$Pt(Me_2SO)_2Cl_2$ was prepared as described in the literature.

All ^{1}H NMR spectra were recorded on either a 300 MHz or a 400 MHz Bruker NMR spectrometer. Peak positions are relative to TMS or solvent residual peak, with TMS as reference. All NMR data were processed with *Mestre-C* software.

Mass spectra were obtained at the Mass Spectrometry Facility at Louisiana State University, Baton Rouge, LA, on a Bruker ProFlex III MALDI-TOF and Hitach M8000 ESI mass spectrometer. The compounds were dissolved in dichloromethane or chloroform using dithranol as the matrix and in methanol for ESI MS.

Scheme 6.1. Synthesis of polyamine PPIX conjugates[a]

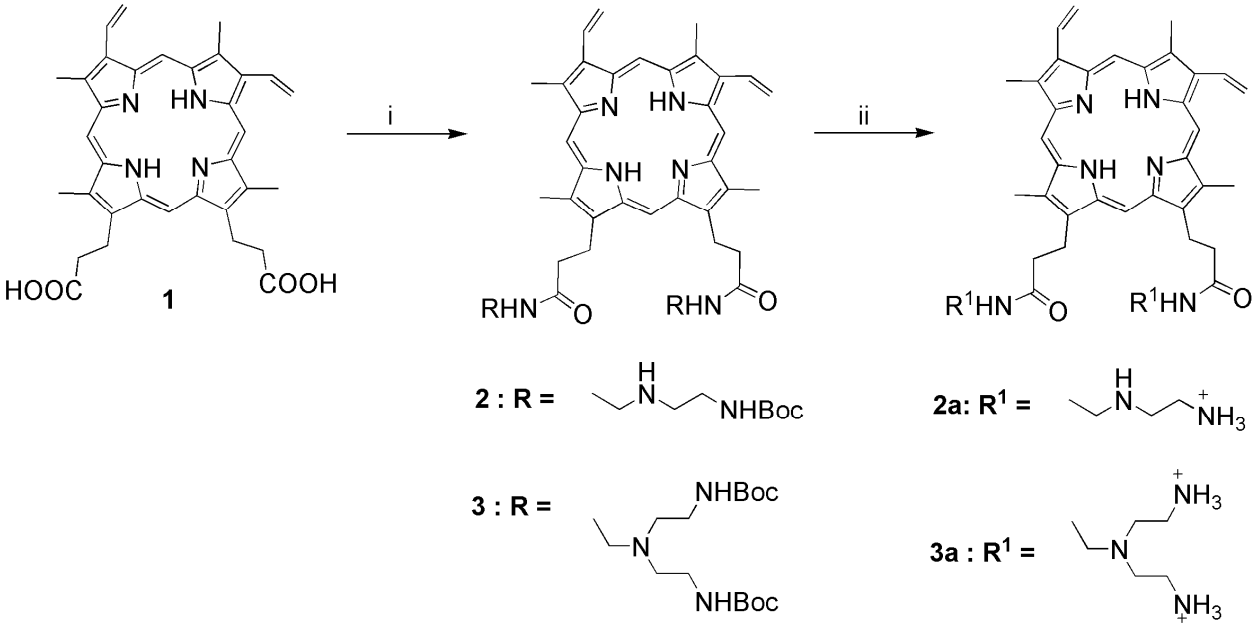

[a] Reagents and conditions: (i) PP (1.1 equiv), polyamine (2.2 equiv), TBTU (2.2), HOBt (2.2 equiv), DIEA (7.7 equiv), DMF, RT, 24 h; (ii) CF_3COOH, RT, 30 min.

6.2.2 General Synthesis of Porphyrin Conjugates. A solution of **1** (0.1g, 0.36 mmol) in 2.0 mL dry DMF was treated with DIEA (0.28g, 2.18 mmol), TBTU (0.23g, 0.72 mmol) and HOBt (0.098g, 0.36 mmol), followed by 0.64 mmol of the respective amine in 0.5 mL of DMF. The reaction mixture was stirred at RT for 24 h, diluted with 10 mL of ethyl acetate, and washed with water (5 × 10 mL). The organic layer was collected and dried over anhydrous Na_2SO_4, filtered, and the solvent evaporated under vacuum. The porphyrin conjugates were isolated by column chromatography on silica gel by eluting with $CHCl_3$/EtOH, 90:10 + 5% TEA.

2,18-Bis[tertbutoxycarbonyldiethlenetriaminyl-*N*-amidoethyl]-3,8,13,17-tetramethyl-7,12-divinylporphyrin (**2**)**:** The general method described above with PP (0.1 g) and dien mono Boc (0.13 g) yielded porphyrin **2** (0.12 g, 35%), ^{1}H NMR (ppm) in DMSO-d_6:

10.30, 10.23 (4H, s, *meso*-H), 8.49 (2H, dd, CH-vinyl), 7.86 (2H, br, -NHCO), 6.50 (2H, d, CH_2-vinyl), 6.42 (2H, br, NHBoc), 6.22 (2H, d, CH_2-vinyl), 4.33 (4H, br, $COCH_2$), 3.72 (6H, d, CH_3-β-pyrrole), 3.62 (6H, d, CH_3-β-pyrrole), 3.06(10H, s, CH_2-proto and CH_2-dien), 2.76 (2H, s, NH-dien), 2.35 (8H, d, CH_2-dien), 1.30 (18H, CH_3-Boc), -3.95 (2H, s, NH-pyrrole). MS (MALDI) m/z: $[M + H]^+$ = 933.708, calcd for $[M + H]^+$ = 933.563.

2,18-Bis[di-tertbutoxycarbonyldiaminodiethylaminoethyl-N-amidoethyl]-3,8,13,17-tetramethyl-7,12-divinylporphyrin (3): The general method described above with PP (0.1 g) and tren bis Boc (0.22 g) yielded porphyrin **3** (0.28 g, 65%). ^{1}H NMR (ppm) in DMSO-d_6: 10.29, 10.24, 10.23, 10.21 (4H, s, *meso*-H), 8.49 (2H, dd, CH-vinyl), 7.85 (2H, br, -NHCO), 6.48 (2H, d, CH_2-vinyl), 6.42 (2H, br, NHBoc), 6.22 (2H, d, CH_2-vinyl), 4.33 (4H, br, $COCH_2$), 4.03 (6H, d, CH_3-β-pyrrole), 3.72 (6H, d, CH_3-β-pyrrole), 3.04(8H, s, CH_2-proto and CH_2-tren), 2.69 (12H, s, CH_2-tren), 2.18 (8H, d, CH_2-tren), 1.26 (36H, CH_3-Boc), -3.94 (2H, s, NH-pyrrole). MS (MALDI) m/z: $[M + H]^+$ = 1220.527, calcd for $[M + H]^+$ = 1220.579.

Deprotection was accomplished in quantitative yield by using trifluoroacetic acid (TFA) (2 mL) at RT for 30 min, followed by evaporation of TFA and washings with diethyl ether. Porphyrins **2a** and **3a** were obtained as green powders.

2,18-Bis[aminoethylaminoethyl-*N*-amidoethyl]-3,8,13,17-tetramethyl-7,12-divinylporphyrin (PP-2(CONHdien), **2a):** ^{1}H NMR (ppm) in DMSO-d_6: ^{1}H NMR (ppm) in DMSO-d_6: 10.34, 10.31, 10.28 (4H, s, *meso*-H), 9.46 (2H, s, NH-dien), 8.49 (2H, dd, CH-vinyl), 8.43 (2H, br, NHCO),8.31 (6H, br, NH_3), 6.47 (2H, d, CH_2-vinyl), 6.24 (2H, d, CH_2-vinyl),4.41 (4H, br, $COCH_2$), 3.66 (12H, d, CH_3 β-pyrrole), 3.49(6H, d, CH_2-proto and CH_2-dien), 3.36 (10H, m, CH_2-proto and CH_2-dien), 3.16 (6H, d, CH_2-dien), -3.95 (2H, s, NH-pyrrole). ESI-MS(m/z): M^+ = 732.4669, calcd for M^+ = 732.4586.

2,18-Bis[diaminodiethylaminoethyl-*N*-amidoethyl]-3,8,13,17-tetramethyl-7,12-divinylporphyrin (PP-2(CONHtren), 3a): ^{1}H NMR (ppm) in DMSO-d_6: 10.37, 10.29, 10.26 (4H, s, *meso*-H), 8.53 (2H, dd, CH-vinyl), 7.92 (2H, br, NHCO), 7.62 (12H, br, NH_3), 6.47 (2H, d, CH_2-vinyl), 6.24 (2H, d, CH_2-vinyl), 4.36 (4H, br, $COCH_2$), 3.75 (6H, d, CH_3 β-pyrrole), 3.64 (6H, d, CH_3 β-pyrrole), 3.06 (12H, s, CH_2-proto and CH_2-tren), 2.58 (8H, s, CH_2-tren), 2.35 (8H, s, CH_2-tren), -3.95 (2H, s, NH-pyrrole). ESI-MS(m/z): M^+ = 818.5310, calcd for M^+ = 818.5431.

6.2.3 Synthesis of the Platinum Complexes of the Porphyrin Polyamine Conjugates.

A suspension of *cis*-$Pt(Me_2SO)_2Cl_2$ (43.7 mg, 0.1 mmol) in methanol (20 mL) was treated with the polyamine PP conjugates **2a** and **3a**, (0.025 mmol), and the reaction mixture was heated at 50 ^oC overnight. The product precipitated in the course of the reaction; the brown suspension was concentrated to 5 mL and the product removed by filtration and washed with water, diethyl ether and dried under vacuum to yield the desired platinum complexes PP-2((CONHdien)Pt(II)Cl_2) and [PP-2((CONHtren)PtCl)]2Cl, which were characterized by ^{1}H NMR spectroscopy.

PP-2((CONHdien)Pt(II)Cl_2) (4). The general method described above with **2a** (20 mg) afforded **4** (Figure 6.1) as a purple solid (15 mg, 47% yield). ^{1}H NMR (ppm) in DMSO-d_6: 10.36, 10.27, 10.24 (4H, s, *meso*-H), 8.57 (2H, dd, CH-vinyl), 8.20 (2H, s, NHCO), 6.70 (2H, br, NH-dien), 6.49 (2H, d, CH_2-vinyl), 6.26 (2H, d, CH_2-vinyl), 5.92 (4H, br, NH_2), 4.39 (4H, br, $COCH_2$), 3.79 (6H, d, CH_3 β pyrrole), 3.67 (6H, d, CH_3 β pyrrole), 3.12 (4H, t, CH_2-Proto), 2.86 (4H, CH_2-dien), 2.65 (4H, CH_2-dien), 2.26 (8H, CH_2-dien), -3.79 (2H, s, NH-pyrrole).

[PP-2((CONHtren)PtCl)]2Cl (5). The general method described above with **3a** (25 mg) afforded **5** (Figure 6.1) as a brown solid (22 mg, 69% yield). ^{1}H NMR (ppm) in DMSO-d_6: 10.39, 10.31, 10.25 (4H, s, *meso*-H), 8.58 (2H, dd, CH-vinyl), 8.27 (2H, s, NHCO), 6.47 (2H, d, CH_2-vinyl), 6.24 (2H, d, CH_2-vinyl), 5.52 (4H, br, NH), 5.16 (4H, br, NH), 4.35 (4H, br,

$COCH_2$), 3.76 (6H, d, CH_3 β pyrrole), 3.65 (6H, d, CH_3 β pyrrole), 3.24 (12H, t, CH_2-proto and CH_2-diene), 3.10 (8H, t, CH_2-tren), 2.97 (4H, t, CH_2-tren), 2.85 (8H, m CH_2-tren), -3.82 (2H, s, NH-pyrrole).

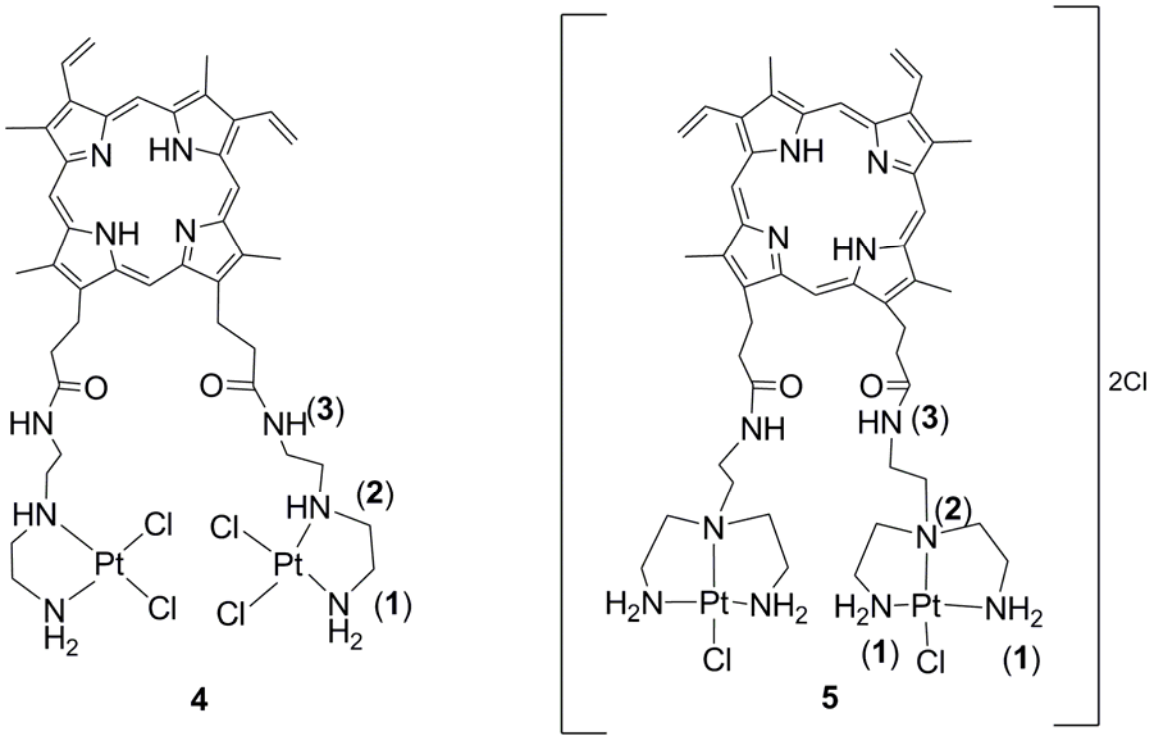

Figure 6.1. PP-Pt(II) complexes synthesized in this study.

6.3 Results and Discussion

Polyamines with Boc-protected groups (Scheme 6.1) were selectively synthesized by following Krapcho's method. The Boc-protecting group can be removed easily by treating with TFA or a solution of 4 M HCl/dioxane. The synthesis of PP-polyamine conjugates **2** and **3** was carried out by reaction of the carboxylic acid groups of PP with the primary amine group of dien mono boc or tren bis Boc in the presence of DIEA, TBTU and HOBt in DMF. After purification by silica column chromatography (eluent: $CHCl_3$/EtOH, 90:10 + 5% TEA), protected polyamine PP conjugates **2** and **3** were obtained in 35% and 48% yields, respectively. ^{1}H NMR spectra of **2**

and **3** in DMSO-d_6 confirmed the synthesis of the PP-polyamine conjugates (**2** and **3**), as the signal of the hydroxyl group at ~12.0 ppm was missing and additional peaks of the amide (NHCO) protons were observed (Figures 6.2 and 6.3). PP-polyamine conjugates (**2** and **3**) were further confirmed by MS MALDI (Figures 6.4 and 6.5), which gave the expected peaks. After cleavage of protecting groups (Boc), the expected compounds **2a** and **3a** were obtained in quantitative yields and confirmed by ^{1}H NMR spectroscopy and mass spectrometry. Treatment of the crude deprotected polyamine PP conjugates with *cis*-Pt$(Me_2SO)_2Cl_2$ in methanol afforded the PP-platinum complexes (Figure 6.1).

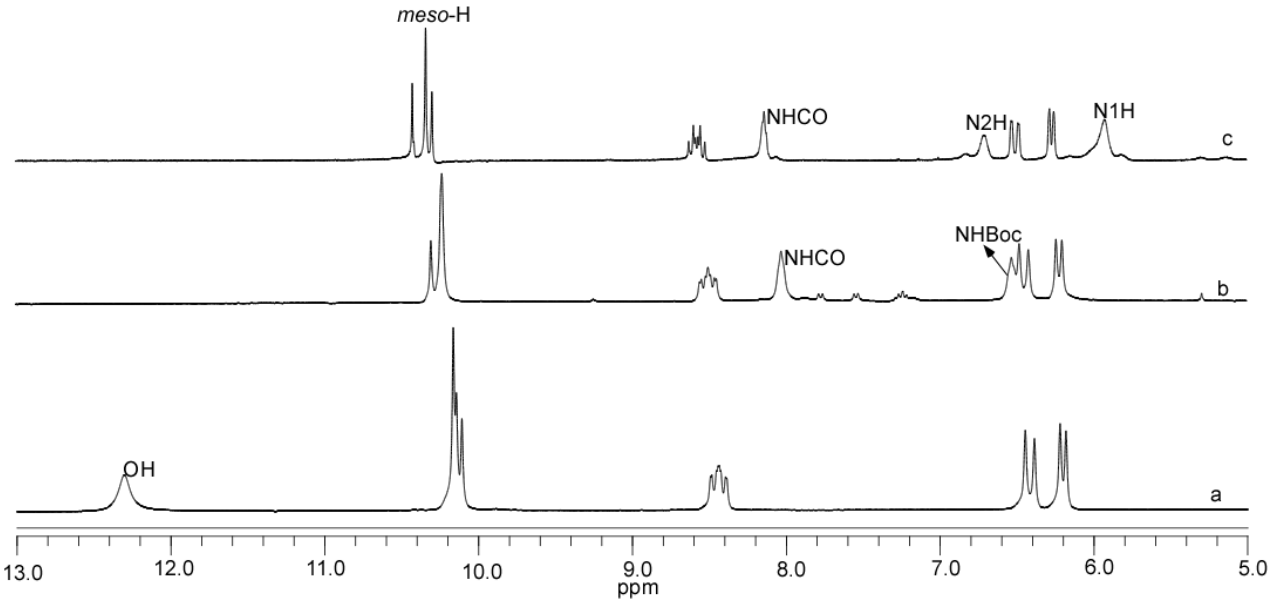

Figure 6.2. ^{1}H NMR region of PPIX (a), **2** (b) and **4** (c) in DMSO-d_6.

PP polyamine conjugates and their platinum complexes were characterized by ^{1}H NMR spectroscopy in DMSO-d_6, and their chemical shifts compared to those of PP in the same solvent (Figures 6.2 and 6.3). The ^{1}H NMR spectra of the porphyrin diacid showed the resonance of two inner pyrrole protons at -4.18 ppm as a singlet. The resonance of the *meso* protons appeared at

10.4 – 10.2 ppm as three singlets in a 2:1:1 ratio. Upon conjugation of the polyamines to the PP diacid groups, the OH peak at 12.30 ppm disappeared, and the amide NH was observed between 7.85 – 8.0 ppm for the two PP-polyamine conjugates (**2** and **3**). The presence of the methyl groups of the tert-butyl groups at ~1.3 ppm confirmed successful conjugation of the polyamines to the PP diacid groups.

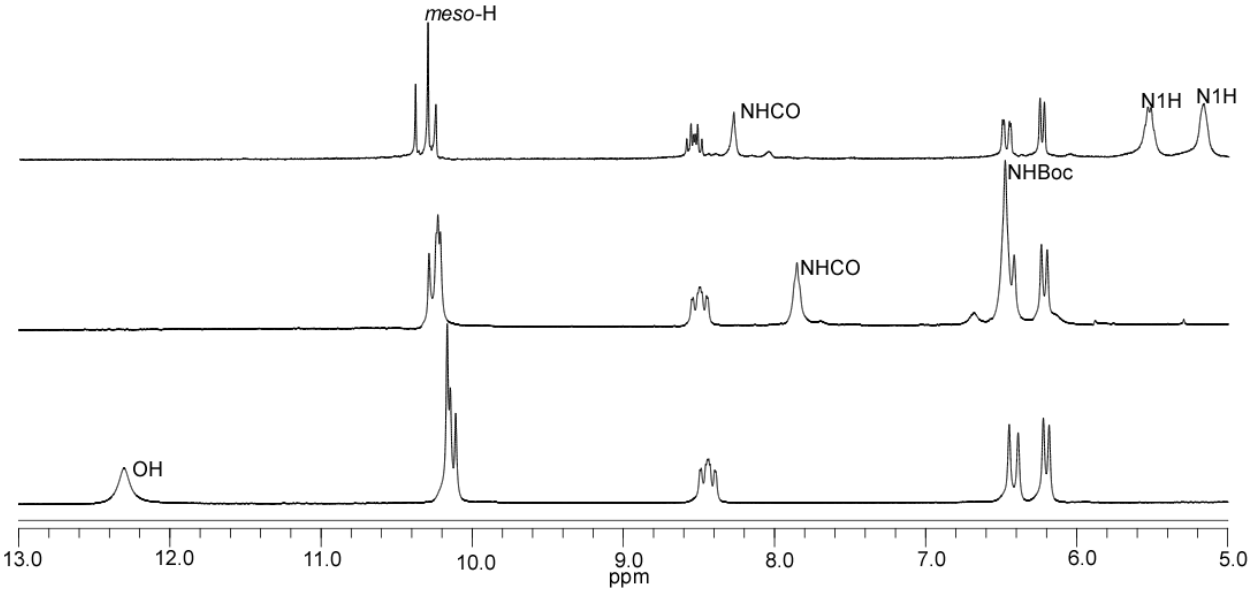

Figure 6.3. ^{1}H NMR region of of PPIX (a), **3** (d) and **5** (e) in DMSO-d_6.

There was a general downfield shift of the PP proton signals of the PP-polyamine conjugates as compared to the parent porphyrin PP diacid. Removal of the Boc-protecting groups was confirmed by ^{1}H NMR spectroscopy (disappearance of the methyl signals of the tert-butyl group and the appearance of the protonated amine groups of the ligands) and ESI-MS, which gave one parent peak of the expected mass (see Experimental Section).

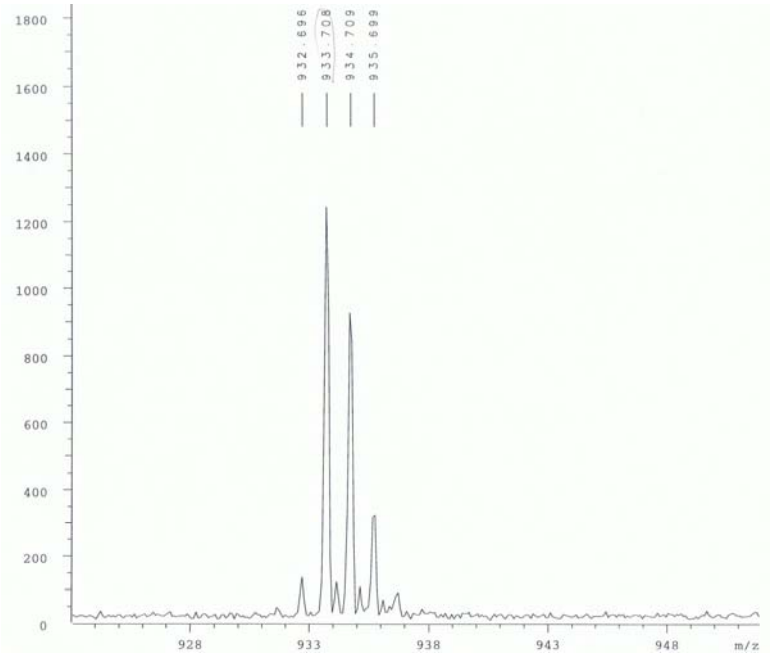

Figure 6.4. MS MALDI spectrum for 2,18-bis[*tert*butoxycarbonyldiethlenetriaminyl-*N*-amidoethyl]-3,8,13,17-tetramethyl-7,12-divinylporphyrin (**2**).

Cis-Pt(Me_2SO)$_2Cl_2$ was treated with the PP-polyamine conjugate (**2a** and **3a**) (Scheme 1) dissolved in methanol at 50 °C for 12 h. The PP-platinum complexes (**4** and **5**) precipitated and were collected by filtration and then washed with methanol to remove the excess of *cis*-Pt(Me_2SO)$_2Cl_2$ and any unreacted ligand. All the PP-platinum complexes synthesized were soluble only in DMSO.

6.3.1 ^{1}H NMR Characterization of PP-Pt(II) Complexes

PP-2((CONHdien)Pt(II)Cl$_2$) (4). Under the conditions used *cis*-Pt(Me_2SO)$_2Cl_2$ and PP-2(CONHdien) formed PP-(dien-Pt)$_2$2Cl$_2$, with PP-2(CONHdien) acting as a bidentate ligand (central N2 and terminal N1) (Figure 6.1). Evidence of this conclusion is the presence of an amide signal N3H in the ^{1}H NMR signal (Figure 6.2) at a shift close to that of the free PP-

2(CONHdien). Soon after dissolving **4** in DMSO-d_6, one major and one minor set of NH signals were observed. The extra set of signals disappeared after ~5 min. Based on a previous study by Christoforou et al.,[21] the minor set of signals was assigned to the dichloride complex and the other set assigned to the monosolvated species, in which only one chloride ligand is replaced by DMSO.

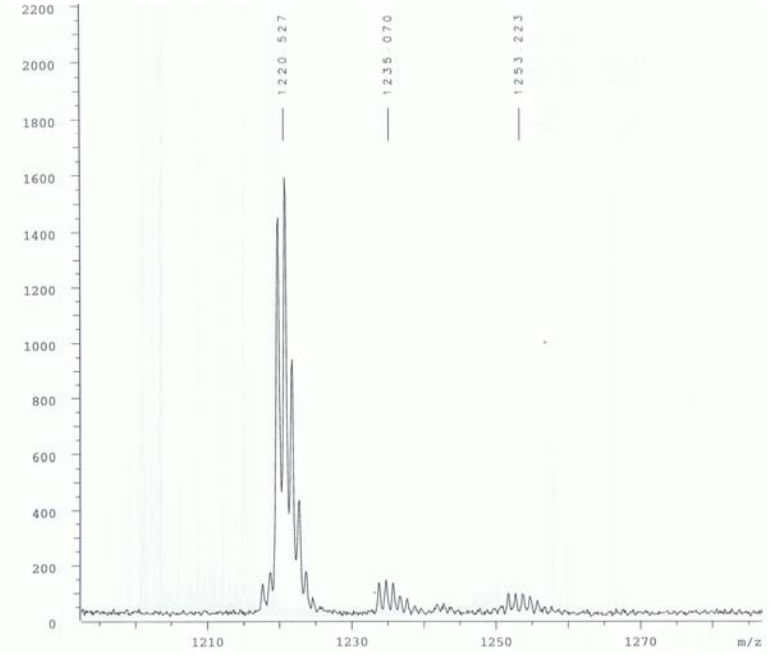

Figure 6.5. MS MALDI spectrum for 2,18-Bis[di*tert*butoxycarbonyldiaminodiethylaminoethyl-*N*-amidoethyl]-3,8,13,17-tetramethyl-7,12-divinylporphyrin (**3**).

[PP-2((CONHtren)PtCl)]2Cl (5). Similarly, under the conditions used, the reaction of *cis*-$Pt(Me_2SO)_2Cl_2$ and PP-2(CONHtren) formed [PP-2((CONHtren)PtCl)]2Cl, with PP-2(CONHtren) acting as a tridentate ligand (central N2 and two terminal N1) (Figure 6.1). The presence of the amide N3H signal (8.5 ppm) confirmed formation of the desired compound

(Figure 6.3). The primary amine N2H signals had shifts close to those of related compounds studied previously.[21] Unlike for PP-2((CONHdien)Pt(II)Cl_2), upon dissolving [PP-2((CONHtren)PtCl)]2Cl in DMSO, no solvolysis species were observed. This unusual behavior was also observed in a related compound, [Pt(DNSH-tren)Cl]Cl, in which only 10% of the solvolysis species was observed; the explanation given was that the presence of an alkyl group on the central N decreases DMSO solvolysis.[21]

6.4 Conclusion and Future Work

We synthesized protoporphyrin IX containing polyamine ligands (PP-2(CONHdien) and PP-2(CONHtren)) that acted as bidentate and tridentate ligands towards platinum (II) complexes, respectively. The synthetic method developed in this work is useful and versatile for conjugating other useful ligands to the protoporphyrin IX. This in turn will provide protoporphyrin IX ligands that can bind different metal fragments with medicinal application.

6.5 References

1. Pratt, W. B.; Ruddon, W. R.; Ensminger, D. W.; Maybaum, J. *The Anticancer Drugs*; 2nd ed.; Oxford University Press: New York, 1994.

2. Keppler, K. B. *Metal Complexes in Cancer Therapy*; VCH: Weinheim, 1993.

3. Von Hoff, D. D.; Schilsky, R.; Reichert, M. C.; Reddick, R. L.; RozencWeig, M.; Young, R. C.; Muggia, M. F. *Cancer Treatment Report* **1979**, *63*, 1527-1531.

4. Boyle, R. W.; Dolphin, D. *Photochem. Photobiol.* **1996**, *64*, 469-485.

5. Dolphin, D. *Can. J. Chem.* **1994**, *72*, 1005-1013.

6. James, D. A.; Swamy, N.; Paz, N.; Hanson, R. N.; Ray, R. *Bioorg. Med. Chem. Lett.* **1999**, *9*, 2379-2384.

7. Sternberg, E. D.; Dolphin, D.; Bruckner, C. *Tetrahedron* **1998**, *54*, 4151-4202.

8. Winkelma.J; Slater, G.; Grossman, J. *Cancer Research* **1967**, *27*, 2060.

9. Winkelman, J. *Cancer Research* **1962**, *22*, 589.

10. Brunner, H.; Arndt, M. R.; Treittinger, B. *Inorg. Chim. Acta* **2004**, *357*, 1649-1669.

11. Brunner, H.; Gruber, N. *Inorg. Chim. Acta* **2004**, *357*, 4423-4451.

12. Brunner, H.; Schellerer, K. M. *Z. Naturforsch., B: Chem. Sci.* **2002**, *57*, 751-756.

13. Brunner, H.; Schellerer, K. M. *Inorg. Chim. Acta* **2003**, *350*, 39-48.

14. Lottner, C.; Bart, K. C.; Bernhardt, G.; Brunner, H. *J. Med. Chem.* **2002**, *45*, 2064-2078.

15. Lottner, C.; Bart, K.-C.; Bernhardt, G.; Brunner, H. *J. Med. Chem.* **2002**, *45*, 2079-2089.

16. Lottner, C.; Knuechel, R.; Bernhardt, G.; Brunner, H. *Cancer Letters* **2004**, *203*, 171-180.

17. Song, R.; Kim, Y. S.; Sohn, Y. S. *J. Inorg. Biochem.* **2002**, *89*, 83-88.

18. Victor N. Nemykin, V. M. M. S. V. V. N. K. *J. Porphyrins Phthalocyanines* **2000**, *4*, 551-554.

19. Brunner, H.; Obermeier, H. *Angew. Chem. Int. Ed.* **1994**, *33*, 2214-2215.

20. Brunner, H.; Scheller, K. M.; Treittinger, B. *Inorg. Chim. Acta* **1997**, *264*, 67-79.

21. Christoforou, A. M.; Marzilli, P. A.; Marzilli, L. G. *Inorg. Chem.* **2006**, *45*, 6771-6781.

CHAPTER 7. CONCLUSIONS

Novel synthetic methodology for preparing porphyrins and their metal derivatives having sulfonamide link was developed. In general the sulfonamide group provided a versatile way to expand porphyrin utility. However, it was necessary to employ a tertiary sulfonamide because otherwise intractable species would be formed. The sulfonamide link can also be used in bioconjugation of useful molecules to the porphyrin.

We achieved the synthesis of pyridyl porphyrins that contained either a secondary or tertiary sulfonamide group. Since sulfonamide groups are known to bind metals, replacing the dissociable proton of the sulfonamide group with a methyl group simplified the synthesis of the metalloporphyrin. Coordinating the pyridyl group with methylcobaloxime unit allowed us to estimate the pK_a of the pyridyl groups of T(*N*-py-4-$CH_2(CH_3)NSO_2Ar$)P) and of TpyP(4) to be close to that of pyridine.

We were able to convert sulfonamide expanded porphyrins bearing pyridyl groups to cationic porphyrins. Most of these new porphyrins contain the same 4-substituted *N*-methylpyridinium group (*N*-Mepy) as in TMpyP(4) and in several other known intercalating porphyrins. However, the *N*-Mepy group in the new porphyrins is not directly attached to the porphyrin ring. The interaction studies of these cationic porphyrins with calf thymus DNA showed that they are outside binders without self stacking in contrast to what is observed with TMpyP(4) which is a known intercalator. Our results on new porphyrins having 4-substituted *N*-Mepy groups that can have separations similar to those in intercalating porphyrins indicate that spacing is not the deciding factor for intercalation into CT DNA. This finding, along with results on porphyrins with *N*-Mepy groups linked at the 2-position, leads us to conclude that direct attachment of the *N*-alkylpyridinium groups to the porphyrin ring in such a way that the *N*-

alkylpyridinium group can become nearly coplanar with the porphyrin ring is necessary in order for intercalation to occur.

APPENDIX A. SUPPLEMENTARY MATERIAL FOR CHAPTER 2

Table A.1. Selected Bond Distances (Å), Angles (deg) of the Methylcobaloxime moieties in $[CH_3Co(DH)_2]_4$TpyP(4) (**9**)

$[CH_3Co(DH)_2]_4$TpyP(4) (**9**)			
Co(1)–N_{eq}	1.883(4)	Co(2)–N_{eq}	1.882(4)
Co(1)–N_{eq}	1.883(4)	Co(2)–N_{eq}	1.883(4)
Co(1)–N_{eq}	1.885(4)	Co(2)–N_{eq}	1.887(5)
Co(1)–N_{eq}	1.887(4)	Co(2)–N_{eq}	1.892(5)
Co(1)–N_{ax}	2.055(4)	Co(2)–N_{ax}	2.079(4)
Co(1)–C(29)	2.002(5)	Co(2)–C(38)	1.999(5)
N(4)–Co(1)–C(29)	177.5(2)	N(4)–Co(2)–C(3)	179.4(2)

Table A.2. ^{1}H NMR Shifts (ppm) of Porphyrin[a] Signals

compound	Hβ[b]	*m*-H	*o*-H	H3,5 (py)	H2,6 (py)	NCH_3	-NH
T(*N*-py-2-CH_2(H)NSO_2Ar)P (**2**)	8.80	8.36	8.18				-2.99
T(*N*-py-4-CH_2(H)NSO_2Ar)P (**3**)	8.76	8.36	8.19	7.43	8.60		-3.01
T(*N*-py-2-CH_2(CH_3)NSO_2Ar)P (**4**)	8.90	8.47	8.25			2.99	-2.94
T(*N*-py-4-CH_2(CH_3)NSO_2Ar)P (**5**)	8.92	8.51	8.30	7.46	8.65	2.93	-2.92

[a] 5 mM in DMSO-d_6. [b] β-pyrrole.

Table A.3. Selected ^{1}H NMR Shifts (ppm) of $[CH_3Co(DH)_2]_4$TpyP(4) (**9**) signals observed after addition of 3,5-lut[a]

Compound	Hβ[b]	-NH
$[CH_3Co(DH)_2]_4$TpyP(4)	8.87, 8.77, 8.76	-3.04, -3.01, -2.97, -2.94, -2.92

[a] 5 mM in $CDCl_3$. [b] β-pyrrole

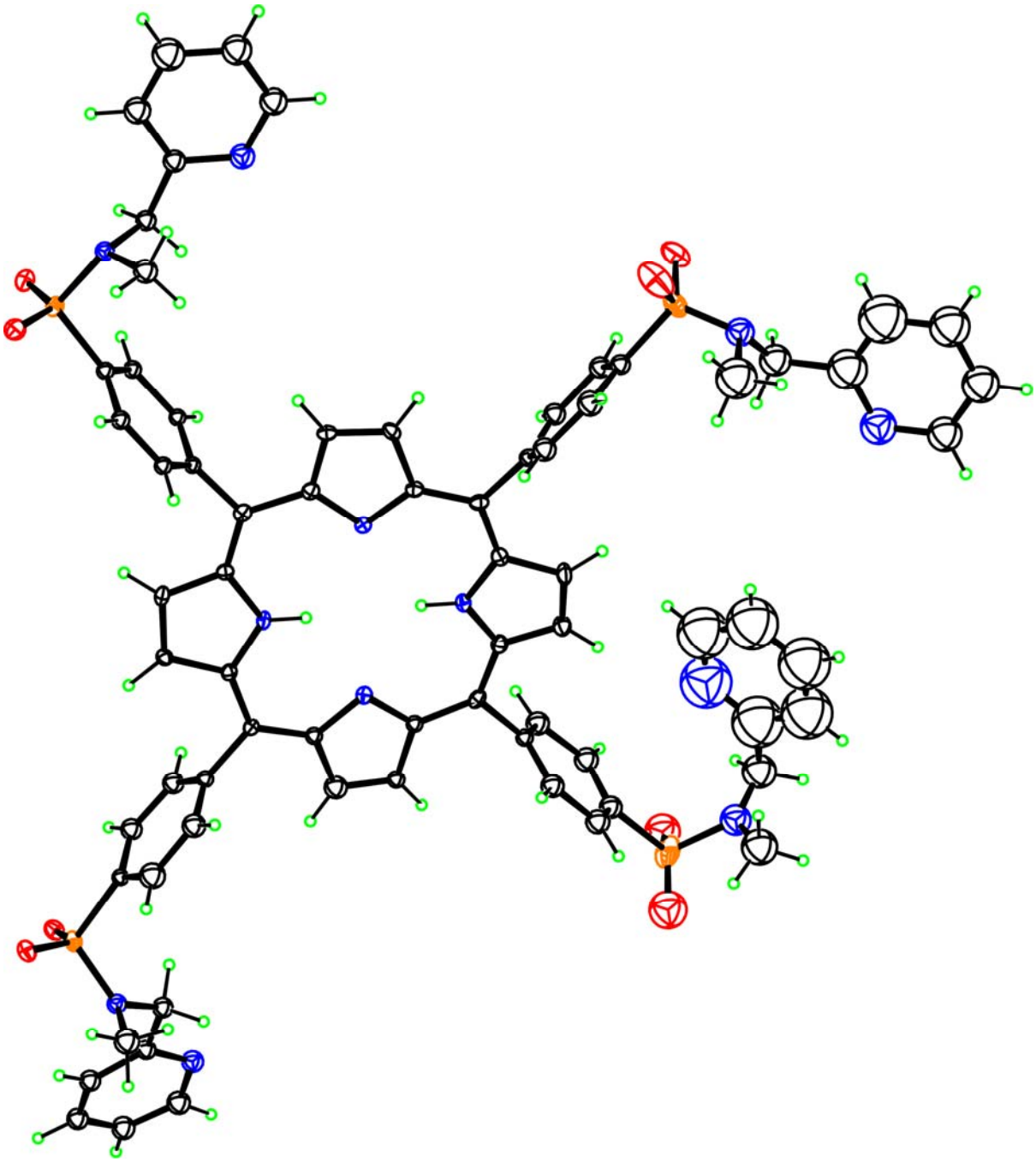

Figure A.1. ORTEP drawing of T(*N*-py-2-$CH_2(CH_3)NSO_2Ar$)P (4) with 50% ellipsoids.

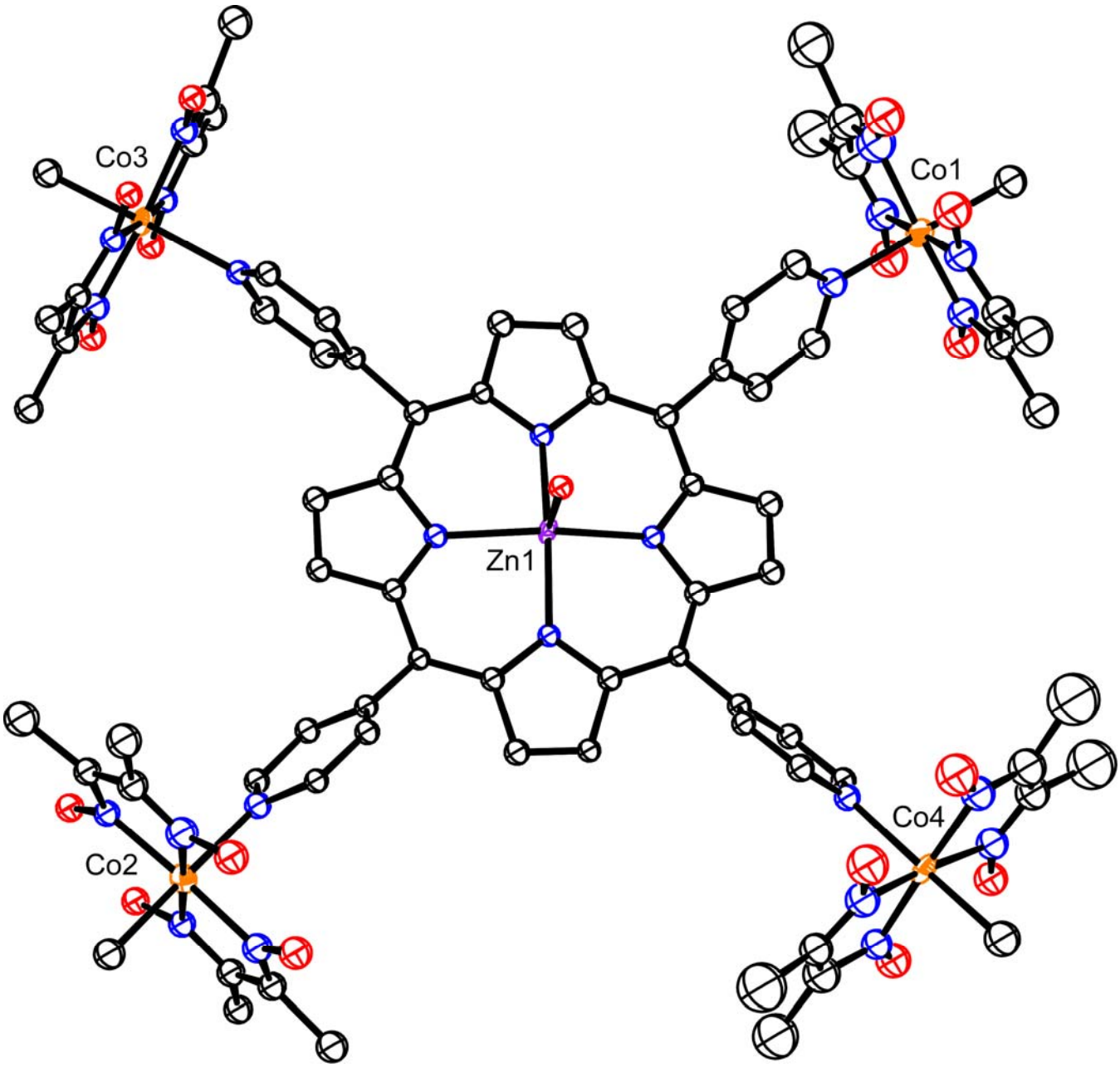

Figure A.2. ORTEP drawing of $[CH_3Co(DH)_2]_4Zn(II)TpyP(4)$ (11) with 50% ellipsoids.

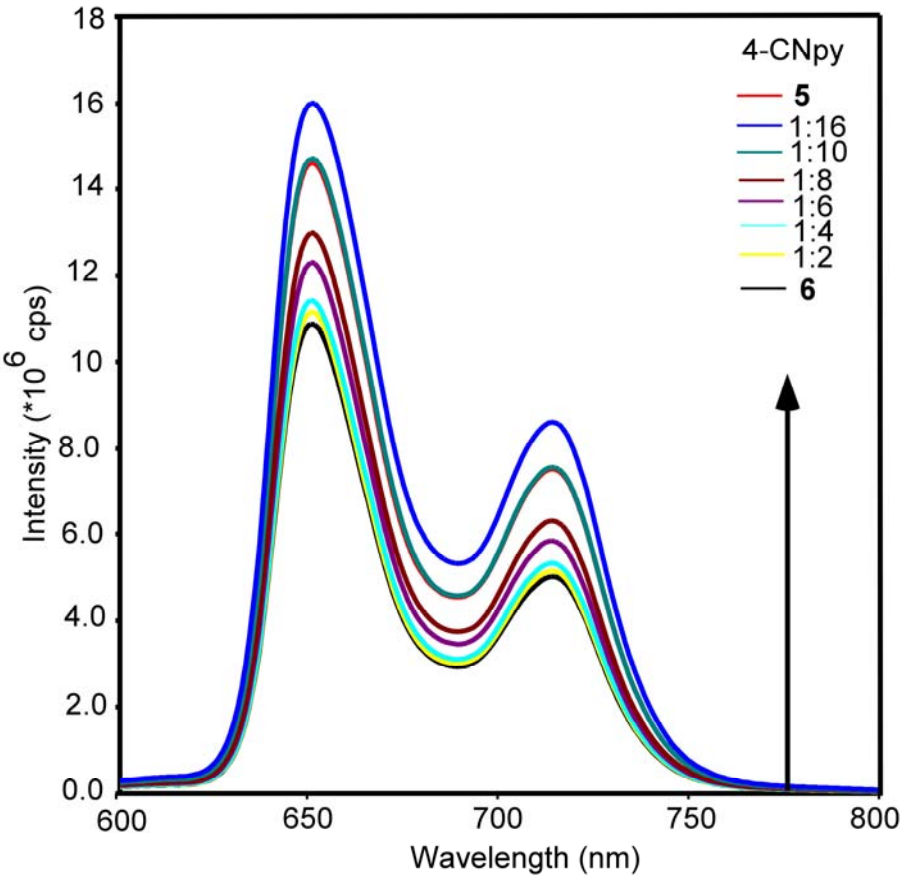

Figure A.3. Emission spectra of $[CH_3Co(DH)_2]_4T(N\text{-py-4-}CH_2(CH_3)NSO_2Ar)P$ (**6**) (5.0 μM) in CH_2Cl_2 with increasing amounts (**6** : pyridine ratio)
of 4-CNpy (excitation wavelength 420 nm).

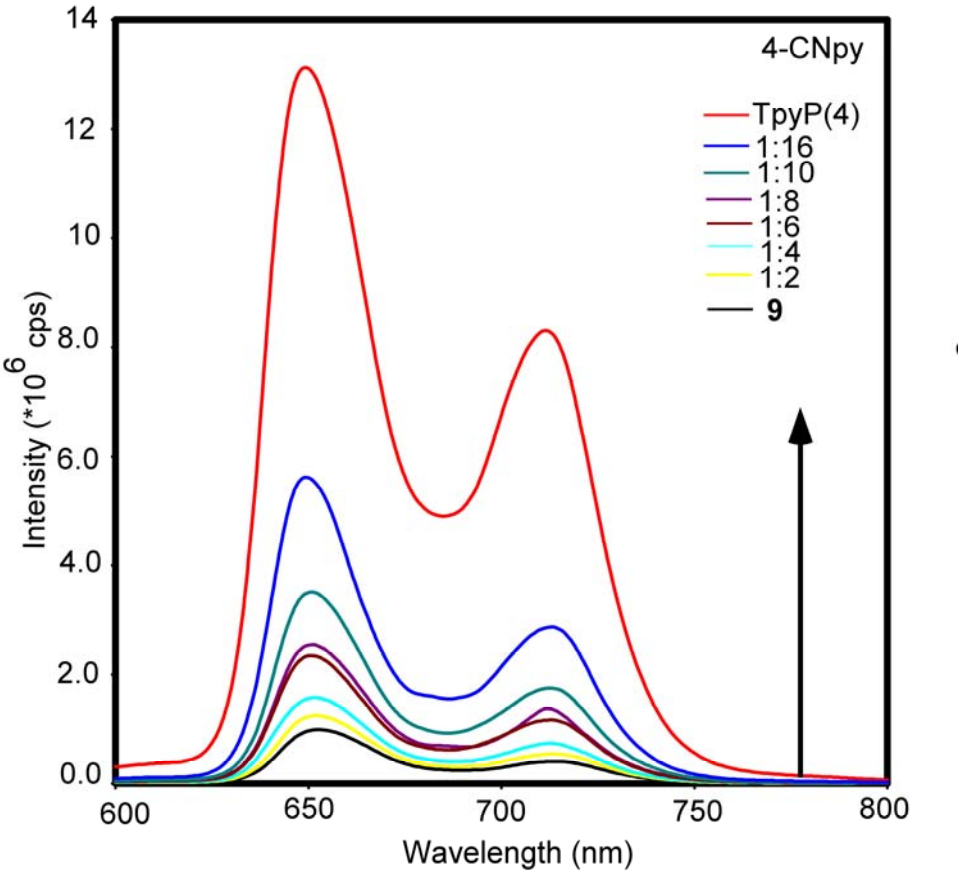

Figure A.4. Emission spectra of $[CH_3Co(DH)_2]_4TpyP(4)$ (**9**) (5.0 μM) in CH_2Cl_2 with increasing amounts (**9** : pyridine ratio) of 4-CNpy (excitation wavelength 420 nm).

APPENDIX B. SUPPLEMENTARY MATERIAL FOR CHAPTER 3

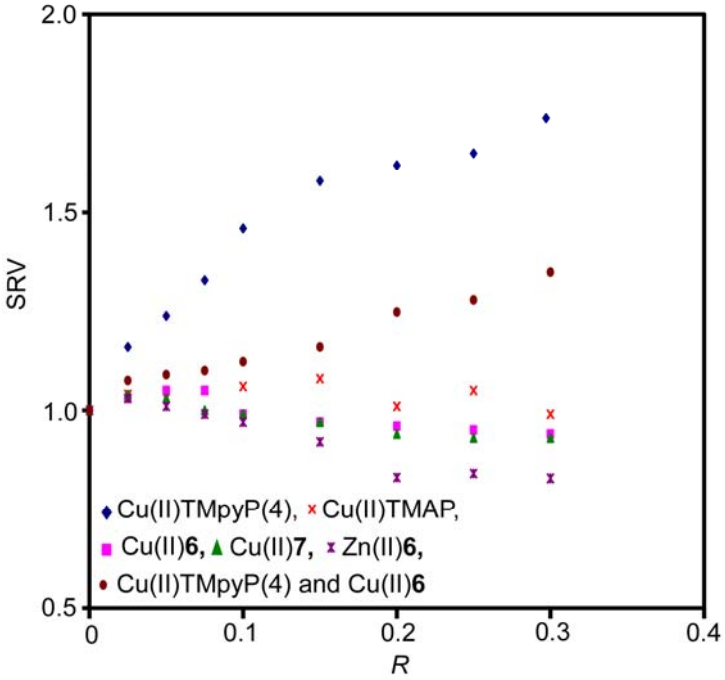

Figure B.1. Plot of SRV vs. *R* for the addition of metalloporphyrins to solutions of CT DNA (75 μM, 100 mM NaCl, pH 7.0).

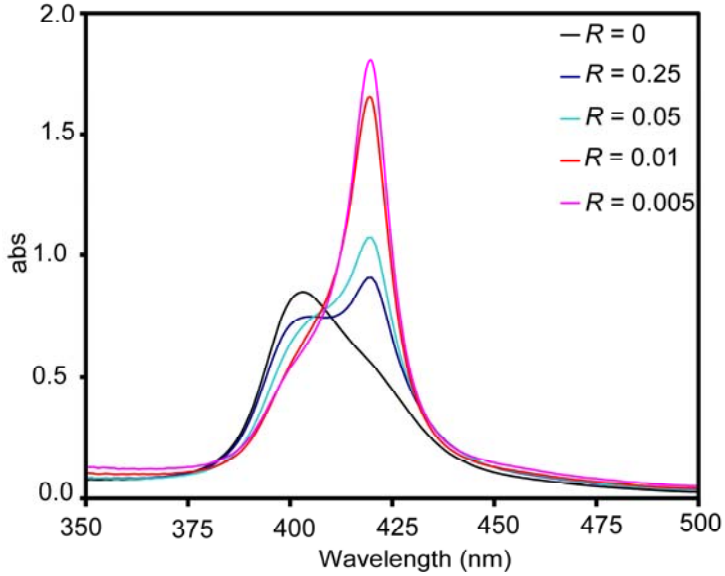

Figure B.2. Effect of CT DNA on the visible spectrum of [Cu(II)T(*N*-Mepy-4-$CH_2(CH_3)NSO_2Ar$)P]Cl_4 (Cu(II)**6**, 7.5 μM) at various *R* values (100 mM NaCl, pH 7.0).

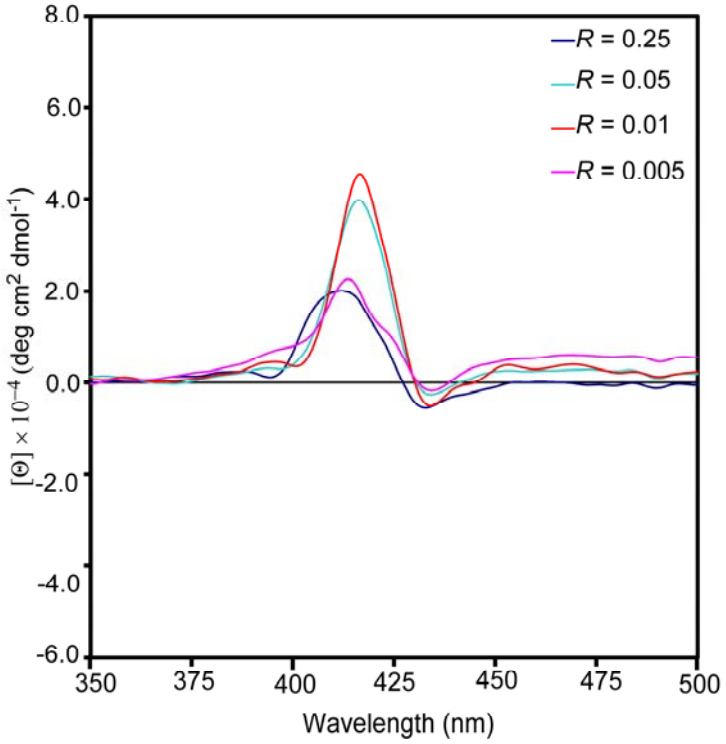

Figure B.3. CT DNA-induced CD spectra of [Cu(II)T(*N*-Mepy-4-$CH_2(CH_3)NSO_2Ar$)P]Cl_4 (Cu(II)**6**, 7.5 μM) at various *R* values (100 mM NaCl, pH 7.0).

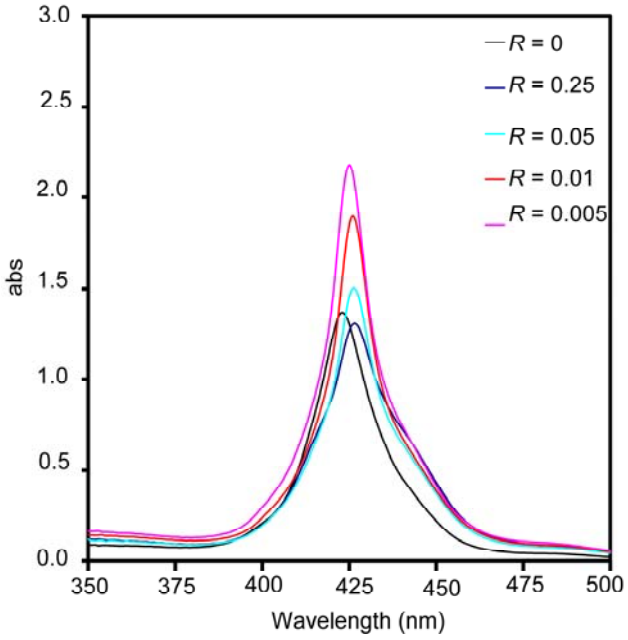

Figure B.4. Effect of CT DNA on the visible spectrum of [Zn(II)T(*N*-Mepy-4-$CH_2(CH_3)NSO_2Ar$)P]Cl_4 (Zn(II)**6**, 7.5 μM) at various *R* values (10 mM NaCl, pH 7.0).

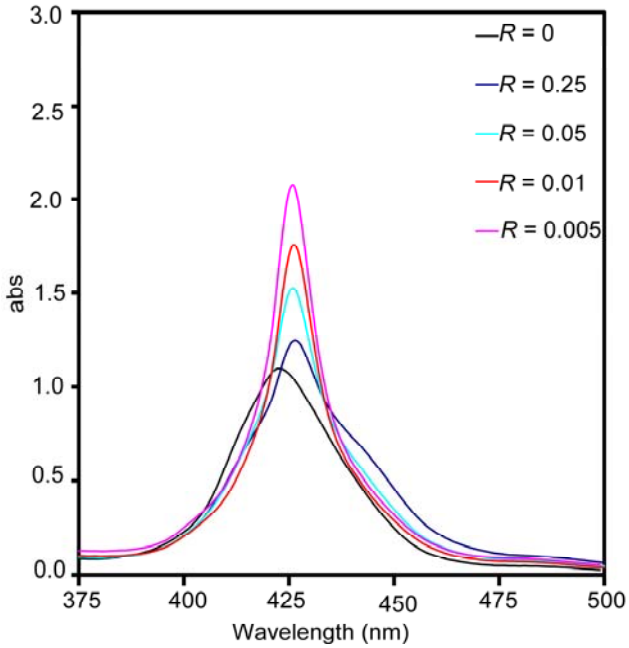

Figure B.5. Effect of CT DNA on the visible spectrum of [Zn(II)T(*N*-Mepy-4-$CH_2(CH_3)NSO_2Ar$)P]Cl_4 (Zn(II)**6**, 7.5 μM) at various *R* values (100 mM NaCl, pH 7.0).

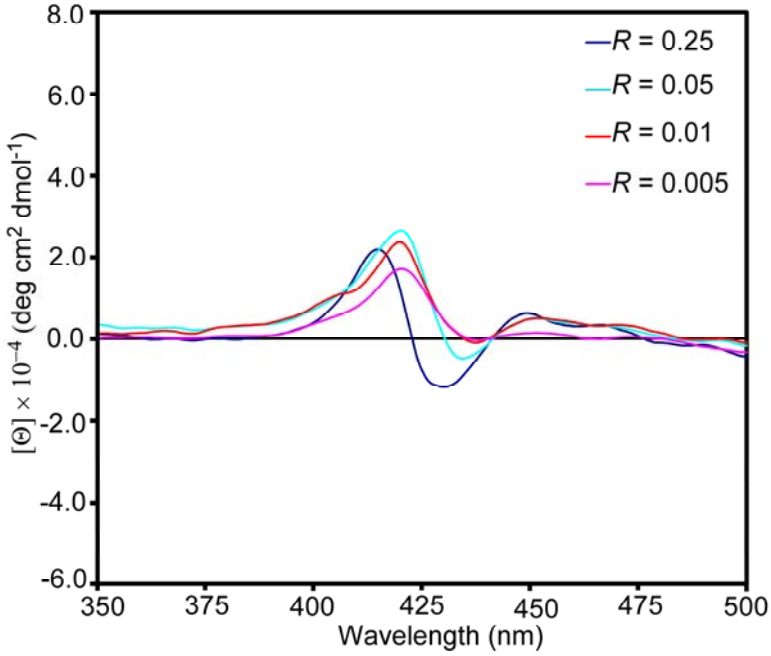

Figure B.6. CT DNA-induced CD spectra of [Zn(II)T(*N*-Mepy-4-$CH_2(CH_3)NSO_2Ar$)P]Cl_4 (Zn(II)**6**, 7.5 μM) at various *R* values (10 mM NaCl, pH 7.0).

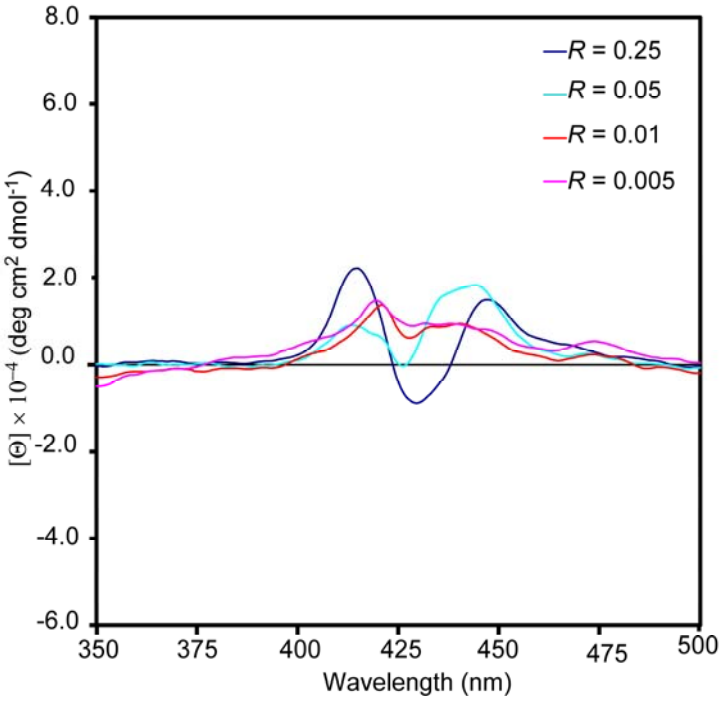

Figure B.7. CT DNA-induced CD spectra of [Zn(II)T(*N*-Mepy-4-$CH_2(CH_3)NSO_2Ar$)P]Cl_4 (Zn(II)**6**, 7.5 μM) at various *R* values (100 mM NaCl, pH 7.0).

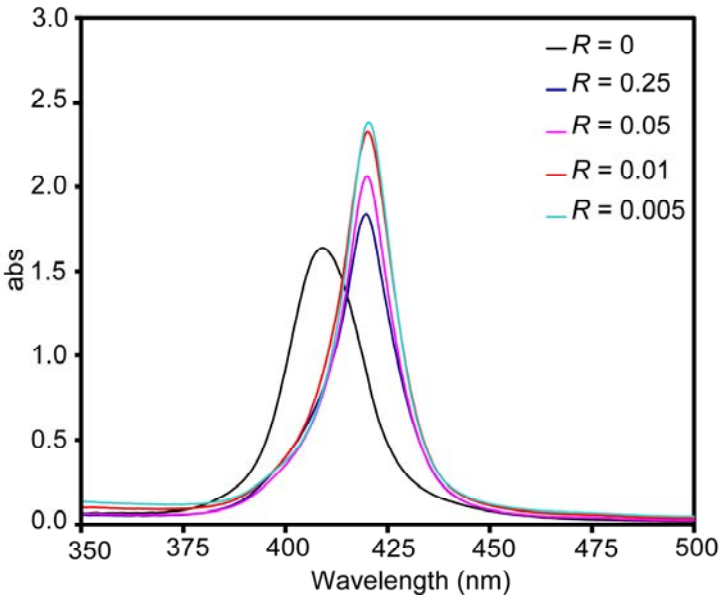

Figure B.8. Effect of CT DNA on the visible spectrum of [Cu(II)T($Et_3NCH_2CH_2)_2NSO_2Ar$)P]Cl_8 (Cu(II)**7**, 7.5 μM) at various *R* values (100 mM NaCl, pH 7.0).

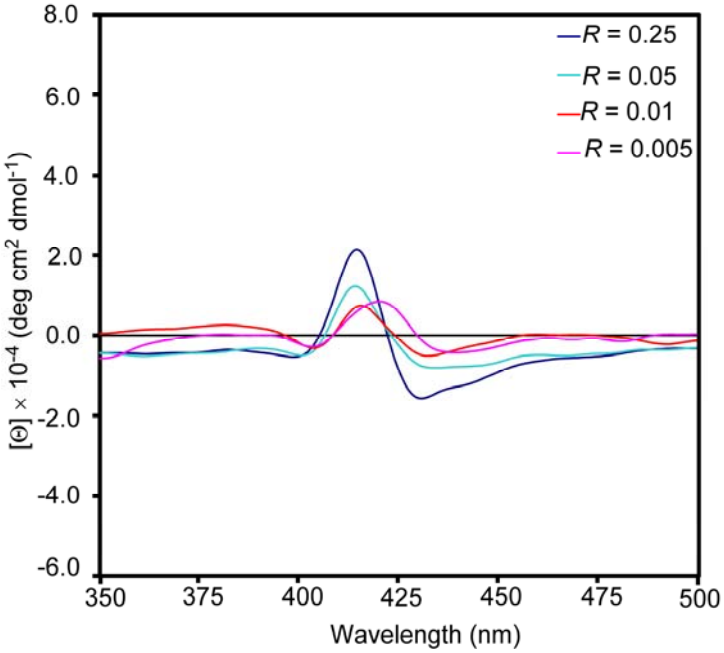

Figure B.9. CT DNA-induced CD spectra of [Cu(II)T($Et_3NCH_2CH_2$)$_2$$NSO_2$Ar)P]$Cl_8$ (Cu(II)**7**, 7.5 μM) at various *R* values (100 mM NaCl, pH 7.0).

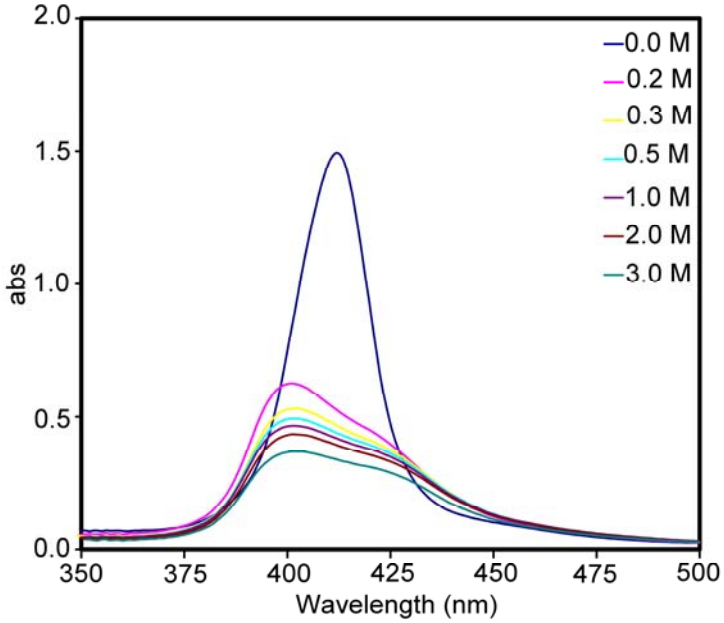

Figure B.10. Effect of NaCl concentration on the visible absorption spectrum of [Cu(II)T(*N*-Mepy-4-$CH_2(CH_3)NSO_2$Ar)P]Cl_4 (Cu(II)**6**, 7.5 μM in water).

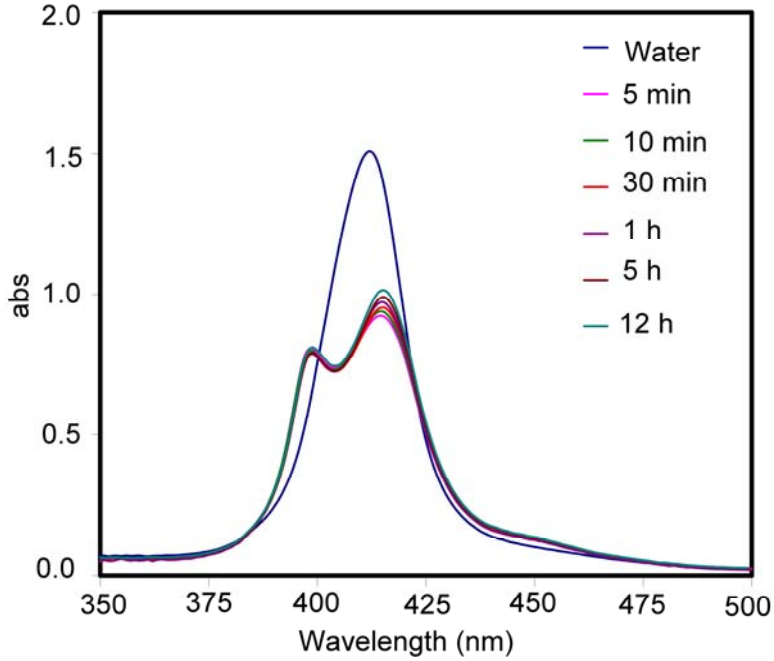

Figure B.11. Visible spectrum monitored with time of [Cu(II)T(*N*-Mepy-4-$CH_2(CH_3)NSO_2Ar$)P]Cl_4 (Cu(II)**6**, 7.5 μM) in 0.1 M SDS. The spectrum in water (dark blue) is also shown.

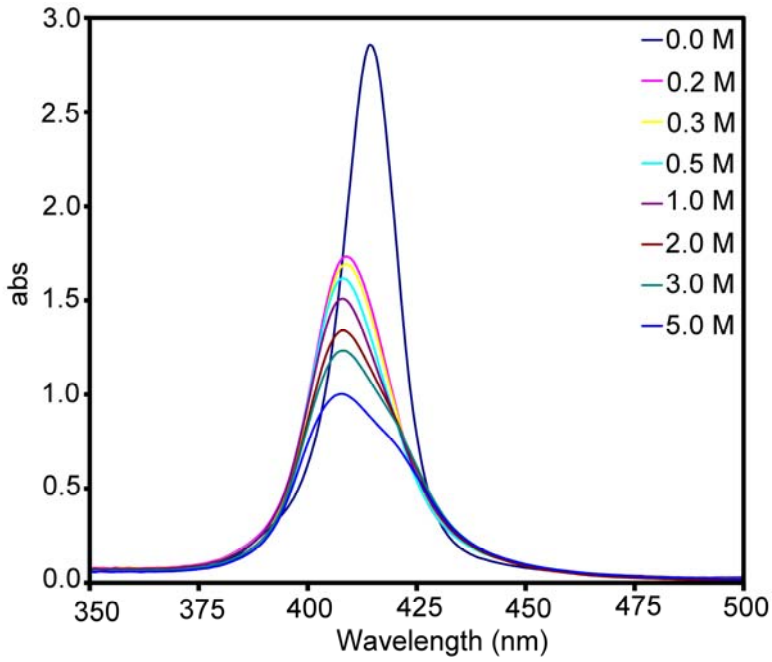

Figure B.12. Effect of NaCl concentration on the visible absorption spectrum of [Cu(II)T($Et_3NCH_2CH_2$)$_2NSO_2Ar$)P]Cl_8 (Cu(II)**7**, 7.5 μM in water).

Table B.1. Visible Spectroscopic Data for [Zn(II)T(*N*-Mepy-4-$CH_2(CH_3)NSO_2Ar$)P]Cl_4 (Zn(II)**6**) in the Presence of CT DNA at pH 7.0[a]

	10 mM NaCl			100 mM NaCl		
R	λ_{So}[b]	$10^{-5} \times \varepsilon_{So}$[c]	$\Delta\lambda$[b] (%*H*)	λ_{So}[b]	$10^{-5} \times \varepsilon_{So}$[c]	$\Delta\lambda$[b] (%*H*)
0	423	1.8		423	1.5	
0.25	426	1.7	3 (6)	426	1.7	3 (-13)
0.05	426	2.0	3 (-11)	426	2.0	3 (-33)
0.01	426	2.5	3 (-39)	426	2.3	3 (-53)
0.005	426	2.9	3 (-61)	426	2.8	3 (-87)

[a] 7.5 μM porphyrin. [b] nm. [c] M^{-1} cm^{-1}.

Table B.2. Effect of NaCl Concentration on the CD Spectrum of [Zn(II)T(*N*-Mepy-4-$CH_2(CH_3)NSO_2Ar$)P]Cl_4 (Zn(II)**6**) in the Presence of CT DNA at pH 7.0[a]

	10 mM NaCl				100 mM NaCl			
R	λ_{+exc}[b]	$10^{-4} \times [\Theta]_{+exc}$[c]	λ_{-s}[b]	$10^{-4} \times [\Theta]_{-s}$[c]	λ_{+exc}[b]	$10^{-5} \times [\Theta]_{+exc}$[c]	λ_{s}[b]	$10^{-4} \times [\Theta]_{-s}$[c]
0.25	415	2.2	430	-1.2	415	2.2	430	-0.8
0.05	420	2.7	434	-0.5	412	0.9		
0.01	420	2.4	437	-0.03	420	1.3		
0.005	420	1.7			421	1.4		

[a] 7.5 μM porphyrin. [b] nm. [c] deg cm^2 $dmol^{-1}$.

Table B.3. Visible Spectroscopic Data for [T(*N*-Mepy-2-CH_2(H)NSO_2Ar)P]Cl_4 (**1**), [T($Me_3NCH_2CH_2$(H)NSO_2Ar)P]Cl_4 (**4**), and [T(*N*-Mepy-2-CH_2(CH_3)NSO_2Ar)P]Cl_4 (**5**) in the Presence of CT DNA at pH 7.0[a]

	1		**4**		**5**	
R	λ_{So}[b] ($10^{-5} \times \varepsilon_{So}$)[c]	$\Delta\lambda$[b] (%*H*)	λ_{So}[b] ($10^{-5} \times \varepsilon_{So}$)[c]	$\Delta\lambda$[b] (%*H*)	λ_{So}[b] ($10^{-5} \times \varepsilon_{So}$)[c]	$\Delta\lambda$[b] (%*H*)
0	414 (2.7)		414 (2.8)		414 (2.6)	
0.25	409 (1.2)	-5 (56)	408 (1.2)	-6 (57)	409 (1.3)	-5 (50)
	422 (1.4)	8 (48)	422 (1.1)	8 (61)	422 (1.5)	8 (42)
0.005	409 (1.3)	-5 (52)	408 (1.1)	-6 (61)	409 (1.2)	-5 (54)
	422 (2.5)	8 (7)	422 (2.4)	8 (14)	422 (2.2)	8 (15)

[a] 7.5 μM porphyrin, 10 mM NaCl. [b] nm. [c] M^{-1} cm^{-1}.

Table B.4. CD Spectral Data for [T(*N*-Mepy-2-CH_2(H)NSO_2Ar)P]Cl_4 (**1**), [T($Me_3NCH_2CH_2$(H)NSO_2Ar)P]Cl_4 (**4**), and [T(*N*-Mepy-2-CH_2(CH_3)NSO_2Ar)P]Cl_4 (**5**) in the Presence of CT DNA at pH 7.0[a]

	1		**4**		**5**	
R	λ_{+exc}[b]	$10^{-4} \times [\Theta]_{+exc}$[c]	λ_{+exc}[b]	$10^{-4} \times [\Theta]_{+exc}$[c]	λ_{+exc}[b]	$10^{-4} \times [\Theta]_{+exc}$[c]
0.25	422	1.5	424	1.8	418	2.6
0.005	422	4.7	418	3.6	418	4.9

[a] 7.5 μM porphyrin, 10 mM NaCl. [b] nm. [c] deg cm^2 $dmol^{-1}$.

VITA

Janet M Manono received her high school Diploma from Ole Tipis Girls' High School, Narok, Kenya, in 1995. She joined University of Nairobi, Kenya, in 1997 and graduated in 2001 with her Bachelor of Science degree (chemistry major). She joined Luigi G. Marzilli group at Louisiana State University, in 2003 and will receive her degree of Doctor of Philosophy in May 15th 2009.